การสังเคราะห์โคพอลิเมอร์ของแลกไทด์และคาโพรแลกโทนที่มีน้ำหนักโมเลกุลต่ำเพื่อใช้เป็นสารยึดติดเนื้อเยื่อและปลดปล่อยยาเททระไซคลิน

นางสาวสุมนา ศรีพุทธิรัตน์

วิทยานิพนธ์นี้เป็นส่วนหนึ่งของการศึกษาตามหลักสูตรปริญญาวิทยาศาสตรมหาบัณฑิต
สาขาวิชาปิโตรเคมีและวิทยาศาสตร์พอลิเมอร์
คณะวิทยาศาสตร์ จุฬาลงกรณ์มหาวิทยาลัย
ปีการศึกษา 2550

SYNTHESIS OF LOW MOLECULAR WEIGHT POLY(LACTIDE-*CO*-CAPROLACTONE) AS TISSUE ADHESIVES AND TETRACYCLINE DRUG RELEASE

Miss Sumana Sriputtirat

A Thesis Submitted in Partial Fulfillment of the Requirements

for the Degree of Master of Science Program in Petrochemistry and Polymer Science

Faculty of Science

Chulalongkorn University

Academic Year 2007

Thesis Title	SYNTHESIS OF LOW MOLECULAR WEIGHT POLY(LACTIDE-*CO*-CAPROLACTONE) AS TISSUE ADHESIVES AND TETRACYCLINE DRUG RELEASE
By	Ms. Sumana Sriputtirat
Field of Study	Petrochemistry and Polymer Science
Thesis Advisor	Associate Professor Somchai Pengprecha, Ph.D.
Thesis Co-advisor	Nuttha Thongchul, Ph.D.

Accepted by the Faculty of Science, Chulalongkorn University in Partial Fulfillment of the Requirements for the Master's Degree

.....Dean of the Faculty of Science
(Professor Supot Hannongbua, Ph.D.)

THESIS COMMITTEE

.....Chairman
(Associate Professor Sirirat Kokpol, Ph.D.)

.....Thesis Advisor
(Associate Professor Somchai Pengprecha, Ph.D.)

..... Thesis Co-advisor
(Nuttha Thongchul, Ph.D.)

.....Member
(Associate Professor Amorn Petsom, Ph.D.)

.....Member
(Associate Professor Wimonrat Trakarnpruk, Ph.D.)

สุมนา ศรีพุทธิรัตน์ : การสังเคราะห์โคพอลิเมอร์ของแลกไทด์และคาโพรแลกโทนที่มีน้ำหนักโมเลกุลต่ำเพื่อใช้เป็นสารยึดติดเนื้อเยื่อและปลดปล่อยยาเททระไซคลิน. (SYNTHESIS OF LOW MOLECULAR WEIGHT POLY(LACTIDE-*CO*-CAPROLACTONE) AS TISSUE ADHESIVES AND TETRACYCLINE DRUG RELEASE) อ. ที่ปรึกษา: รศ. ดร. สมใจ เพ็งปรีชา, อ. ที่ปรึกษาร่วม: ดร. ณัฏฐา ทองจุล, 101 หน้า.

พอลิเมอร์ที่สังเคราะห์จากแลกไทด์สามารถใช้ประโยชน์อย่างแพร่หลายในทางการแพทย์ เช่น นำไปใช้เป็นสารยึดติดและใช้ควบคุมการปลดปล่อยยา ซึ่งวัสดุที่ใช้นั้นต้องสามารถยึดติดเนื้อเยื่อได้และสามารถปลดปล่อยยาได้นานตลอดช่วงการรักษา และที่สำคัญคือเมื่อวัสดุนี้สลายตัวทางชีวภาพจะต้องไม่มีผลข้างเคียงหรือเป็นพิษต่อผู้ใช้ โดยงานวิจัยนี้ได้สังเคราะห์โคพอลิเมอร์แบบเปิดวงของแลกไทด์และคาโพรแลกโทนที่มีน้ำหนักโมเลกุลต่ำที่ใช้ตัวเริ่มต้นปฏิกิริยาร่วมที่มีจำนวนหมู่ไฮดรอกซิลแตกต่างกันและใช้สแตนนัส ออกโตเอตเป็นตัวเร่งปฏิกิริยา โดยทำการสังเคราะห์ให้โคพอลิเมอร์มีความยาวแขนเท่ากันและมีน้ำหนักโมเลกุลใกล้เคียงกัน และทำการวิเคราะห์ด้วยเทคนิค ^{1}H NMR, GPC และ DSC จากการสังเคราะห์โคพอลิเมอร์ทั้งหมด พบว่า ดี-ซอบิทอลไม่เหมาะสำหรับใช้เป็นตัวเริ่มต้นปฏิกิริยาร่วมในการสังเคราะห์โคพอลิเมอร์เพื่อใช้เป็นสารยึดติดเนื้อเยื่อและปลดปล่อยยา และโคพอลิเมอร์ที่มีความยาวแขนเท่ากันสามารถควบคุมอุณหภูมิคล้ายแก้วให้อยู่ระหว่าง 20-25 องศาเซลเซียส ในการเตรียมแผ่นฟิล์มผสมระหว่างโคพอลิเมอร์กับไคโตซาน พบว่าอัตราส่วนที่เหมาะสมในการเตรียม คือ 70/30 โคพอลิเมอร์/ไคโตซาน และนำไปทดสอบสมบัติในการยึดติดโดยใช้ T-peel test พบว่าแผ่นฟิล์มผสมระหว่างโคพอลิเมอร์ที่ใช้เพนทาอีรีทริทอลเป็นตัวเริ่มต้นปฏิกิริยาร่วมกับไคโตซาน (CO-PTOL/CH) มีสมบัติในการยึดติดสูงที่สุด และนำแผ่นฟิล์ม CO-PTOL/CH ไปทดสอบการปลดปล่อยยาเททระไซคลิน ไฮโดรคลอไรด์ในสารละลายฟอสเฟตบัฟเฟอร์ที่อุณภูมิ 37 องศาเซลเซียส พบว่าแผ่นฟิล์ม CO-PTOL/CH ที่บรรจุเททระไซคลิน ไฮโดรคลอไรด์ 5% โดยน้ำหนัก สามารถลดอัตราการปลดปล่อยยาในเวลา 7 วัน เมื่อเทียบกับแผ่นฟิล์มไคโตซานซึ่งสอดคล้องกับพฤติกรรมการบวมน้ำ นอกจากนั้นแผ่นฟิล์มนี้ยังสามารถปลดปล่อยยาออกจากแผ่นฟิล์มได้ 84.08% ดังนั้นแผ่นฟิล์มนี้จึงเหมาะที่จะใช้ปลดปล่อยยาเททระไซคลิน ไฮโดรคลอไรด์มากที่สุด

สาขาวิชา ปิโตรเคมีและวิทยาศาสตร์พอลิเมอร์ ลายมือชื่อนิสิต สุมนา ศรีพุทธิรัตน์

ปีการศึกษา 2550 ลายมือชื่ออาจารย์ที่ปรึกษา

ลายมือชื่ออาจารย์ที่ปรึกษาร่วม ณัฏฐา ทองจุล

487 25242 23: MAJOR PETROCHEMISTRY AND POLYMER SCIENCE
KEY WORD: TISSUE ADHESIVE / DRUG RELEASE / POLY(LACTIDE-*CO*-CAPROLACTONE) / LOW MOLECULAR WEIGHT / TETRACYCLINE

SUMANA SRIPUTTIRAT: SYNTHESIS OF LOW MOLECULAR WEIGHT POLY(LACTIDE-*CO*-CAPROLACTONE) AS TISSUE ADHESIVES AND TETRACYCLINE DRUG RELEASE. THESIS ADVISOR: ASSOC. PROF. SOMCHAI PENGPRECHA, Ph.D., THESIS COADVISOR: NUTTHA THONGCHUL, Ph.D., 101 pp.

Lactide-based polymers are widely used in various biomedical applications including surgical fixation devices and controlled drug delivery system. An ideal tissue adhesive and drug release system must adhere to the tissue substrates and sustain drug throughout the wound healing process. Additionally, it should biodegrade without side effect or systematic toxicity. Ring-opening copolymerization of L-lactide and ε-caprolactone using alcohols with different numbers of hydroxyl groups as co-initiator was prepared in the presence of $Sn(Oct)_2$. Two series of low molecular weight copolymers with similar arm length and molecular weight were synthesized and characterized by ^1H NMR, GPC and DSC. Among all of the copolymers synthesized, D-sorbitol was not suitable to be used as co-initiator for copolymerization as tissue adhesive and drug release system and T_g of copolymers with similar arm length are controlled between 20-25°C. In film preparation, copolymer was incorporated to chitosan at suitable ratio (70/30, copolymer/chitosan, w/w). Blend film of copolymer using pentaerythritol as co-initiator and chitosan (CO-PTOL/CH) gave the highest adhesive property that measured by T-peel test. The tetracycline hydrochloride (TCH) release from blend film was investigated in phosphate buffer saline at 37°C. The CO-PTOL/CH (5% TCH) can prolong the release of TCH within 7 days compared with chitosan film which is consistent with swelling behavior. Furthermore, this film can release drug with high %drug release (84.08%). Therefore, it is the most suitable TCH drug release system.

Field of Study: Petrochemistry and Polymer Science Student's Signature: Sumana Sriputtirat

Academic Year: 2007 Advisor's Signature: Somchai Pengprecha

Co-advisor's Signature: Nuttha Thongchul

ACKNOWLEDGEMENTS

I would like to express my appreciation to my advisor Assoc. Prof. Dr. Somchai Pengprecha for his kind supervision, instruction and encouragement during my research. I would also like to thank my co-advisor Dr. Nuttha Thongchul for her help and advice. I would like to thank Assoc. Prof. Dr. Sirirat Kokpol, Assoc. Prof. Dr. Amorn Petsom and Assoc. Prof. Dr. Wimonrat Trakarnpruk for their valuable suggestions and comments as committee members.

In addition, I wish to thank the Institute of Biotechnology and Genetic Engineering for all facilities and grant. Appreciation is also extended to the Graduate School of Chulalongkorn University for granting partial support to conduct this research.

I would like to acknowledge for supporter, Assist. Prof. Dr. Varawut Tangpasuthadol for his assistance with GPC analysis and Dr. Nanthika Khongcharoenpong for providing tetracycline hydrochloride.

Special thanks also give to all members of Institute of Biotechnology and Genetic Engineering for valuable friendship and helpfulness as well as all of my friends, especially Miss Supaporn, Miss Wilasinee, Miss Panitha, Mr. Pichaet, Miss Paweena, Miss Wasinee, Miss Arpudsorn and my younger sisters in laboratory for encouragement.

Finally, I wish to express my deep sense of appreciation to my beloved family and lovely friends for their inspiration, understanding, great support and encouragement throughout my study.

CONTENTS

Page

ABSTRACT (THAI)..... iv
ABSTRACT (ENGLISH)..... v
ACKNOWLEDGEMENTS..... vi
CONTENTS..... vii
LIST OF TABLES..... x
LIST OF FIGURES..... xii
LIST OF SCHEMES..... xvi
LIST OF ABBREVIATIONS AND SYMBOLS..... xvii

CHAPTER I INTRODUCTION..... 1
1.1 Introduction..... 1
1.2 Objectives..... 3
1.3 Scope of research..... 4

CHAPTER II THEORY AND LITERATURE REVIEWS..... 5
2.1 Block copolymer 5
2.1.1 Classification of block copolymers..... 6
2.1.2 Synthetic methods of block copolymers..... 7
2.2 “Coordination-insertion” ring-opening polymerization..... 10
2.3 Poly(lactide-*co*-caprolactone)..... 11
2.3.1 Lactide 11
2.3.2 Caprolactone..... 12
2.3.3 Catalyst/Co-initiator systems for the ring-opening polymerization of lactides and lactones..... 12
2.4 Tissue adhesive..... 16
2.4.1 Definition..... 16
2.4.2 Development of tissue adhesive 16
2.5 Controlled drug release system..... 18
2.5.1 Fundamental requirements for release system..... 18

Page

2.5.2 Advantages of controlled release..... 19
2.5.3 Transdermal drug delivery system..... 20
2.5.4 Methods of achieving controlled release..... 21
2.6 Tetracycline hydrochloride (TCH) as model drug..... 23
2.6.1 Physicochemical properties..... 23
2.6.2 Uses and administration..... 24
2.6.3 Pharmacokinetics..... 24
2.6.4 Adverse effects..... 24
2.7 Chitosan..... 25
2.7.1 Structure of chitosan..... 25
2.7.2 Chitosan in pharmaceutical application..... 26

CHAPTER III EXPERIMENTAL..... 27
3.1 Materials..... 27
3.2 Instruments/Equipments..... 28
3.3 Methodology..... 29
3.3.1 Synthesis of lactide..... 29
3.3.1.1 Synthesis of low molecular weight polylactide 29
3.3.1.2 Ring formation of L-lactide using zinc powder as catalyst..... 30
3.3.2 Synthesis of low molecular weight poly(lactide-*co*-caprolactone) using stannous(II) 2-ethylhexanoate as catalyst..... 31
3.3.3 Copolymer characterization..... 33
3.3.3.1 Proton nuclear magnetic resonance spectrometer (^{1}H NMR)..... 33
3.3.3.2 Gel permeation chromatograph (GPC)..... 33
3.3.3.4 Differential scanning calorimeter (DSC)..... 33
3.3.4 Preparation and characterization of film..... 34
3.3.4.1 Preparation of blend films..... 34
3.3.4.2 Morphology study..... 35
3.3.4.3 Swelling property..... 35

Page

3.3.5 *In vitro* tissue adhesion..... 36
3.3.6 *In vitro* tetracycline hydrochloride (TCH) release study..... 37
3.3.6.1 Calibration curve of tetracycline hydrochloride..... 37
3.3.6.2 *In vitro* tetracycline hydrochloride release..... 37

CHAPTER IV RESULTS AND DISCUSSION..... 39
4.1 Synthesis of L-lactide..... 39
4.1.1 Synthesis of low molecular weight polylactide..... 39
4.1.2 Ring formation of L-lactide using zinc powder as a catalyst..... 39
4.2 Synthesis and characterization of low molecular weight poly(lactide-*co*-caprolactone) using alcohols with different numbers of hydroxyl groups.. 41
4.2.1 Proton nuclear magnetic resonance spectroscopy (^{1}H NMR) analysis..... 44
4.2.2 Gel permeation chromatography (GPC) analysis..... 51
4.2.3 Differential scanning calorimetry (DSC) analysis..... 51
4.3 Preparation and characterization of blend film..... 53
4.3.1 Morphology study..... 55
4.3.2 Swelling property..... 59
4.4 *In vitro* tissue adhesion..... 60
4.5 *In vitro* tetracycline hydrochloride release study..... 61
4.5.1 Effect of TCH content on the dissolution profiles..... 62
4.5.2 Effect of the molecular weight of copolymer in matrixes on the dissolution profiles..... 64

CHAPTER V CONCLUSIONS AND SUGGESTION..... 68
5.1 Conclusions..... 68
5.2 Suggestion for future work..... 69

REFERENCES..... 70
APPENDICES..... 75
VITA..... 101

LIST OF TABLES

Table		Page
3.1	Composition of blend film.....	35
4.1	The %yield and physical appearance of low molecular weight copolymers prepared by using alcohols with different numbers of hydroxyl groups.....	42
4.2	Composition of low molecular weight copolymers prepared by using alcohols with different numbers of hydroxyl groups.....	50
4.3	Characterization of low molecular weight copolymers prepared by using alcohols with different numbers of hydroxyl groups.....	52
4.4	The appearance of blend films.....	53
4.5	Adhesive failure strength (AFS) of blend films.....	60
4.6	The percentage of drug content.....	61
4.7	The release rate of TCH from the blend films with various drug loading contents in PBS pH 7.4 at 37°C.....	64
4.8	The release rate of TCH from the 5% drug-loaded films with various copolymers in PBS pH 7.4 at 37°C.....	66
4.9	Comparison of Formulation C with other drug delivery device.....	67
B1	The swelling percent of blend films in phosphate buffer saline (pH 7.4).....	91
C1	Absorbance of tetracycline hydrochloride in PBS at 276.7 nm.....	94
D1	Percentage of TCH from blend film (Formulation B) in PBS at 37°C.....	96
D2	Percentage of TCH from blend film (Formulation C) in PBS at 37°C.....	97

Table **Page**

D3 Percentage of TCH from blend film (Formulation D) in PBS at 37°C..... 98

D4 Percentage of TCH from chitosan film (Formulation A) in PBS at 37°C..... 99

D5 Percentage of TCH from blend film (Formulation E) in PBS at 37°C..... 100

LIST OF FIGURES

Figure		Page
1.1	Structures of (a) L-lactide and (b) ε-caprolactone.....	2
2.1	Structures of (a) random, (b) alternating, (c) graft and (d) block copolymer.....	5
2.2	A schematic presentation of (a) AB di-block, (b) ABA tri-block, (c) $(AB)_n$ multiblock and (d) star-shaped block copolymer.....	7
2.3	The structures of lactide in different stereoisomer.....	11
2.4	The structure of caprolactone.....	12
2.5	The structure of stannous(II) 2-ethylhexanoate.....	13
2.6	Schematic plot of the change in modulus as function of temperature.....	17
2.7	Hypothetical serum drug concentrations of various oral dosage forms.....	19
2.8	Basic approaches of patch constructions.....	20
2.9	(a) Dissolution-controlled, (b) diffusion-controlled and (c) biodegradable systems.....	22
2.10	Chemical structure of tetracycline hydrochloride.....	23
2.11	Chemical structure of chitosan.....	25
3.1	Experimental set up for low molecular weight PLLA synthesis.....	30
3.4	Experimental set up for L-lactide ring formation.....	31
3.5	T-peel specimens.....	36
4.1	(a) Condensate reservoir and (b) white solid crystal of L-lactide.....	40

Figure **Page**

4.2 Recrystallized L-lactide..... 40

4.3 (a) Experimental set up for P(LA-*co*-CL) synthesis under nitrogen atmosphere, (b) P(LA-*co*-CL) in round bottom flask and (c) purified P(LA-*co*-CL)..... 41

4.4 Structures of (a) similar arm length and (b) similar molecular weight copolymers..... 43

4.5 ^{1}H NMR spectrum of P(LA-*co*-CL) prepared by using 1,4-butanediol as co-initiator (CO-BD)..... 45

4.6 The photograph of film with various compositions..... 54

4.7 Scanning electron micrographs of the blend films surface (x1000 and x10,000)..... 56

4.8 Scanning electron micrographs (cross section) of the blend films with and without TCH ((a) and (b) respectively)..... 58

4.9 Scanning electron micrographs of the blend films surface (x10000) after preparation for about 1 month..... 58

4.10 Swelling behavior of various ratios of copolymer/chitosan films in PBS. 59

4.11 The dissolution profiles of TCH from the blend films with various drug loading contents in 7 days interval in PBS pH 7.4 at 37°C..... 63

4.12 The amount of drug released profiles of TCH from the blend films with various drug loading contents in PBS pH 7.4 at 37°C..... 63

4.13 The dissolution profiles of TCH from the 5% drug-loaded films with various copolymers in 7 days interval in PBS pH 7.4 at 37°C..... 65

Figure **Page**

A1 ^{1}H NMR spectrum of L-lactide..... 77

A2 ^{1}H NMR spectrum of P(LA-*co*-CL) prepared by using 1,4-butanediol as co-initiator with similar arm length..... 78

A3 ^{1}H NMR spectrum of P(LA-*co*-CL) prepared by using pentaerythritol as co-initiator with similar arm length..... 79

A4 ^{1}H NMR spectrum of P(LA-*co*-CL) prepared by using D-sorbitol as co-initiator with similar arm length..... 80

A5 ^{1}H NMR spectrum of P(LA-*co*-CL) prepared by using 1,4-butanediol as co-initiator with similar molecular weight..... 81

A6 ^{1}H NMR spectrum of P(LA-*co*-CL) prepared by using pentaerythritol as co-initiator with similar molecular weight..... 82

A7 ^{1}H NMR spectrum of P(LA-*co*-CL) prepared by using D-sorbitol as co-initiator with similar molecular weight..... 83

A8 The chromatogram of P(LA-*co*-CL) prepared by using 1,4-butanediol as co-initiator with similar arm length..... 84

A9 The chromatogram of P(LA-*co*-CL) prepared by using pentaerytritol as co-initiator with similar arm length..... 84

A10 The chromatogram of P(LA-*co*-CL) prepared by using D-sorbitol as co-initiator with similar arm length..... 85

A11 The chromatogram of P(LA-*co*-CL) prepared by using 1,4-butanediol as co-initiator with similar molecular weight..... 85

A12 The chromatogram of P(LA-*co*-CL) prepared by using pentaerythritol as co-initiator with similar molecular weight..... 86

Figure **Page**

A13 The chromatogram of P(LA-*co*-CL) prepared by using D-sorbitol as co-initiator with similar molecular weight..... 86

A14 DSC chromatogram of P(LA-*co*-CL) prepared by using 1,4-butanediol as co-initiator with similar arm length..... 87

A15 DSC chromatogram of P(LA-*co*-CL) prepared by using pentaerytritol as co-initiator with similar arm length..... 87

A16 DSC chromatogram of P(LA-*co*-CL) prepared by using D-sorbitol as co-initiator with similar arm length..... 88

A17 DSC chromatogram of P(LA-*co*-CL) prepared by using 1,4-butanediol as co-initiator with similar molecular weight..... 88

A18 DSC chromatogram of P(LA-*co*-CL) prepared by using pentaerythritol as co-initiator with similar molecular weight..... 89

A19 DSC chromatogram of P(LA-*co*-CL) prepared by using D-sorbitol as co-initiator with similar molecular weight..... 89

C1 Calibration curve of tetracycline hydrochloride in PBS at 276.7nm..... 94

LIST OF SCHEMES

Scheme **Page**

2.1 The proposed reaction pathway for the ROP of a cyclic ester by the coordination-insertion mechanism..... 10

2.2 Production of L-lactide by dehydration 2 molar of lactic acid..... 11

2.3 The main ROP mechanism proposals with $Sn(Oct)_2$ as catalyst, (a) complexation of a monomer and alcohol prior to ROP and (b) formation of a tin-alkoxide before ROP of cyclic ester..... 14

3.1 Synthesis of low molecular weight poly(L-lactide)..... 29

3.2 Ring formation of L-lactide..... 30

3.3 Polymerization of P(LA-*co*-CL)..... 32

LIST OF ABBREVIATIONS AND SYMBOLS

°C	degree celsius
nm	nanometer
µm	micrometer
mm	millimeter
cm	centimeter
cm^2	square meter
M	molar
N	normal
µl	micro-liter
ml	milli-liter
ppm	parts per million
LA	L-lactide
CL	ε-caprolactone
LMW	low molecular weight
P(LA-*co*-CL)	poly(lactide-*co*-caprolactone)
ROP	ring-opening polymerization
PCL	poly(ε-caprolactone)
PLLA	poly(L-lactide)
CH	chitosan
T_g	glass transition temperature
^{1}H NMR	proton nuclear magnetic resonance spectroscopy
GPC	gel permeation chromatography
DSC	differential scanning calorimetry
SEM	scanning electron microscopy
UV-VIS	ultraviolet visible
$Sn(Oct)_2$	stannous(II) 2-ethylhexanoate
DAD	dialdehyde dextran
T_a	temperature of application
T_b	body temperature
TCH	tetracycline hydrochloride
g	gram
mg	milligram

µg	microgram
BD	1,4-butanediol
PTOL	pentaerythritol
SB	D-sorbitol
MHz	megaHertz
δ	chemical shifts
$\overline{M}_w$	molecular weight average by weight
$\overline{M}_n$	molecular weight by number
PDI	polydispersity
THF	tetrahydrofuran
$CHCl_3$	chloroform
min.	minute
h.	hour
v/v	volume by volume
w/w	weight by weight
kV	kilovolt
PBS	phosphate buffer saline
rpm	rounds per minute
OH	hydroxyl group
AFS	adhesive failure strength
N/cm	Newton per centimeter width

CHAPTER I

INTRODUCTION

1.1 Introduction

The skin is often known as "the largest organ of the human body". The skin is composed of two major layers of tissue. The outer epidermis which provides protection, and prevents micro-organisms from entering the body. The inner dermis, which is composed of blood vessels and accessory structures (hair, nails, sweat glands, and sebaceous glands), and collagen fibres and elastin which give the skin its strength and flexibility. Therefore, the skin is damaged easily, for example, the skin is torn, cut or punctured (an *open* wound), or where blunt force trauma causes a contusion (a *closed* wound). When skin wounds occur, from the understanding of the wound healing process, wound management aids are important in promoting wound healing. Wound management is performed by initial cleansing and debridement after antiseptic procedures have been completed the wound was covered with dressing to stop bleeding and preventing wound infection (Forter *et al.*, 1995). Wound management has several methods for example, use of wound dressing such as gauze-based dressings, paste bandages, suturing or stapling the tissue.

Lactide-based polymers are widely utilized in a variety of biomedical applications including surgical fixation devices and controlled drug delivery (Agrawal *et al.*, 2006; Gallardo *et al.*, 1998; Lee *et al.*, 2005; Peppas, 1997 and Wang *et al.*, 2002). The use of lactide-based polymers as bioadhesives for human tissue is emerging as a preferred alternative to suturing. An ideal tissue adhesive must have sufficient viscosity prior to use; thus, adheres to the tissue substrates rapidly. Additionally, the adhesive should biodegrade without side effect or systematic toxicity, and must provide strong and complete closure throughout the healing process (Cohn *et al.*, 2004 and Reece *et al.*, 2001). The existing adhesives in clinical use such as fibrin sealants, albumin-based compounds, cyanoacrylates, hydrogels (polyethylene glycol polymers), collagen-based adhesive (Montanaro *et al.*, 2001). Although

surgical adhesives have performed satisfactorily in many instances, each material has limitations.

Fibrin sealants and albumin-based compounds, show substantially lower mechanical bonding capabilities and they are manufactured from human blood or plasma, the menace of the transmission of infective agent cannot be completely ruled out.

Alkyl cyanoacrylates, which cure rapidly and form strong tissue joints, are often toxic to tissue and elicit dose-dependent carcinogenicity (Cohn *et al*., 2004 and Reece *et al*., 2001).

In earlier research, tissue adhesives have been developed in several forms (English *et al.*, 1989 and Mai-ngam *et al*., 2005). But those methods have shown several drawbacks including:

- Synthesis process and application are complicate.
- Their polymerization reaction is noticeably exothermic and may result in thermal damage to tissues.

Co-oligomers consisting of l-lactide (LA) (Fig.1 (a)) and ε-caprolactone (CL) (Fig.1 (b)) using trimethylolpropane (TMP) as co-initiator, are prepared as tissue adhesives that do not entail any chemical reaction during their application, their use being based solely on their temperature-dependent rheological behavior (Cohn *et al*., 2004), adhesive property depended on lactide component and chain entanglement.

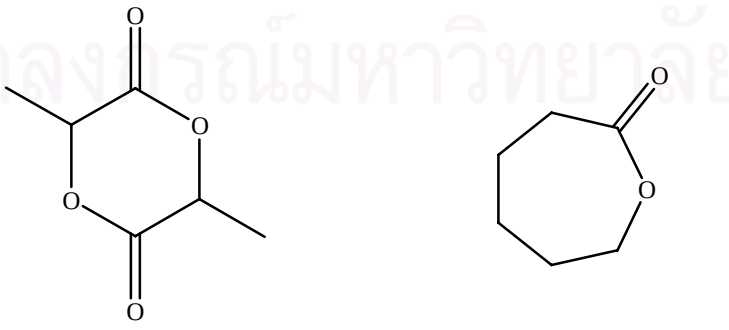

(a) (b)

Figure 1.1 Structures of (a) L-lactide and (b) ε-caprolactone.

This research focuses on development of copolymer from biocompatible and biobased monomer for use as tissue adhesive and drug release system.

Antibiotics drug, substance that prevent the growth or reproduction of bacteria within the body and reduced many inflammation because of infection, was selected as a model drug. By applying antibiotics on tissue adhesive film or wound dressing patch, this could help reduce many bacterial infections both in small wound such as incision wound, acne wound and large wound such as burn wound, postoperative wound. In addition copolymer with adhesive property can help enhance scab formation comparing with traditional wound dressing management simple which is done by applying antibiotic on wound and covering with dressing such as gauze dressing to provide wound protection from the external environment during the formation of the scab, it was expected that copolymer used in this study helps protect wound from dryness and injury during daily cleansing. Since, gauze dressing is a dry dressing which interfere growing epithelial cells on a wound when opening it, therefore causing injury during wound cleansing.

In this work, we have attempted to synthesize low molecular weight poly(L-lactide-*co*-ε-caprolactone) by ring-opening polymerization (ROP). The effect of co-initiator was investigated. It was expected that the obtained copolymer would have glass transition temperature (T_g) approximately at 20-25°C and the viscosity of the copolymer could have changed with the temperature; therefore, at body temperature the copolymer adhesive could hold the injured tissue together. After the preparation, the biodegradable and biocompatible copolymer was evaluated as a new tissue adhesive and drug release system. Tetracycline was selected as a model drug due to its application to treat a wide range of infections.

1.2 Objectives

1. To synthesize low molecular weight poly(L-lactide-*co*-ε-caprolactone) using different type of co-initiator.

2. To characterize the resulting copolymer by ^{1}H NMR, GPC and DSC.

3. To study the adhesive properties of copolymer.

4. To study the *in vitro* drug release of tetracycline.

1.3 Scope of research

In this research, the activities involved in synthesis of low molecular weight poly(L-lactide-*co*-ε-caprolactone) that would be as tissue adhesive and tetracycline drug release as follows:

1. Literature survey.

2. Synthesis of low molecular weight poly(lactide-*co*-caprolactone).

    - Synthesis of lactide
    - Synthesis of poly(lactide-*co*-caprolactone) by ring-opening copolymerization using different co-initiator.
        i. Butanediol
        ii. Pentaerythritol
        iii. Sorbitol as co-initiator.

3. Characterization of copolymer by ^{1}H NMR, GPC and DSC techniques.

4. Preparation and characterization of copolymer/chitosan film.

5. Determination of adhesive property of copolymer by T-peel test.

6. *In vitro* drug release of tetracycline.

CHAPTER II

THEORY AND LITERATURE REVIEWS

2.1 Block copolymer (Kumar *et al*., 2001)

Copolymers are defined as polymers composed of several different monomer units and are classified into four types by monomer placement namely, random copolymers, alternating copolymers, graft copolymers and block copolymers (Yokoyama, 1992).

Random polymers are the statistical arrangement of copolymer having repeating units in their backbone. Alternating copolymers are synthesized by the alternate placement of monomers. Both block and graft copolymers are composed of several segments and they differ in the intersegment linkage site as graft copolymers are defined by chemically linked pair of homopolymers, while block copolymer are composed of terminally connected structures and thus, graft polymers have a comb type structure as shown in Figure 2.1. The focus in this review is on the block copolymer.

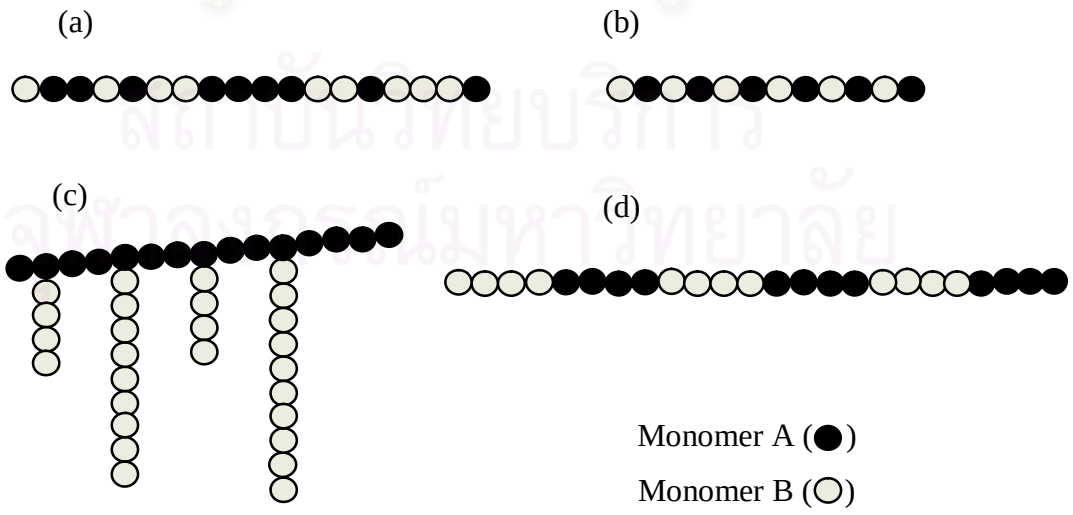

Figure 2.1 Structures of (a) random, (b) alternating, (c) graft and (d) block copolymer.

2.1.1 Classification of block copolymers

The block copolymers have received much attention, since the different homopolymer properties are maintained in the block copolymer, and this allows easy modification of the polymer characteristics (Stridsberg *et al*, 2002). Block copolymers are classified into several types by sequential arrangement of component segment including:

a) The simplest block copolymer is AB-type block copolymer, which is composed of one segment of A unit of homopolymer with B units of other homopolymer (Figure 2.2 (a)).

b) Both terminals of B unit are connected at the terminal of A unit, and thus, it is referred to as an ABA type block copolymer (Figure 2 (b)).

c) A and B segment is connected many times and referred to as a multiblock copolymer (Figure 2.2 (c)).

d) Star-shaped block copolymers. In this family of block copolymers, unit A has multi-arm functionality and copolymerize with the blocks of B and shows a star-like shape. The number of arms of the star-shaped block copolymers depends on the number of functional groups on block A (Figure 2.2 (d)).

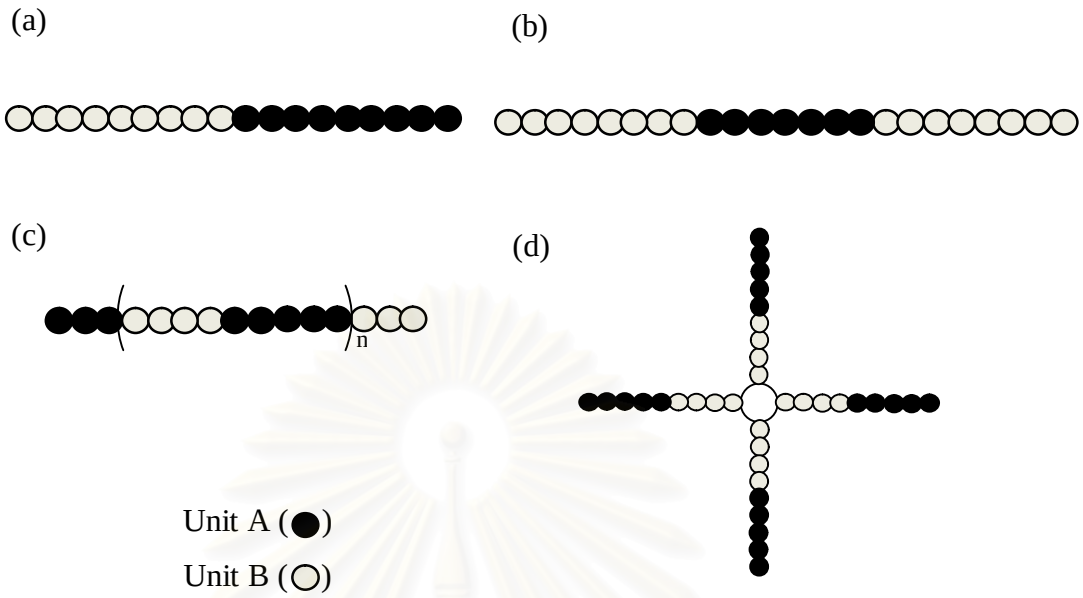

Figure 2.2 A schematic presentation of (a) AB di-block, (b) ABA tri-block, (c) $(AB)_n$ multiblock and (d) star-shaped block copolymer.

2.1.2 Synthetic methods of block copolymers

The synthesis of block copolymers exhibits well-defined properties and structure, the pre-requisite for biodegradation having requisite properties, and to achieve these aims, the synthetic structure leading to copolymers should comply the following:

- The molecular weight of backbone chain/arm of star-shaped block copolymers along with the single unit block is adjustable;
- The copolymers, polymer block and arms of star-shaped block have a very narrow molecular weight distribution;
- The type, number and arrangement of the polymer blocks and arms of star-shaped block are known;

- The chemical structure can be analyzed exactly and is as uniform as possible;

- The polymer does not contain non-removable impurity e.g. homopolymers, starting components having low molecular weight etc.

Block copolymers can be polymerized by a large of well known polymerization techniques, including anionic, radical, cationic, ring-opening, photo, group transfer and Ziegler/Natta polymerization. The most widely used technique is living polymerization, in which the molecular weight of the individual blocks (variation of initiator/monomer ratio), the volume ratio (variation of monomer/monomer ratio), as well as the block arrangement (AB, ABA, BAB), can be adjusted in a desired manner. The most widely used techniques to synthesize block copolymers are as follows:

Sequential addition of the monomer

This is the most widely used technique with a possibility to synthesize AB, ABC and ABA by using monofunctional initiating system and BAB and CBABC by using bifunctional initiator.

Addition of the monomers at the same time

This method is applicable when reactivity of the monomers is different and permits a mono and bifunctional initiation (Ferruti *et al*, 1995; Penco *et al*, 1996). Due to different reactivities of monomer, polymerization of second monomer starts just after the completion of polymerization of more reactive first monomer. This variant is applicable only if the polymerization parameter of the monomers is different otherwise it will proceed to gradient polymers.

Coupling of homo- or block copolymers

Coupling of terminal functionalized homo- and block copolymers can be used to synthesize AB, ABA and star-shaped block copolymers. However, a successful synthesis is dependent on several preconditions such as: The coupling reaction proceeds completely and without any side-reaction; A 100% end group functionality of copolymers is a necessary condition to approach a complete coupling reaction; Both types of homopolymers are available in the exact mole ratio of the functional end groups. There are many types of initiators, which can induce the living polymerization, among them, anionic initiators are representative ones due to long history of studies and actual applications to polymer industries.

Site transformation technique

Recently, site transformation technique has been applied to synthesize the block copolymers in which monomers with completely different chemical structures can be polymerized by sequential addition with a change in the polymerization technique (Kitayama *et al*, 1991)

2.2 “Coordination-insertion” ring-opening polymerization

The coordination-insertion mechanism, also known as pseudoanionic ring-opening polymerization, involves the coordination of a monomer at the carbonyl oxygen to active species (Zhong *et al*., 2001). This coordination enhances the electrophilicity of the C-O group and the nucleophilicity of the OR group, hence, allowing “insertion” of monomer into the metal-oxygen bond to occur (Mecerreyes *et al*., 1999).

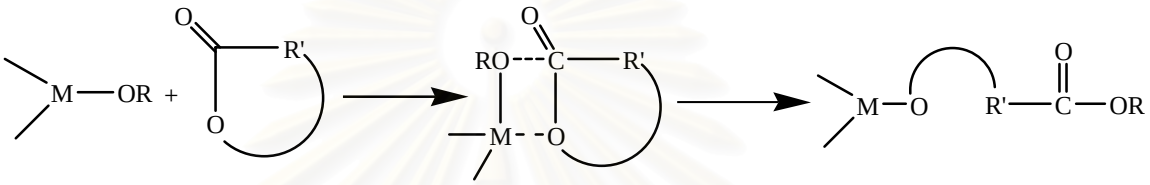

Scheme 2.1 The proposed reaction pathway for the ROP of a cyclic ester by the coordination-insertion mechanism.

Scheme 2.1 shows a schematic presentation of the coordination-insertion mechanism. The growing chain remains attached to the metal through an alkoxide bond during the propagation. The reaction is terminated by hydrolysis forming a hydroxyl end group. With functional alkoxy-substituted initiators, macromers with end groups active in post-polymerization reactions are produced (Stridsberg *et al*, 2002).

The coordination-insertion type of polymerization has been thoroughly investigated since it possibly yields well-defined polyesters through living polymerization. When two monomers of similar reactivity are used, block copolymers can be formed by sequential addition to the living system.

2.3 Poly(lactide-*co*-caprolactone)

2.3.1 Lactide

A cyclic dimer of lactide produced from the dehydration of lactic acid. When dilactide is prepared from racemic lactic acid, the three isomers that result are D-lactide, L-lactide and *meso*-lactide.

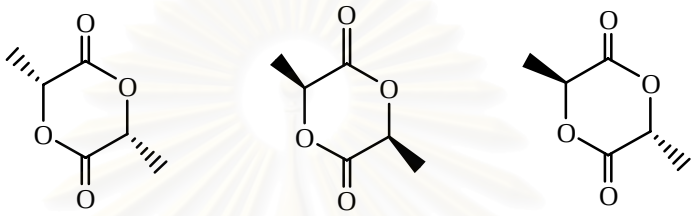

Figure 2.3 The structures of lactide in different stereoisomer.

The meso isomer can be removed, but D and L-lactide are enantiomers that comprise the racemic form, *rac*-lactide. When *rac*-lactide is polymerized with simple catalysts, an amorphous polymer results from an essentially random incorporation of D and L-lactide units in the growing chain. Since the properties of the racemic polymer are not suitable for most practical applications, commercial processes presently utilize L-lactide produced from L-lactic acid.

Scheme 2.2 Production of L-lactide by dehydration 2 molar of lactic acid.

2.3.2 Caprolactone

Caprolactone is a cyclic ester, known as a lactone, with a ring size of seven. It is a clear colorless liquid that is miscible with most organic solvents except aliphatic hydrocarbons. It reacts slowly with water to form 6-hydroxyhexanoic acid. Caprolactone is prepared by oxidation of cyclohexanone with peracetic acid.

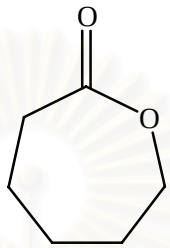

Figure 2.4 The structure of caprolactone.

The lactone ring is easily opened with nucleophiles including alcohols and water. Caprolactone is a monomer used in the manufacture of various polymers including polycaprolactone. It is also used in synthetic fibers, polyurethane elastomers, plastics, adhesive fabrics, and coatings.

2.3.3 Catalyst/Co-initiator systems for the ring-opening polymerization of lactides and lactones

Multivalent metal (Al, Fe, Ti, Sn, Y) alkoxides and covalent metal carboxylates such as stannous(II) 2-ethylhexanoate are the two main classes of initiators currently utilized for the synthesis of biodegradable aliphatic polyesters and their copolymers. Stannous and aluminum alkoxides are the most widely used initiators for the preparation of well-defined aliphatic polyesters of controllable molar mass and narrow molar mass distributions.

Stannous(II) 2-ethylhexanoate ($Sn(Oct)_2$)

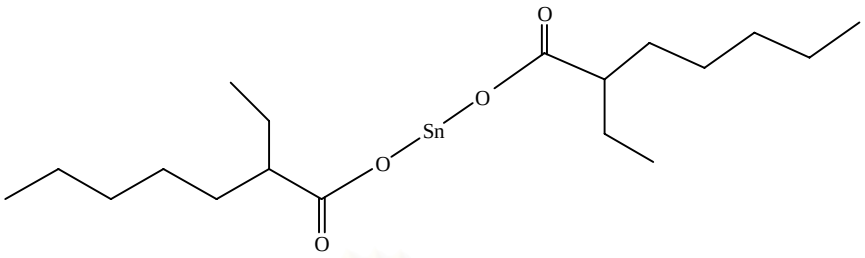

Figure 2.5 The structure of stannous(II) 2-ethylhexanoate.

Stannous(II) 2-ethylhexanoate or tin (II) 2-ethylhexanoate, commonly refered to stannous octoate ($Sn(Oct)_2$), is a frequently used catalyst in the ROP of lactones and lactides. $Sn(Oct)_2$ has been approved as a food additive by the American Food and Drug Administration (FDA) (Kricheldorf *et al.*, 1995). The mechanism of polymerization has been widely discussed. Despite several proposals over a long period of time, until now the ROP mechanism has not been elucidated. The $Sn(Oct)_2$ is not thought to be the actual initiator since the molecular weight does not depend on the monomer to $Sn(Oct)_2$ molar ratio. The most promising mechanism is a coordination-insertion mechanism where a hydroxyl functional group is thought to coordinate to $Sn(Oct)_2$, forming the initiating tin alkoxide complex (Dutkeiwicz *et al.*, 2003 and Kricheldorf *et al.*, 1995). Unfortunately $Sn(Oct)_2$ chemistry also has its downsides, including difficulty in controlling the molecular weight of the polymer since any presence of water or other hydroxyl functionality is likely to initiate the system along with large amounts of transesterification reactions (Kricheldorf *et al.*, 1985).

Coordination-insertion mechanism can be proposed into two slightly different reaction pathways (Stridsberg *et al.*, 2002).

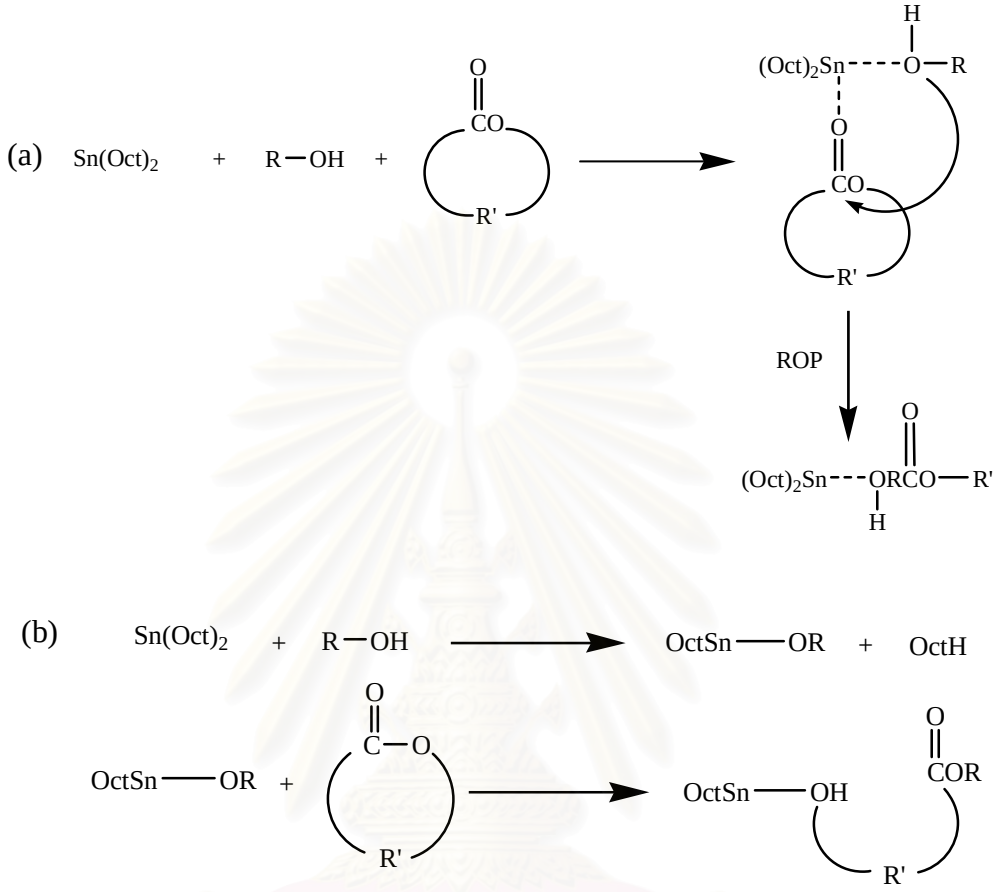

Scheme 2.3 The main ROP mechanism proposals with $Sn(Oct)_2$ as catalyst, (a) complexation of a monomer and alcohol prior to ROP and (b) formation of a tin-alkoxide before ROP of cyclic ester.

Scheme 2.3 shows two different mechanisms. In the first mechanism, the co-initiating alcohol functionality and the monomer are both coordinated to the $Sn(Oct)_2$ complex during propagation. Secondly, $Sn(Oct)_2$ complex is converted into a tin alkoxide before complexing and ring-opening of the monomer. Direct observation of this tin alkoxide complex has been reported by using MALDI-TOF spectrometry for both lactide and cyclic ester polymerization.

The $Sn(Oct)_2$ catalyst is a strong transesterification agent, and the resulting co-polymers normally have a randomized microstructure. The increasing of reaction

temperature or reaction time will also increase the amount of transesterification reactions.

The ROP of lactide with $Sn(Oct)_2$ is fairly slow and it is desirable for economic and commercial reasons to increase the rate of polymerization. The addition of an equimolar amount of triphenylphosphine was increased the rate, and as an additional advantage, this compound delays the occurrence of the undesirable back-biting reactions.

Co-initiator

Several mechanisms have been proposed for the $Sn(Oct)_2$ induced polymerization. According to the most recent results, $Sn(Oct)_2$ first reacts with compounds containing hydroxyl groups to form a tin alkoxide that acts an actual initiator in the polymerization. Hence, the use of alcohol as co-initiator increases the reaction rate of polymerization. The propagation is stopped via a chain transfer with another alcohol molecule, which causes the polymerization to yield hydroxyl-terminated polymers with molecule weight depending on the ratio of monomer to co-initiator (Korhonen *et al*., 2001).

However, the polymerizations with $Sn(Oct)_2$ are initiated by hydroxyl containing compounds. These hydroxyl-groups can either be purposely added to the reaction mixture or appear as impurities in the monomer or catalyst itself as a result of the production method and the fact that $Sn(Oct)_2$ is extremely hygroscopic (Kricheldorf *et al*., 1985).

The synthesis of star-shaped, biodegradable polymers using a wide variety of multifunctional hydroxy-terminated co-initiators such as pentaerythritol (Kricheldorf *et al*., 2005 and Korhonen *et al*., 2001) and dipentaerythritol (Choi *et al*., 2005) are extensively reported.

2.4 Tissue adhesive

2.4.1 Definition

Tissue adhesive can be broadly defined as any substance with characteristics that allow for polymerization. This polymerization must either hold tissues together or serve as a barrier to leakage. Some sources call them tissue glues, but the word *glue* confers expectations that tissue adhesives, as a group, are not designed to meet (Reech *et al*., 2001)

2.4.2 Development of tissue adhesive

Series of thermo-responsive chitosan-*g*-poly-*N*-isopropylacrylamide with different grafting compositions were synthesized to develop tissue adhesive that can be used easily. The association temperature of these copolymers (32.5-34°C) in water make them suitable candidates for utilizing as tissue adhesives. The liquid adhesives become solid after wound closure due to the body temperature (37°C) that exceeds their association temperature. To compose tissue adhesives, dialdehyde dextran (DAD) was used as a crosslinker (Mai-ngam *et al*., 2005)

A family of biocompatible and biodegradable lactide/caprolactone co-oligomer was synthesized (Cohn *et al*., 2004). Application of this tissue adhesive does not entail any chemical reaction during its application, its use being based solely on its temperature-dependent rheological behavior. Its working concept capitalizes on the behavior of specially designed, low molecular weight block copolymers that display low viscosity at the temperature of application (T_a) and become much more viscous once at body temperature (T_b). The initial low viscosity and substantial flowability exhibited by these materials at Ta; allow their straightforward application at the site of performance, displaying also enhanced conformability and better attachment to the tissues. The pronounced raise in viscosity these materials are required to exhibit as they cool down to physiological temperature, is a key requisite if these oligomers are to successfully perform as adhesives. Lastly, since biocompatibility and biodegradability are additional indispensable attributes, the

oligomers synthesized were tailored so that they as well as their degradation products, are non-toxic.

Since the performance of these adhesives is based on their temperature-dependent rheological behavior, special attention was given to the interdependence existing between temperature, molecular weight and rheological properties, as schematically plotted in Figure 2.6. Low molecular weight polymers have much lower viscosities and display a sharp decrease in viscosity at a temperature slightly above their typically low glass transition temperatures. Due to this behavior, low molecular weight polymers were selected.

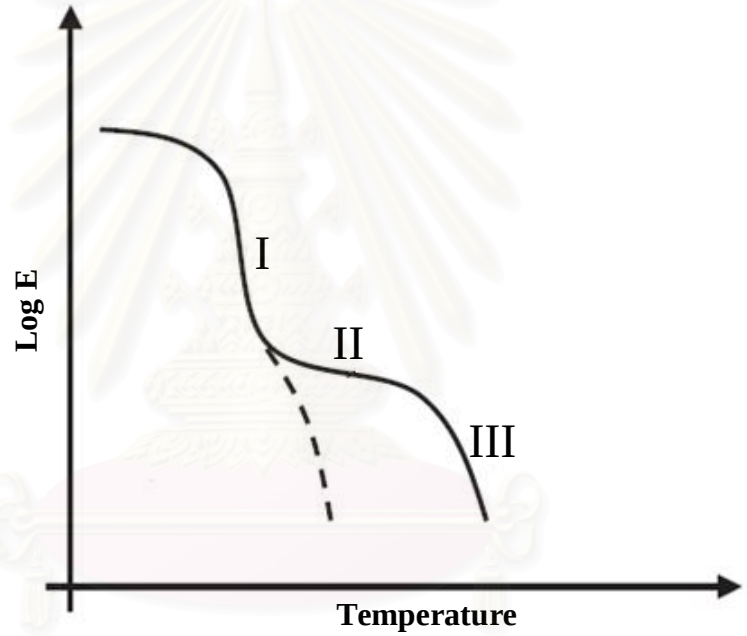

Figure 2.6 Schematic plot of the change in modulus as function of temperature.

2.5 Controlled drug release system

Controlled release may be defined as a technique or method in which active chemicals are made available to a specified target at a rate and duration designed to accomplish an intended effect. A definition perhaps more acceptable to the chemist and engineer may be:

Controlled release is the permeation-moderated transfer of an active material from a reservoir to a target surface to maintain a predetermined concentration or emission level for a specified period of time.

In its broadest sense, the concept of controlled or sustained release of biologically active agents has existed for over three decades. Early commercial applications of the technology occurred in both the pharmaceutical and agricultural industries.

2.5.1 Fundamental requirements for release system

There are several major factors to consider during the development of drug delivery system. Biocompatibility with the human environment is essential since the system is adhered to tissue. All agents must be chemically inert, noncarcinogenic, hypoallergenic, and mechanically stable. If proper biocompatibility is not achieved, many untoward effects can occur such as capsular contracture, unexpected release of the drug, tissue damage, or infection of the area surrounding applied (Dash *et al*., 1998)

2.5.2 Advantages of controlled release

Controlled release system provides numerous benefits over conventional dosage form. Controlled release dosage forms are able to control the rate of drug delivery, the target area of drug administration and maintain therapeutic levels of drug with narrow fluctuations (Figure 2.7) (Kim, 2000). That can reduce toxic and/or undesirable side effects of the drug. The serum concentration of drug released from controlled release dosage form fluctuates within the therapeutic range over a long period of time. Conventional therapies may require administration of the dosage form either one, two, or multiple times a day (Dash *et al*., 1998). That makes it possible to reduce the frequency of drug administration and improvement in treatment efficiency.

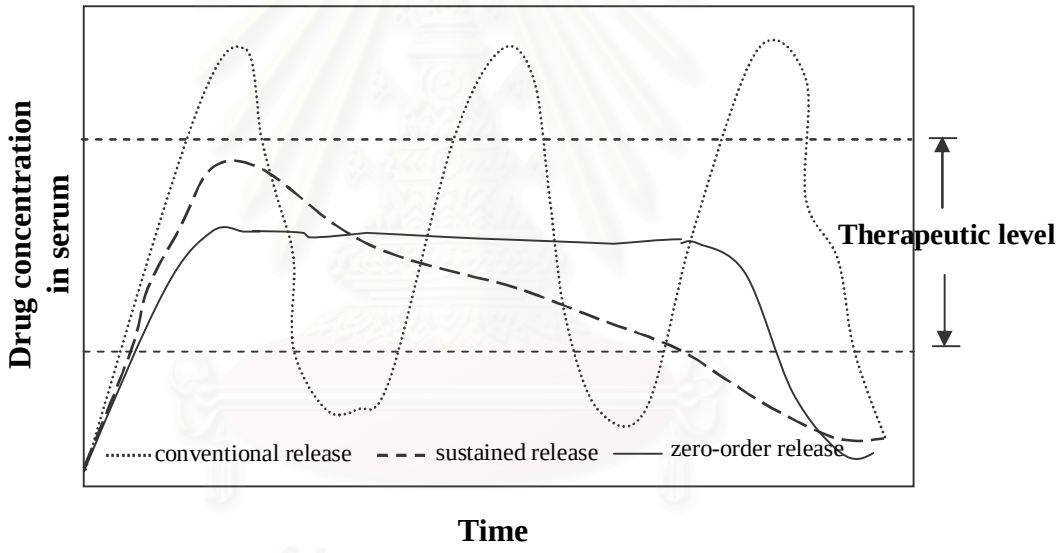

Figure 2.7 Hypothetical serum drug concentrations of various oral dosage forms.

2.5.3 Transdermal drug delivery system

All of technologies can classified into the four common configurations that used in transdermal drug delivery system as shown in Figure 2.8.

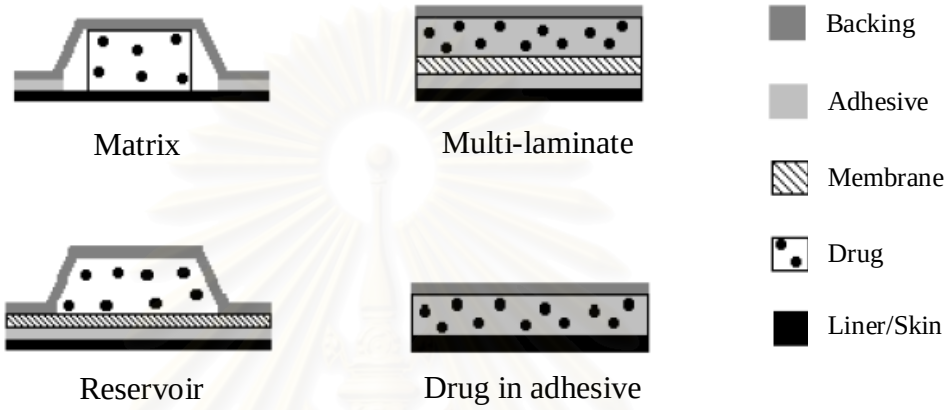

Figure 2.8 Basic approaches of patch constructions.

a) Reservoir, in which the drug is placed in liquid and delivered to the skin across a rate moderating membrane.

b) Matrix, in which the drug is placed within a non-adhesive polymeric material, typical a hydrogel or soft polymer.

c) Drug in adhesive, in which the drug is placed which in an adhesive polymer.

d) Multi-laminate, which is similar to the drug in adhesive design but which incorporates an additional layer of pressure sensitive adhesive to cover the entire patch and affix it to the skin.

2.5.4 Methods of achieving controlled release

There are five major types of controlled release device designs, as follow:

1) Dissolution-controlled systems
2) Diffusion-controlled systems
3) Biodegradable systems
4) Osmotic systems
5) Mechanical pumps

The choice of method for achieving controlled release in a particular application depends on a number of factors such as the coat, the potency and the properties of the agent, the environment of use, and any requirement for biodegradability. Perhaps the most critical factor is the release rate required. In the following sections, three of the more superior controlled release systems (1-3) will be described in details.

Dissolution-controlled systems

The sustained-release preparations of drugs could be made by decreasing their rate of dissolution. The approaches to achieve this include preparing appropriate salts or derivatives, coating the drug with a slowly dissolving material, or incorporating it into a tablet with a slowly dissolving carrier. Figure 2.9 (a) shows that the dissolution controlled systems can be made to be sustaining in different design.

Diffusion-controlled systems

In diffusion-controlled systems the active agent is homogeneously dissolved or dispersed throughout the polymer mass (Figure 2.9 (b)). The release pattern depends on the geometry of the system, the identity and nature of the polymer or other carrier material, and the loading of the agent.

Biodegradable systems

The diffusion-controlled devices previously outlined are permanent, in that the membrane or matrix of the device remains after its delivery role is completed. In some applications a device that degrades during or subsequent to its delivery role is required. Many polymer systems have been prepared that slowly biodegrade when placed in the body. With such polymers, it is, in principle, possible to program the release of an active agent by dispersing the material within the polymer, with erosion of the polymer effecting release of the agent. A typical system is shown on Figure 2.9 (c).

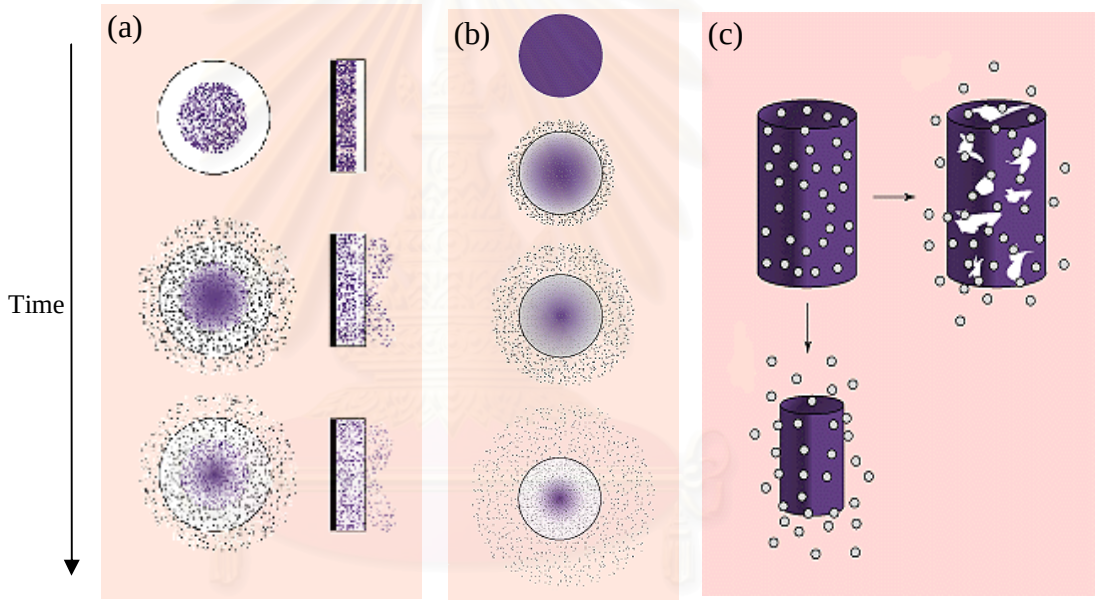

Figure 2.9 (a) Dissolution-controlled, (b) diffusion-controlled and (c) biodegradable systems (Peppas, 1997).

2.6 Tetracycline hydrochloride (TCH) as model drug

Tetracycline is a wide spectrum antibiotic affecting anaerobic and facultative organisms, gram-positive and gram-negative bacteria and mycoplasms, through potent bacteriostatic activity (Pataro *et al.*, 2003).

2.6.1 Physicochemical properties

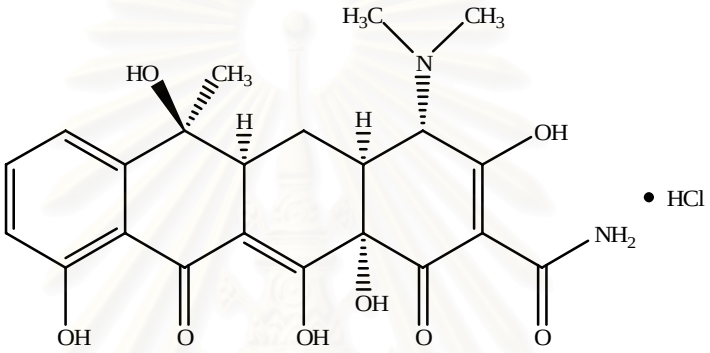

Figure 2.10 Chemical structure of tetracycline hydrochloride.

Solubility in water : Freely soluble, freely soluble in alkali hydroxide and carbonates solutions; sparingly soluble in alcohol; practically insoluble in chloroform and in ether.

Stability : Stable in air, but exposure to strong sunlight causes it darken. It loses potency in solutions of pH below 2 and is rapidly destroyed by alkali hydroxide solutions.

2.6.2 Uses and administration

Adults appointed on the inside of 0.25 g every 6 hours, if necessary, 2 g per day. Children over 7 years appoint 25 mg/kg every six hours. For treating moderate to severe acne, the TCH dosage is 125 mg to 500 mg twice daily.

2.6.3 Pharmacokinetics

Bioavailabilities are approximately 60-80% via oral. The presence of food or dairy products can significantly reduce the amount of TCH absorbed, with reductions of 50% or more possible. However, bioavailabilities are less than 40% via intramuscular. TCH as a class, are widely distributed to heart, kidney, lungs, muscle, pleural fluid, bronchial secretions, sputum, bile, saliva, urine, synovial fluid, ascitic fluid, and aqueous and vitreous humor. TCH cross the placenta, enter fetal circulation and are distributed into milk.

TCH are eliminated unchanged primarily via glomerular filtration. Patients with impaired renal function can have prolonged elimination half-lives and may accumulate the drug with repeated dosing. These drugs apparently are not metabolized, but are excreted via both biliary and nonbiliary routes and may become inactive after chelation with fecal materials. The elimination half-life of TCH is approximately 6-11 hours.

2.6.4 Adverse effects

TCH side effects may include nausea, fever, diarrhea, vomiting, loss of appetite, pain in the abdomen, constipation, allergic reactions (skin rashes, itching) and photosensitization (increased skin sensitivity to sunlight). However, children given TCH therapy for even short periods can develop permanent yellow/gray staining of teeth and bones (Pataro *et al.*, 2003).

2.7 Chitosan

Chitosan, a polycationic biopolymer, was discovered by Rouget in 1859 and gave a name by Hoppe-Seyler in 1894 (Pual *et al*., 2000). It is generally obtained by alkaline deacetylation of chitin, which is the second abundant polysaccharide next to cellulose. Chitin is the principal component of protective cuticles of crustaceans such as crabs, shrimps, lobsters, prawns and cell walls of some fungi such as *aspergillus* and *mucor*. In plants, chitin is present in hyphae or spores of molds (Sigha *et al*, 2004).

2.7.1 Structure of chitosan

Chitosan $(C_6H_{11}O_4N)_n$, a natural linear biopolyaminosaccharide, is a copolymer of β-[1-4]-linked 2 –acetamido-2-deoxy-D-glucopyranose and 2-amino-2-deoxy-D-glucopyranose. It has one primary amine group and two free hydroxyl groups for each C6 building unit (Figure 2.11). Both reactive primary amine and hydroxyl group can be used to chemically alter its properties under mild reaction conditions. The polymer differs from chitin in that a majority of the N-acetyl groups in chitosan are hydrolyzed. The degree of hydrolysis (deacetylation) has a significant effect on the solubility and rheological properties of the polymer. The amine group on polymer has a pKa in the range of 5.5 to 6.5, depending on the source of the polymer. At pH below 6.5 (dilute acid solution), chitosan is soluble as the glucosamine units can be converted into a soluble form ($R\text{--}NH_3^+$). It gets precipitated in alkaline solution (pH above 7) or with polyanions. The pH-sensitivity, coupled with the reactivity of the primary amine groups, make chitosan a unique polymer for oral drug delivery applications.

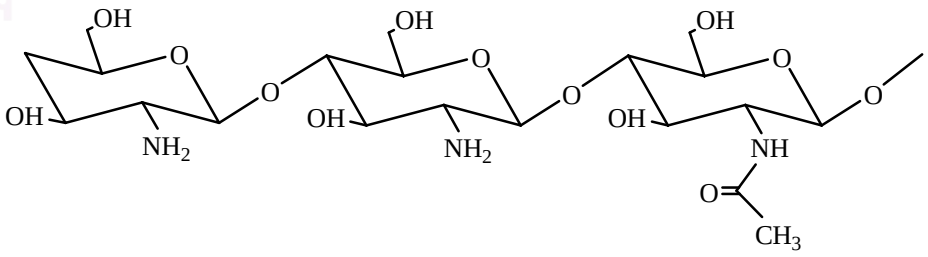

Figure 2.11 Chemical structure of chitosan.

2.7.2 Chitosan in pharmaceutical application

Chitosan has been considerable interesting in the medical and pharmaceutical fields. In addition to the good biocompatibility, biodegradability and low toxicity of chitosan, it has a number of desirable properties that make study of it interesting. Indeed, chitosan is known for it is polycationic polymer, forming gels most readily in acidic environments, such as that in the stomach. This makes chitosan interesting in relation to the development of slow release dosage forms for oral administration.

Chitosan were widely prepared for controlled drug release. Monolayer multilayer composite systems were prepared. Monolayer composite systems made of ipriflavone loaded poly(lactide-*co*-glycolide) (PLGA) micromatrices in a chitosan film form, were obtained by emulsification/casting/evaporation technique. Multilayer films, made of three layers of polymers (chitosan/PLGA/chitosan) compared to monolayer films for their *in vitro* characteristics. Significant differences in swelling, degradation and drug release were highlighted, depending on film structure and composition. *In vitro* experiments demonstrated that the composite micromatricial films represent a suitable dosage form to prolong ipriflavone release for 20 days (Perugini *et al.*, 2003).

In 2007, chitosan film containing fucoidan was investigated its suitability for the treatment of dermal burns on rabbits (Szer *et al*., 2007) and novel wound dressings composed of chitosan film and minocycline hydrochloride were prepared (Aoyagi *et al*., 2007). Chitosan also promotes wound and burn healing properties, enhances the functions of inflammatory cells such as polymorphonuclear leukocytes, macrophages, fibroblasts and it is beneficial for the large open wounds of animals.

Therefore, copolymer/chitosan matrix system could promote wound healing and prolong drug release for wound healing interval.

CHAPTER III

EXPERIMENTAL

3.1 Materials

All of the AR grade chemicals and L-lactic acid from the suppliers were used without further purification. Commercial grade solvents were distilled before use.

Chemical	*Grade*	*Company*
L-lactic acid	Commercial grade	Archer Daniels Midland
Zinc powder	AR grade	Merck
ε-Caprolactone	AR grade	Aldrich
1,4-Butanediol	AR grade	Fluka
Pentaerythritol	AR grade	Sigma
D-Sorbitol	AR grade	Aldrich
Stannous(II) 2-ethylhexanoate	AR grade	Sigma
Ethyl acetate	Commercial grade	U&V
Methanol	Commercial grade	CAL
Chloroform	AR grade	Merck
Dichloromethane	Commercial grade	Merck
Tetrahydrofuran	HPLC grade	Fischer
Acetone	Commercial grade	LBS
Ethanol	AR grade	Merck
Chloroform-d	AR grade	Merck
Chitosan	-	TMECO
Acetic acid glacial 100%	AR grade	Merck
Glycerin	AR grade	J.T. Baker
Tetracycline hydrochloride	AR grade	Sigma
Phosphate buffer saline (PBS)	AR grade	Fluka
Nitrogen gas	High purity 99.99%,	Thai Industrial Gas

3.2 Instruments/Equipments

Instruments/Equipments	*Model*	*Company/Country*
Electronic balance	: FX180 : FX-3000	A&D, Japan
Nuclear Magnetic Resonance Spectrometer (NMR)	: Varian mercury-400 spectrometer	Varian, USA
Gel Permeation Chromatograph (GPC)	: Waters 150-CV Degas: ERC-3415α Column: Waters Styragel HR columns (HR 1, 3, and 4), PL-gel 10 µm Pump: Waters 600 Controller Refractive Index Detector: Waters 2414	Waters, USA
Differential Scanning Calorimeter (DSC)	: NETZSCH DSC204F1 Phoenix	Phoenix, USA
Centrifuge	: KR-20000T	Shimadzu, Japan
Vacuum Drying Oven	: DP 41	Yamato Scientific, Japan
Tensile tester	: 5583	Instron, USA
Micrometer	-	Matui

Instruments/Equipments	*Model*	*Company/Country*
Micropipette (100-1000 µl)	: Volumate	Mettler Toledo
Rotary incubator shaker	: G-25	New Brunswick Scientific Co., Inc. U.S.A.
Scanning electron microscope	: JSM-5800 LV	Jeol, Japan
UV-VIS Spectrophotometer	: UV-160	Shimadzu, Japan

3.3 Methodology

3.3.1 Synthesis of lactide

L-lactide synthesis was divided into two steps. The first step was to produce low molecular weight PLLA and the second step was L-lactide ring formation by decomposition of low molecular weight PLLA.

3.3.1.1 Synthesis of low molecular weight polylactide

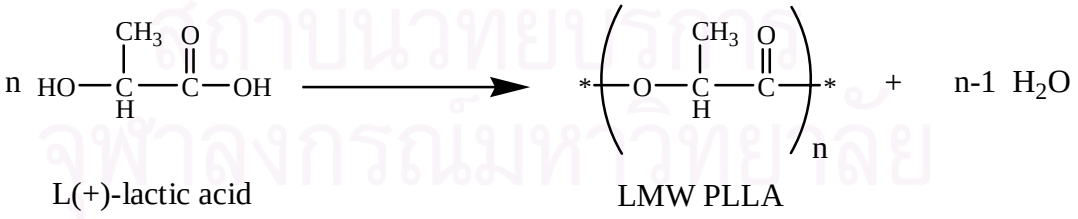

L(+)-lactic acid LMW PLLA

Scheme 3.1 Synthesis of low molecular weight poly(L-lactide).

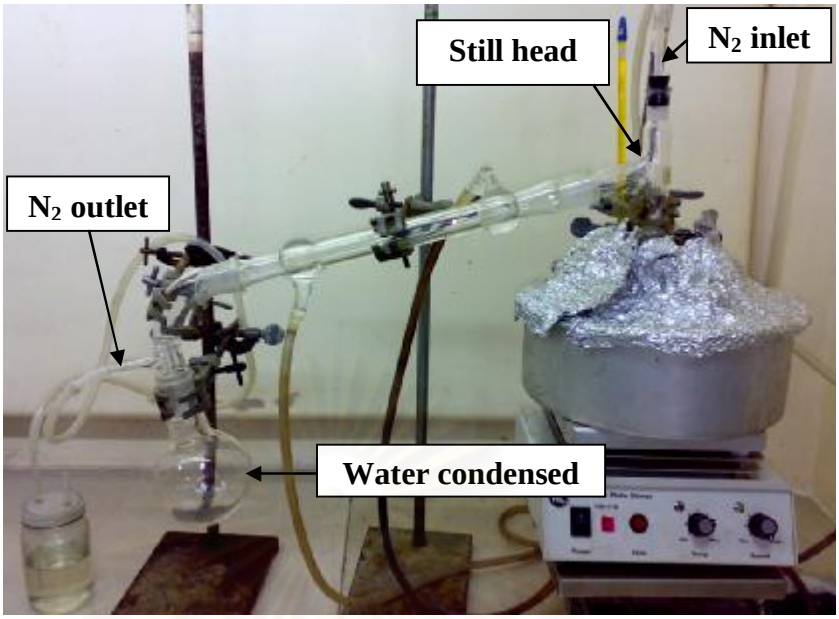

Figure 3.1 Experimental set up for low molecular weight PLLA synthesis.

First L-lactic acid solution (150 g) was heated at 140°C for 2 hours under a dry nitrogen atmosphere. High vacuum was applied in this step for 30 minutes to remove water which initially presented in L-lactic acid solution and obtained from polymerization. Later, the reaction mixture was heated to 160°C for 3 hours and no water was condensed to obtain low molecular weight PLLA.

3.3.1.2 Ring formation of L-lactide using zinc powder as a catalyst

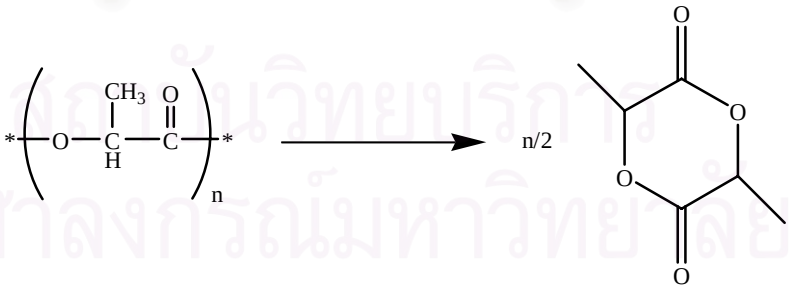

LMW PLLA L-lactide

Scheme 3.2 Ring formation of L-lactide.

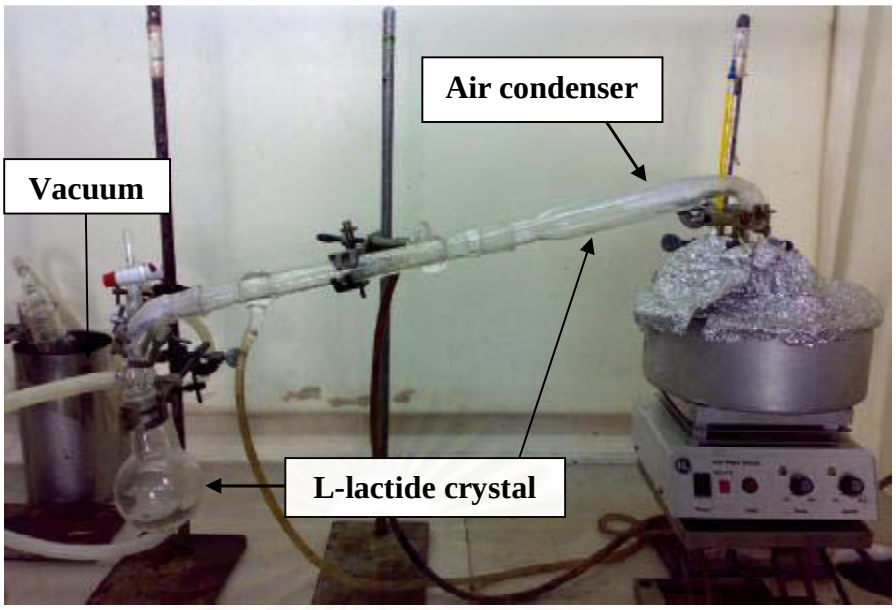

Figure 3.2 Experimental set up for L-lactide ring formation.

In this step, low molecular weight of polylactide was heated with zinc (weight ratio of catalyst to low molecular weight polylactide is 1/100) at 160^{o}C for 30 minutes. After that high vacuum was applied and the reaction mixture was heated to 220-230^{o}C until L-lactide crystal was formed. The L-lactide crystal was removed and washed with cold de-ionized water to remove excess L-lactic acid and then vacuum filtered. L-lactide crude was purified by dissolved in warm ethyl acetate to remove insoluble materials and filtered. The filtrate was then heated to evaporate the remaining ethyl acetate and precipitate white needle-like crystal of L-lactide. L-lactide crystal was purified for 3 times and dried in vacuum oven for 24 hours before use.

3.3.2 Synthesis of low molecular weight poly(lactide-*co*-caprolactone) using stannous(II) 2-ethylhexanoate as catalyst

Low molecular weight copolymers of L-lactide (LA) and ε-caprolactone (CL) were synthesized using the following equation.

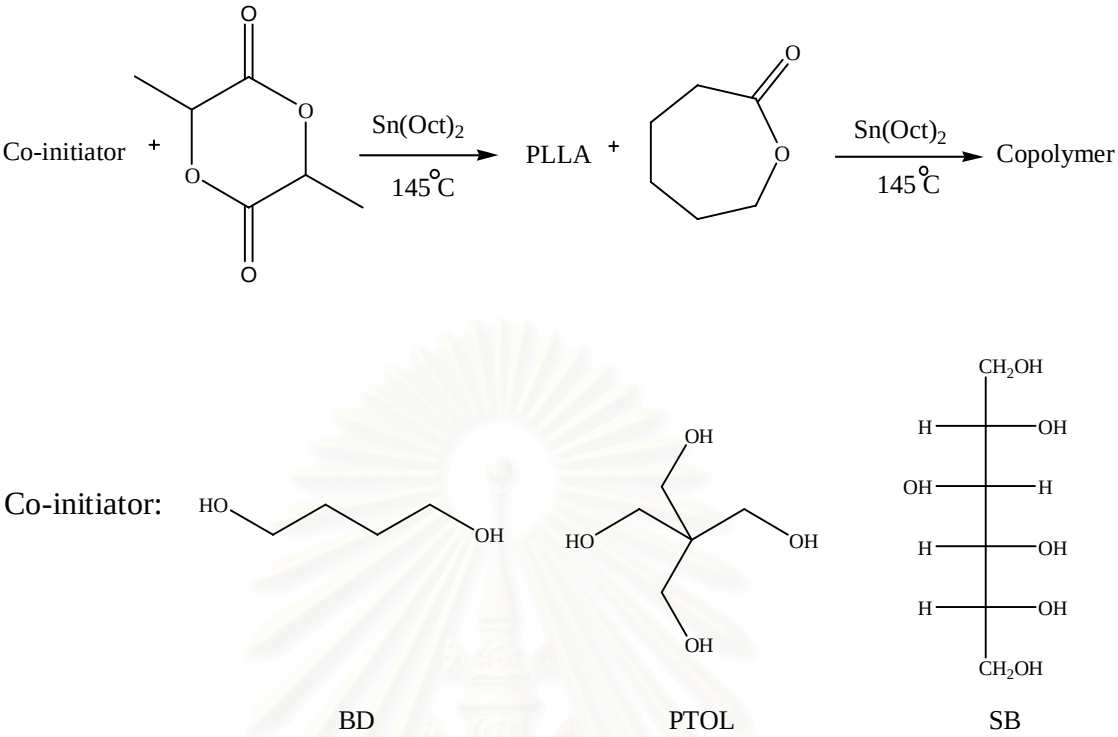

Scheme 3.3 Polymerization of P(LA-*co*-CL).

All copolymerizations were prepared using alcohols with different numbers of hydroxyl groups (1,4-butanediol (BD), pentaerythritol (PTOL) and D-sorbitol (SB)) as co-initiator by step-by-step ring opening polymerization. L-lactide and co-initiator was added to 25 ml three-neck round bottomed flask containing a magnetic bar and sealed with a rubber septum. The reaction was carried out at 145°C for 150 minutes per block under a dry nitrogen atmosphere. Stannous(II) 2-ethylhexanoate ($Sn(Oct)_2$) in toluene was added at a 1/400 catalyst/lactone molar ratio when the monomer was melt. When reaction was finished, ε-caprolactone was added to the reaction and process in a similar procedure. The reaction was absolutely finished when appropriate arm length of copolymer was achieved. The crude products were dissolved in chloroform, precipitated several times in methanol, and dried in vacuum oven at 30°C for 24 hours. Finally, copolymer was kept under vacuum at room temperature.

3.3.3 Copolymer characterization

The resulting copolymers were characterized by ^{1}H NMR, GPC, and DSC.

3.3.3.1 Proton nuclear magnetic resonance spectrometer (^{1}H NMR)

Proton (^{1}H) nuclear magnetic resonance analysis was used to characterize L-lactide and copolymer products. The sample was dissolved in chloroform-d ($CDCl_3$) and vortexed until clear solution was obtained. The NMR experiment was carried out by using Varian mercury-400 spectrometer ^{1}H NMR operating at 400 MHz. Chemical shifts (δ) were reported in parts per million (ppm) relative to the residual protonated solvent signal as a reference.

3.3.3.2 Gel permeation chromatograph (GPC)

Gel permeation chromatography (GPC) was used to determined molecular weight of copolymer products ($\overline{M}_w$ and $\overline{M}_n$) and polydispersity index (PDI). The copolymer sample (15 mg) was dissolved in tetrahydrofuran (THF) (3 ml) and filtered by syringe filter (diameter 13 mm. 0.45 µm. nylon). GPC chromatogram of copolymer was obtained from Waters 150-CV chromatography equipped with PL-gel 10 µm mixed B 2 columns (MW resolving range = 500-10,000,000) at 35^{o}C. Tetrahydrofuran was used as an eluent with the flow rate of 1.0 ml/min. Degassed THF mobile phase was passed through the column for 20 minutes before injected. The sample volume 100 µl was injected and run for 40 minutes. Polystyrenes (MW = 5,460-1,290,000) were used as standards for calibration. The molecular weight was determined by a reflection index detector.

3.3.3.3 Differential scanning calorimeter (DSC)

Differential scanning calorimeter was determined by NETZSCH DSC204F1 Phoenix. Technique in which the difference in energy input into a substance and a

reference material is measured as a function of temperature, while the substance and reference material are subjected to a controlled temperature program.

This technique determined the physical property of semi-crystalline products. In this research, DSC technique was used to study glass transition temperature (T_g) of copolymer products. Copolymer was weighed in a sample pan about 10-13 mg. The temperature was started at 20^{o}C, heated to 160^{o}C (heating rate 20^{o}C/min) and isothermal for 3 minutes. In this step, copolymer would be completely molten. Liquid nitrogen was used to reduce temperature until -50^{o}C (cooling rate 20^{o}C/min) and isothermal for 3 minutes. Some semi-crystalline copolymer were precipitated quickly but the amorphous could not be precipitated in a short time. The sample was heated to 200^{o}C (heating rate 20^{o}C/min) until completely molten again. The empty pan was used as standard calibration. The amorphous could be changed from glass-like to rubber-like at glass transition temperature.

3.3.4 Preparation and characterization of film

3.3.4.1 Preparation of blend films

Poly(lactide-*co*-caprolactone) particles were prepared by the modified spontaneous emulsification-solvent diffusion method (modified-SESD method) in chitosan solution (Baimark *et al*., 2007). The chitosan solution was prepared using 1% (v/v) acetic acid aqueous solution as the solvent. The preparation of blend film was typically undertaken as follows. P(LA-*co*-CL) was dissolved in 5 ml acetone/ethanol (4/1, v/v). The P(LA-*co*-CL) solution was then added drop-wise into 2% chitosan solution containing 0.5% (w/w) glycerine. This mixture was stirred at 600 rpm. The various P(LA-*co*-CL)/chitosan composites were prepared, and their composite ratio are summarized in Table 3.1. The P(LA-*co*-CL) particles suspended in chitosan solution was obtained. Then, the film casting was done on a Petri dish and solvent was removed in a fume hood over a 5 hours period. The prepared film was dried at 30°C for 72 hours and kept under vacuum at room temperature for a week before characterization.

Table 3.1 Composition of blend film.

Film composition (copolymer/chitosan) (w/w)	*Total weight (g)*	*Copolymer[a] (g)*	*Chitosan[b] (g)*
90/10	0.5	0.45	0.05
	1	0.9	0.1
80/20	0.5	0.4	0.1
	1	0.8	0.2
70/30	0.5	0.35	0.15
	1	0.7	0.3

[a]amount of copolymer in 5 ml acetone/ethanol (4/1, v/v) mixture solvents.
[b]amount of chitosan in 2% chitosan solution (w/w).

3.3.4.2 Morphology study

The thickness of the appropriated copolymer/chitosan films was measured with a micrometer at 5 different locations (center and 4 corners) and mean thickness was calculated. The values were the average of 3 experiments.

Morphological characteristics were studied by scanning electron microscopy (SEM), using an electron microscope Jeol JSM-5800 LV (Jeol LTD, Tokyo, Japan). The prepared films were mounted on metal grids with doublesided adhesive tape and coated with gold under high vacuum before observation. The surface morphology of coated samples was examined by scanning electron microscopy at 10 kV. The photographs were taken at different magnifications.

3.3.4.3 Swelling property

The swelling property of the films was examined by measuring the water absorption content. The films were cut into 2x2 cm^2 and weighed before immerged in glass bottles containing 50 ml of phosphate buffer saline (PBS) (pH 7.4) at room temperature. At an appropriate time interval, the films were taken out, and the excess

water was removed carefully with filter paper then weighed immediately. The average of three measurements was plotted vs time. The degree of swelling was determined as follows:

$$\% \ of \ swelling = \left(\frac{W_t - W_0}{W_0} \right) \times 100$$

Where W_t is the weight of film at time t, and W_0 is the weight of film at time zero.

3.3.5 *In vitro* tissue adhesion

The adhesive strength was tested by T-peel test. The adhesive strength tests were performed *in vitro* using 30 µm thick polyamide (6/6 Nylon) films as substrates. The film sample (2.5x5 cm^2) was adhered to substrate and cut into 2.5x10 cm^2 (Figure 3.3). The tests (T-Peel Test ASTM D 1876) were performed using an Instron machine (model 5583) and Adhesive Failure Strength (AFS) values were determined and reported in Newton per cm width units (N/cm width). The measurements were performed at a 30 mm/min crosshead speed at 37°C. Each test was repeated three times.

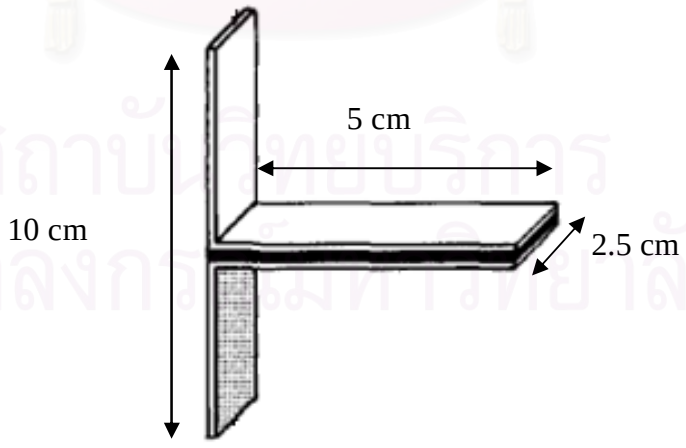

Figure 3.3 T-peel specimens.

3.3.6 *In vitro* tetracycline hydrochloride (TCH) release study

Drug-loaded copolymer/chitosan blend films with appropriated composition ratio were prepared in 2.5, 5 and 10% (w/w).

3.3.6.1 Calibration curve of tetracycline hydrochloride

Twenty five mg TCH was accurately weighed and dissolved in PBS pH 7.4 into a 50 ml volumetric flask and adjusted to volume (500 ppm). The solution was used as stock solution.

The 0.05, 0.1, 0.2, 0.3, 0.4 and 0.5 ml of stock solution was individually pipetted into a 5 ml volumetric flask and then diluted to volume with PBS. The final concentration of each solution was 5, 10, 20, 30, 40 and 50 ppm, respectively.

The absorbance of standard solutions was determined by UV-VIS spectrophotometer at 276.7 nm. The PBS was used as a reference solution. Each concentration was determined in triplicates. The absorbance and calibration curve of TCH in PBS pH 7.4 are shown in Table C1 and Figure C1 (Appendix C), respectively.

3.3.6.2 *In vitro* tetracycline hydrochloride release

The *in vitro* drug release of tetracycline hydrochloride was investigated. Drug loaded polymer square films (30 mm x 30 mm x 0.1 mm, about 80 mg weight) were cut from dry films. Each film was immersed in flask containing pH 7.4 phosphate buffer saline (PBS) as a releasing medium (50 ml). The sealed flask were placed in an incubator shaker at 37±1°C and shaken at a frequency of 110 rpm. At the end of the predetermined time intervals (e.g. 0.25, 0.5, 0.75, 1, 2, 3, 4, 5, 6, 7, 8, 10, 12 hours and daily for 7 days or until drug release rate was constant), dissolution medium (3 ml) were removed from each flask. An equal volume of fresh medium (3 ml) was replaced into each dissolution flask, to maintain a constant volume of medium during the dissolution test. Each sample solution was centrifuged and diluted to a suitable concentration if necessary. The UV absorption was measured by UV-VIS

spectrophotometer at 276.7 nm. All experiments were performed in triplicate. The amount of TCH released was calculated by interpolation from a calibration curves containing increasing concentrations of TCH. A cumulative correction was made for the previously removed sample to determine the total amount of drug release.

CHAPTER IV

RESULTS AND DISCUSSION

4.1 Synthesis of L-lactide

L-lactide synthesis was divided into two steps. The first step was to produce low molecular weight PLLA. In the second step, L-lactide was produced by ring formation from the decomposition of low molecular weight PLLA.

4.1.1 Synthesis of low molecular weight polylactide

L-lactic acid was heated until temperature reached 100°C under nitrogen atmosphere so that water present in L-lactic solution was removed and condensed into the condensate reservoir in Figure 4.1 (a). The temperature was maintained at 100-115°C for 2-3 hours to remove water and by product. When temperature reached 140°C, the solution was changed from white clear liquid to very light yellow liquid. Later, the vacuum pressure was applied for 30 minutes to further remove water from the reaction.

4.1.2 Ring formation of L-lactide using zinc powder as a catalyst

The zinc powder was added into the light yellow liquid obtained in 4.1.1 and the reaction mixture was heated to 160^{o}C for 30 minutes or until water was not condensed into the condensate reservoir. Then, the temperature was increased to 220-230^{o}C and the vacuum pressure was applied until white solid crystal of L-lactide was formed (Figure 4.1 (b)). The L-lactide crystal was purified by recrystallization several times from ethyl acetate. The white needle-like crystal of L-lactide was kept under vacuum in refrigerator (Figure 4.2).

(a) (b)

Figure 4.1 (a) Condensate reservoir and (b) white solid crystal of L-lactide.

The L-lactide crystal was characterized by ^{1}H NMR technique. From ^{1}H NMR spectrum in Figure A1 (Appendix A), the chemical shift at 5.07 ppm was assigned for the methine proton (-C<u>H</u>-CH_3), and 1.66 ppm for methyl protons (-CH-C<u>H</u>$_3$).

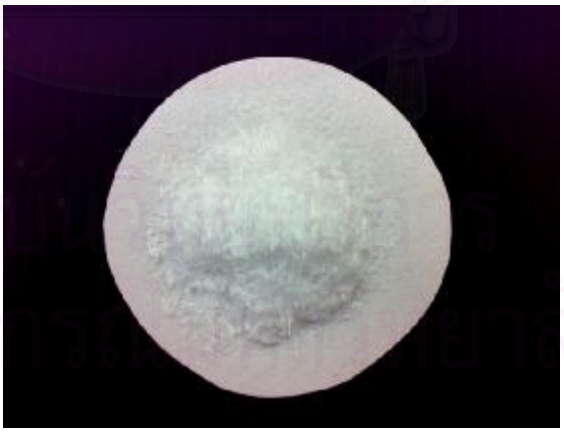

Figure 4.2 Recrystallized L-lactide.

4.2 Synthesis and characterization of low molecular weight poly(lactide-*co*-caprolactone) using alcohols with different numbers of hydroxyl groups.

A series of low molecular weight copolymers (LMW) of L-lactide (LA) and ε-caprolactone (CL) possessing variations in arm number and arm length were synthesized through step by step ring opening polymerization of LA and CL using alcohols with different numbers of hydroxyl groups in the presence of $Sn(Oct)_2$. All LMW copolymers were synthesized under nitrogen atmosphere shown in Figure 4.3 (a). After the reaction was finished, the crude copolymer turned yellowish viscous and then became solidify at room temperature. The physical appearances of purified LMW copolymers are shown in Table 4.1.

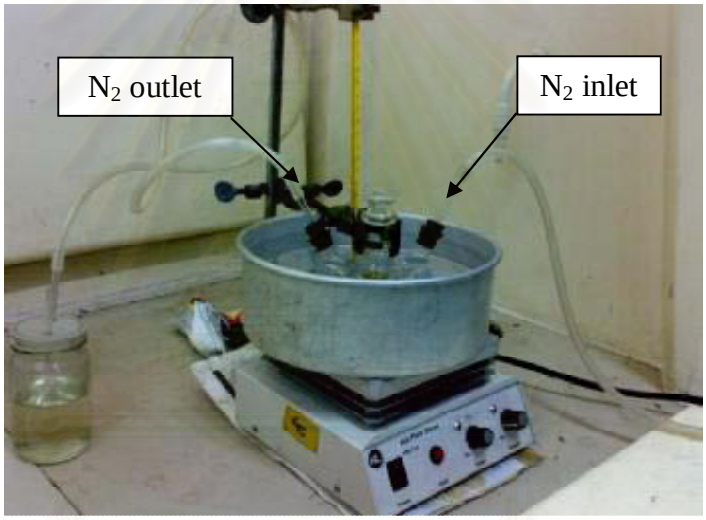

(a)

(b)

(c)

Figure 4.3 (a) Experimental set up for P(LA-*co*-CL) synthesis under nitrogen atmosphere, (b) P(LA-*co*-CL) in round bottom flask and (c) purified P(LA-*co*-CL).

Table 4.1 The %yield and physical appearance of low molecular weight copolymers prepared by using alcohols with different numbers of hydroxyl groups.

Copolymer	*Co-initiator*	*%yield*	*Physical appearance*
Similar arm length			
CO-BD	1,4-Butanediol	75.67±3.74	White solid
CO-PTOL	Pentaerythritol	77.44±2.68	White solid
CO-SB	D-sorbitol	62.2±6.62	White solid
Similar molecular weight (~10,000 g/mol)			
CO-BD (10,000)	1,4-Butanediol	68.28±8.36	White solid
CO-PTOL (10,000)	Pentaerythritol	77.84±4.13	Yellowish solid
CO-SB (10,000)	D-sorbitol	65.15±8.06	Yellowish viscous

The structure of the copolymers obtained depended on the functionality of the alcohol used as the co-initiator. Difunctional alcohols yielded linear copolymers, while alcohols with OH functionalities higher than 2 gave branched and star-shaped copolymers.

In this research, variations in the number of arms were obtained through utilization of 1,4-butanediol (BD), pentaerythritol (PTOL) and D-sorbitol (SB) to obtain linear, four and six-arm, star-shaped, P(LA-*co*-CL)s respectively. The similar arm length and molecular weight of copolymer was copolymerized (Figure 4.4). By controlling the monomer to co-initiator molar ratio, the difference in arm length and molecular weight could be achieved. Copolymers with similar arm length have 24 LA unit and 4 CL unit. Whereas copolymers with similar molecular weight (10,000 g/mol), arm length decreased when OH groups of co-initiator increased. The resulting copolymers were characterized by ^{1}H NMR, GPC and DSC.

(a) Similar arm length

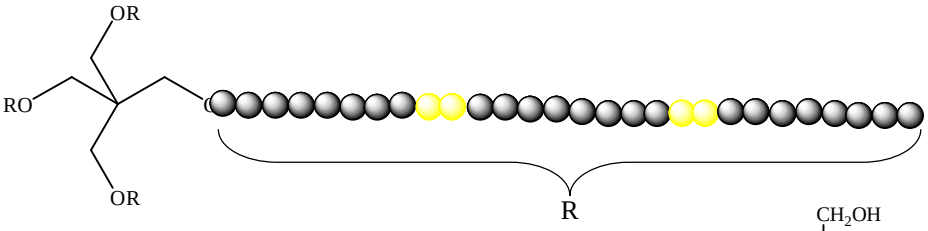

Co-initiator:

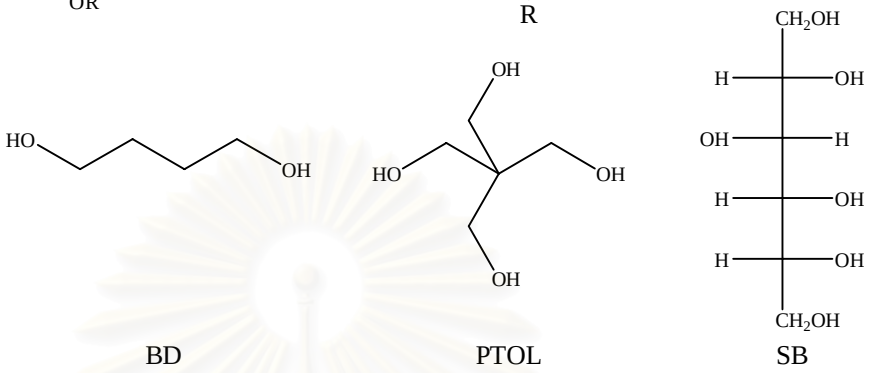

(b) Similar molecular weight (~10,000 g/mol)

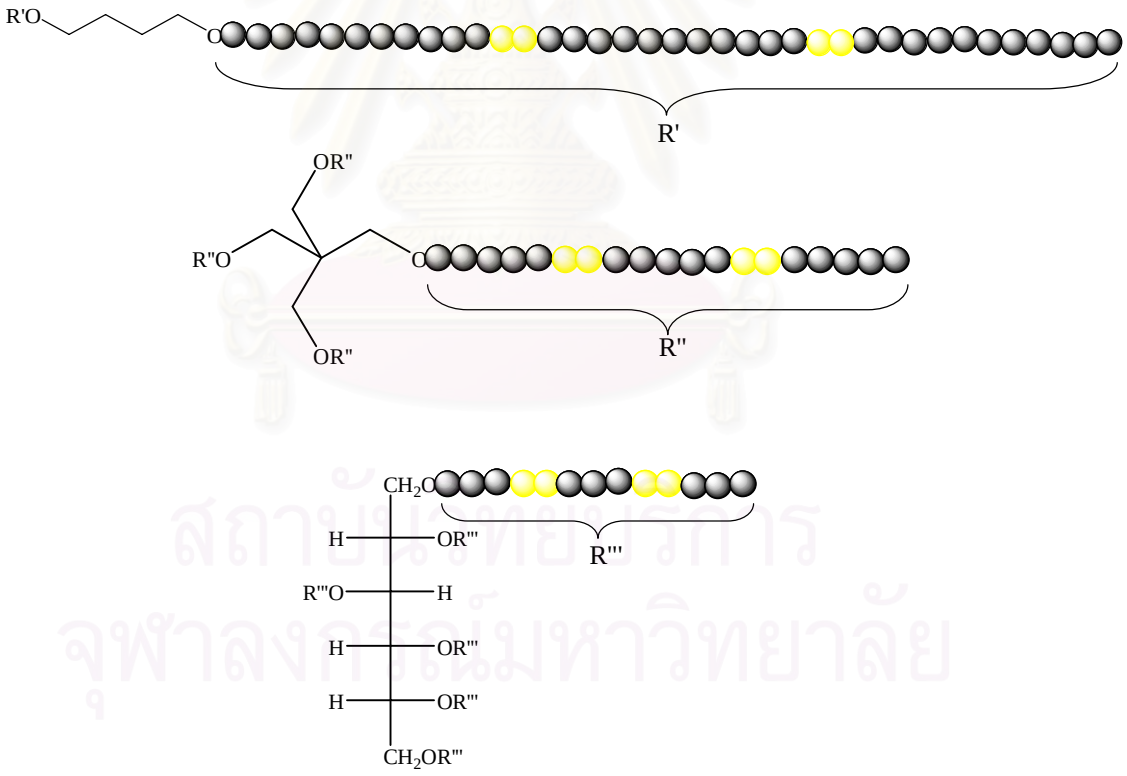

L-lactide unit ( ), ε-caprolactone unit ( )

Figure 4.4 Structures of (a) similar arm length and (b) similar molecular weight copolymers.

4.2.1 Proton nuclear magnetic resonance spectroscopy (^{1}H NMR) analysis

Characterization of the P(LA-*co*-CL)s with ^{1}H NMR spectroscopy was performed. ^{1}H NMR analysis was used to characterize the copolymer compositions. The example of ^{1}H NMR spectrum of two-arm or linear P(LA-*co*-CL) is shown in Figure 4.5. The signal of the methine proton (-C<u>H</u>-CH_3, *a*) of PLLA repeat unit is at 5.20 ppm. The methine proton (-C<u>H</u>-OH, *b*) of the chain end unit is at 4.35 ppm. The methylene protons of PCL repeat unit are at 4.00-4.20 and 2.23-2.41 ppm (-C<u>H_2</u>-O-, *c* and -C<u>H_2</u>-COO-, *d* respectively). The methyl group (-CH-C<u>H_3</u>, *e*) of PLLA repeat unit and the methylene protons (-C<u>H_2</u>-CH_2-, *f* and *g*) of PCL repeat unit are at 1.37-1.70 ppm. Similarly, copolymerization of LA and CL with PTOL and SB afforded well-defined four, six-arm, star-shaped P(LA-*co*-CL). The four and six-arm, star-shaped copolymer showed the typical proton signals of the P(LA-*co*-CL) main chain as found in two-arm (Figures A3-A7, Appendix A).

From ^{1}H NMR results, monomer ratio, arm length, number of hydroxyl group and molecular weight could be calculated from integral peak (Korhonen *et al*., 2001).

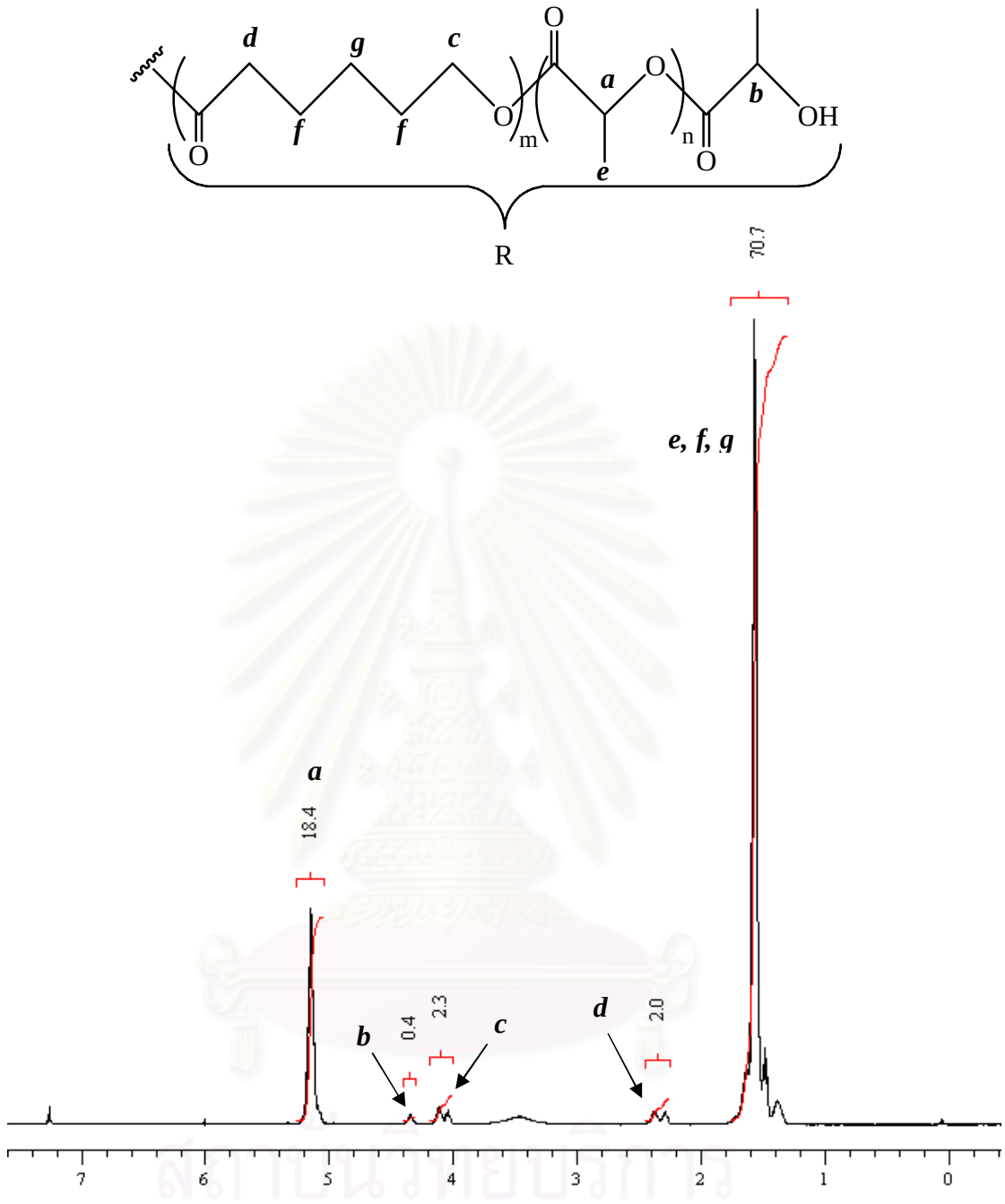

Figure 4.5 ^{1}H NMR spectrum of P(LA-*co*-CL) prepared by using 1,4-butanediol as co-initiator (CO-BD).

Monomer ratio

The chemical composition of P(LA-*co*-CL) was determined from the ^{1}H NMR spectrum in two methods by calculating:

1) The ratio of the integral peak areas corresponding to the lactoyl (L, repeating units of PLLA, *a*) methine protons at 5.20 ppm and the other peak.

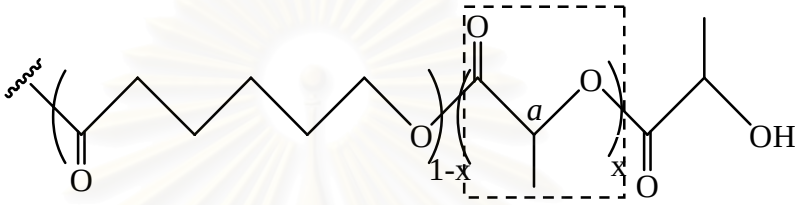

$10(CH_2CH_2CH_2CH_2CH_2)$ H	1(CH) H $3(CH_3)$ H
Total 10 H	4 H

T = Total of integral peak

A = Peak integral of interested monomer

x = Mole fraction of interested monomer

$$A = x$$

$$T = 4x+10(1-x)$$

$$\frac{A}{T} = \frac{x}{4x+10(1-x)} = \frac{x}{10-6x}$$

$$x = \frac{10(\frac{A}{T})}{1+6(\frac{A}{T})} \qquad (1)$$

2) The ratio of the integral peak areas corresponding to the lactoyl (L, repeating units of PLLA, *a*) methine protons at 5.20 ppm and the CL methylene protons at 4.00-4.20 ppm (CL, repeating units of PCL, *c*).

$$Mole\ fraction\ of\ lactoyl = \frac{a}{a+c} \qquad (2)$$

Example of CO-BD (Figure 4.5)

From equation (1)

$$\frac{A}{T} = \frac{18.4}{18.4+2.3+2.0+70.7} = \frac{18.4}{93.4} = 0.197$$

$$x = \frac{10(0.197)}{1+6(0.197)} = 0.90$$

$$1-x = 0.10$$

Mole fraction of L and CL is 0.9 and 0.1 respectively. #

From equation (2)

$$Mole\ fraction\ of\ lactoyl = \frac{a}{a+c} = \frac{18.4}{18.4+2.3} = 0.89$$

Mole fraction of L and CL is 0.89 and 0.11 respectively. #

From the peak area integrations, the copolymer composition can be determined as showed in Table 4.2.

It was observed that the composition, the LA to CL ratio of the copolymer obtained was lower than the calculated theoretical values (Table 4.2). Besides, it was found that only trace amounts of moisture affected the molecular weight and composition of the copolymer.

According to above method, the copolymer composition was calculated in different method. However, the composition that calculated in two different methods was corresponded to the LA and CL mole ratio. Therefore, average chain length and initiating OH were calculated via the ratio of the integral peak areas of LA and CL unit.

Average chain length and initiating OH

Average lactide chain lengths were calculated by comparing the peak integrals of chain methine protons of LA (*a* , 5.20 ppm) with those of methine proton next to the terminal hydroxyl group (*b*, 4.35 ppm). This gives the chain length in lactide units as presented in Equation (3).

$$LA\ Chain\ length = \frac{a+b}{2b} \quad (3)$$

Average caprolactone chain lengths were calculated by similar equation with the peak integrals of methylene protons of PCL repeat unit (*c*, 4.00-4.20 ppm).

$$CL\ Chain\ length = \frac{c}{b} \quad (4)$$

The average of hydroxyl groups in the co-initiator that take part in the polymerization process was determined by comparing the theoretical chain length with the chain length determined by ^{1}H NMR as in Equation (5).

$$Initiating\ OH = \frac{theoretical\ chain\ length}{chain\ length\ determined\ by\ ^{1}H\ NMR} \times functionality \quad (5)$$

Example of CO-BD (continued)

From equation (3), (4) and (5)

$$LA\ Chain\ length = \frac{a+b}{2b} = \frac{18.4+0.4}{2(0.4)} = 23.5$$

$$CL\ Chain\ length = \frac{2.3}{0.4} = 5.75$$

$$Initiating\ OH = \frac{theoretical\ chain\ length}{chain\ length\ determined\ by\ ^{1}H\ NMR} \times functionality$$

$$= \frac{24+4}{23.5+5.75} \times 2 = \frac{28}{29.25} \times 2 = 1.91$$

Linear P(LA-*co*-CL) (CO-BD) had a theoretical chain length of 24 LA unit and 4 CL unit, whereas the chain length determined by ^{1}H NMR was 23.5 and 5.75 respectively. The result corresponds to value of 1.91 as the average number of OH groups initiating polymerization. This is also similar to four-arm P(LA-*co*-CL) (Table 4.2). Whereas the initiating OH of six-arm P(LA-*co*-CL) using D-sorbitol as co-initiator, that determined by ^{1}H NMR, was greater than the theoretical value. Probably, the difference between the calculated and theoretical values is due to the lower activity of the secondary OH groups. However, the calculated values were considerably greater than 2, which would correspond to the primary OH groups (Korhonen *et al.*, 2001).

Table 4.2 Composition of low molecular weight copolymers prepared by using alcohols with different numbers of hydroxyl groups.

Copolymer	*Arms*	*Mole fraction*						*Average chain length*						*No. of OH gr.*	
		Theory[a]		*^{1}H NMR*				*Theory*[a]			*^{1}H NMR*				
		L[b]	*CL*	*L*[b, c]	*CL*	*L*[b, d]	*CL*	*LA*	*CL*	*Total*	*LA*	*CL*	*Total*	*Theory*	*^{1}H NMR*
CO-BD	2	0.92	0.08	0.90	0.10	0.89	0.11	24	4	28	23.50	5.75	29.25	2	1.91
CO-PTOL	4	0.92	0.08	0.90	0.10	0.91	0.09	24	4	28	23.25	4.75	28.00	4	4.00
CO-SB	6	0.92	0.08	0.88	0.12	0.90	0.10	24	4	28	29.67	6.33	36.00	6	4.67
CO-BD (10,000)	2	0.94	0.06	0.94	0.06	0.95	0.05	33	4	37	35.17	3.64	38.83	2	1.91
CO-PTOL (10,000)	4	0.88	0.12	0.87	0.13	0.89	0.11	15	4	19	14.25	3.33	17.58	4	4.32
CO-SB (10,000)	6	0.82	0.18	0.82	0.18	0.79	0.21	9	4	13	12.67	6.50	19.17	6	4.07

[a]feed mol ratio of LA and CL, [b]L = Lactoyl unit, [c]determined by ^{1}H NMR (eq. (1)) and [d]determined by ^{1}H NMR (eq. (2)).

4.2.2 Gel permeation chromatography (GPC) analysis

The $\overline{M}_w$, $\overline{M}_n$ and PDI of P(LA-*co*-CL)s obtained from GPC are shown in Table 4.3 and the chromatogram is shown in Figures A8-A13 (Appendix A). Copolymers were synthesized by using alcohols with different numbers of hydroxyl groups with the similar chain length and similar molecular weight. It was observed that copolymer with similar chain length, increasing the number of OH increased the molecular weight of copolymer. For copolymer initiated with SB, the $\overline{M}_w$ closely corresponded to the theoretical values. For copolymer initiated with BD and PTOL, the differences between theoretical molecular weight and GPC results were much smaller.

Excellent agreement existed between the ^{1}H NMR and GPC, and the $\overline{M}_w$ was in agreement with the targeted molecular weight. The PDI for the linear and four-arm, star-shaped P(LA-*co*-CL) were narrow while the PDI for the six-arm, star-shaped P(LA-*co*-CL)s were relatively broad. It can be attributed to increased steric hindrance with increasing arm molar mass, number of arms and transesterification reactions.

From ^{1}H NMR and GPC, this copolymer composition is similar to the LA and CL feed mole ratio. Therefore, the synthesized reaction was taken to near-quantitative conversion.

4.2.3 Differential scanning calorimetry (DSC) analysis

The glass transition temperature (T_g) of copolymer was measured by DSC. The chromatograms are shown in Figures A14-A20. It is expected that the T_g of synthesized copolymers could be between 20-25°C that so the viscosity of the copolymer could have changed such the temperature; therefore, at body temperature the copolymer adhesive could hold the injured tissue together. According to the thermal properties of homopolymer, PLLA is about 37% crystalline, with a melting point of 175-178°C and a glass transition temperature of 60-65°C. Whereas PCL is a semicrystalline polymer with a melting point of 59-64°C and a glass transition

temperature of -60°C (Younes *et al.*, 2004). Therefore, T_g was decreased with the incorporation of caprolactone molecules into the chains of lactide.

The T_g of copolymers are shown in Table 4.3. It was found that the T_g of copolymers change with the copolymers composition. With increase of LA/CL ratio, the T_g of copolymer increased from 10.8 to 31.6°C. Copolymers with similar arm length (24/4, LA/CL), T_g of copolymers using BD, PTOL and SB was observed nearly at 21.4, 22.8 and 25.9°C respectively. Whereas copolymers with similar weight (~10,000 g/mol), in case of copolymers with the presence of BD and SB as co-initiator (CO-BD (10,000) and CO-SB (10,000) respectively), T_g was observed at 31.6°C and 10.8°C. The T_g of CO-BD (10,000) is higher than appropriate temperature interval due to high LA/CL ratio and the T_g of CO-SB (10,000) is lower than appropriate temperature interval because of low LA/CL ratio. Therefore the T_g of copolymer increased when the LA/CL ratio increased

Table 4.3 Characterization of low molecular weight copolymers prepared by using alcohols with different numbers of hydroxyl groups.

Copolymer	*Molecular weight*		*GPC*			*T_g (°C)*	
	Theory[a]	*^{1}H NMR*	*$\overline{M}_n$*	*$\overline{M}_w$*	*PDI*	*Onset*	*Midpoint*
CO-BD	7914	7824	6169	8006	1.3	21.4	23.9
CO-PTOL	15784	15694	11645	14895	1.28	22.8	25.5
CO-SB	23654	23487	13041	18248	1.4	25.9	29.7
CO-BD (10,000)	10506	10537	9870	11295	1.14	31.6	35.9
CO-PTOL (10,000)	10600	10648	8657	10080	1.16	20.6	24.5
CO-SB (10,000)	10694	10621	7409	10252	1.38	10.8	15.7

[a]Feed mole ratio.

4.3 Preparation and characterization of blend film

Poly(lactide-*co*-caprolactone)/chitosan blend films were prepared followed the modified spontaneous emulsification-solvent diffusion method (modified-SESD method) at different film composition (Table 3.1). Using this method, the particles dispersed in chitosan matrix could be prepared (Baimark *et al.*, 2007). The appearances of films are shown in Table 4.4 and Figure 4.6. The presence of chitosan in the film helped improve the flexibility of the films since the chitosan is highly flexible. It was found that the appropriate composition was 70/30 (copolymer/chitosan, w/w).

Table 4.4 The appearance of blend films.

Film composition	*Total weight (g)*	
(copolymer/chitosan) (w/w)	*0.5*	*1.0*
90/10	-	-
80/20	±	-
70/30	+	+

- Film does not form.
± Film forms but could be not peeled out from Petri dish.
+ Film forms and could be peeled out from Petri dish.

Total weight: 0.5 g 1.0 g

(a) 70/30 (CO-BD/CH)

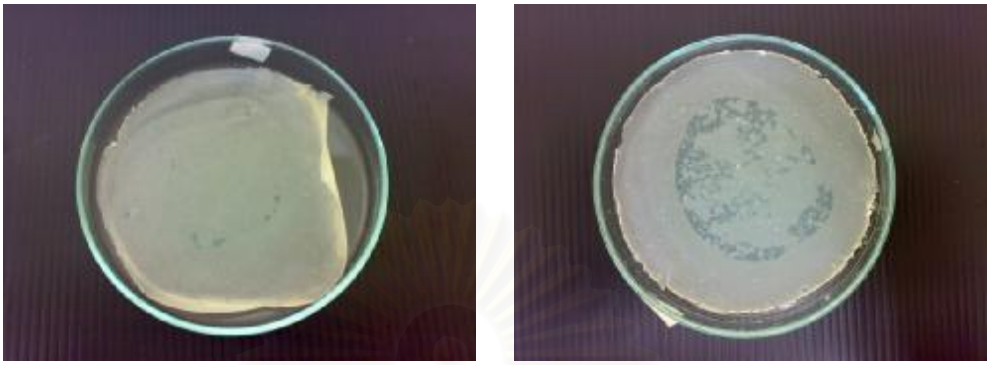

(b) 80/20 (CO-BD/CH)

(c) 90/10 (CO-BD/CH)

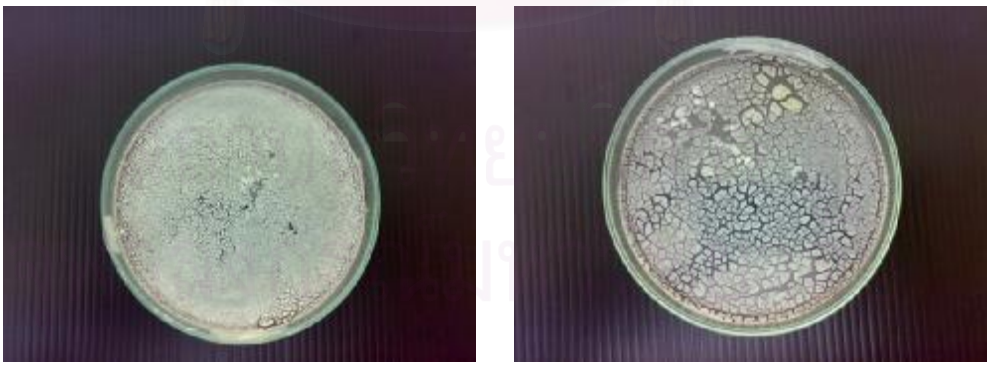

Figure 4.6 The photograph of film with various compositions

4.3.1 Morphology study

The thickness of the chitosan and blend film was determined by micrometer. It was found to be in the range of 0.10–0.15 mm.

Scanning electron microscopy (SEM) was used to directly investigate the structure of the copolymer/chitosan blends. The SEM micrographs of the surface and cross section of 70/30 (w/w) copolymer/chitosan blend films are shown in Figures 4.7 and 4.8, respectively.

Similar morphology was observed in all blend films. It is observed that the surfaces of blend films were rougher and more opaque than those of chitosan film (Figure 4.7). The diameters of pores observed on the film surface were ranging from 0.5-1 μm. The particle sizes were approximately ranging from 0.2-1 μm with spherical shape. TCH loaded blend film was prepared. The embryonic copolymer microspheres TCH have been formed and entrapped in the chitosan matrix. TCH was incorporated in copolymer hole and partially dissolved in chitosan matrix. TCH seems to show no affect on film morphology (Figure 4.7 (g)).

Looking at the film cross section, it can be seen that the copolymer particles dispersed into chitosan matrix (Figure 4.8 (a) and (b)). The cross-section micrographs in Figure 4.8 (a) showed that the incorporation of TCH gave higher porosity inside the film. As the results of ionic interactions between the NH_4^+ groups of chitosan and the COO^- of TCH, the strong network was formed when drug was incorporated in blend film.

When the blend film was prepared, morphology of film was changed with the increasing time. Figure 4.9 shows the blend film after preparation for approximately 1 month.

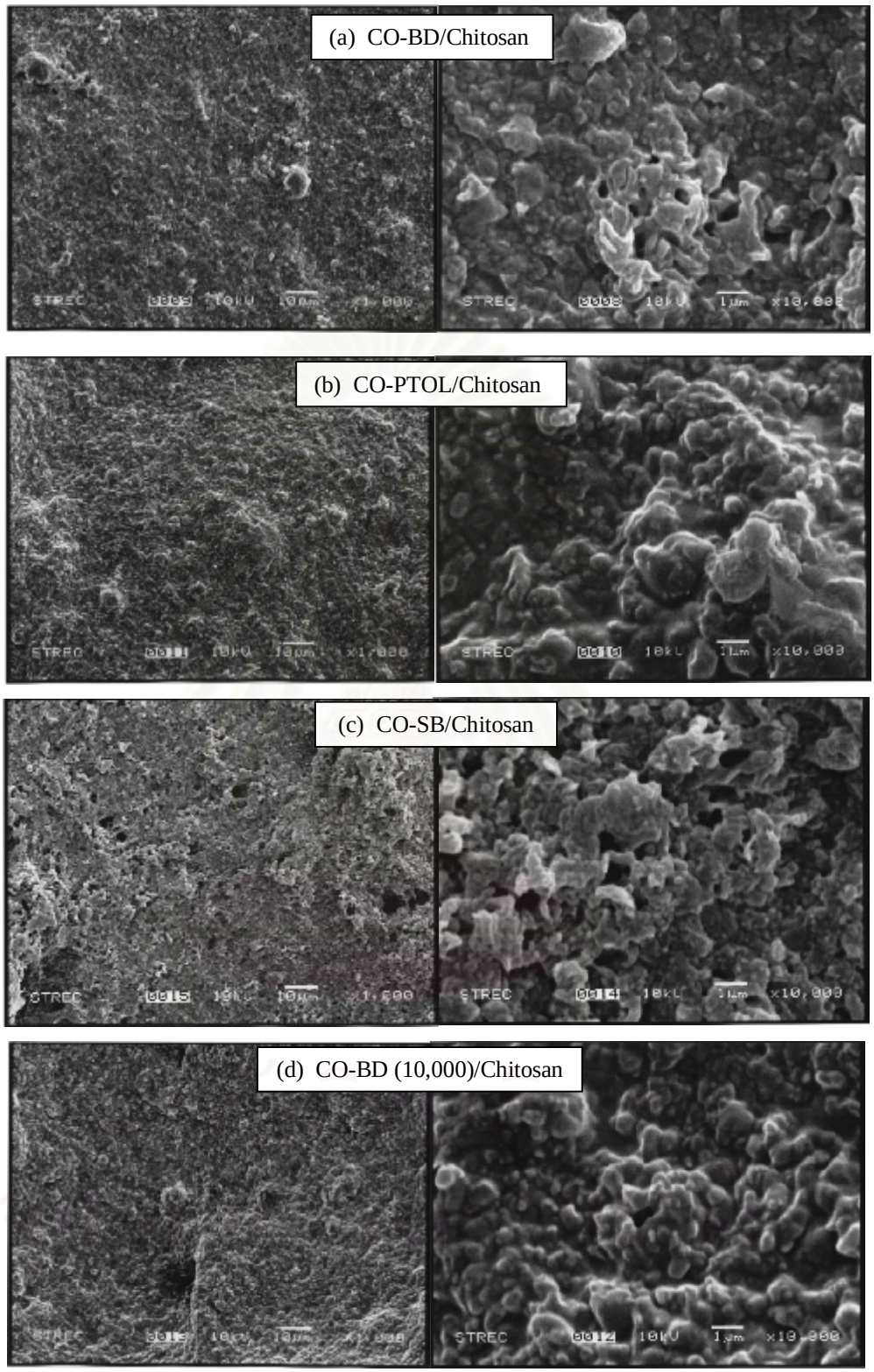

Figure 4.7 Scanning electron micrographs of the blend films surface (x1000 and x10,000).

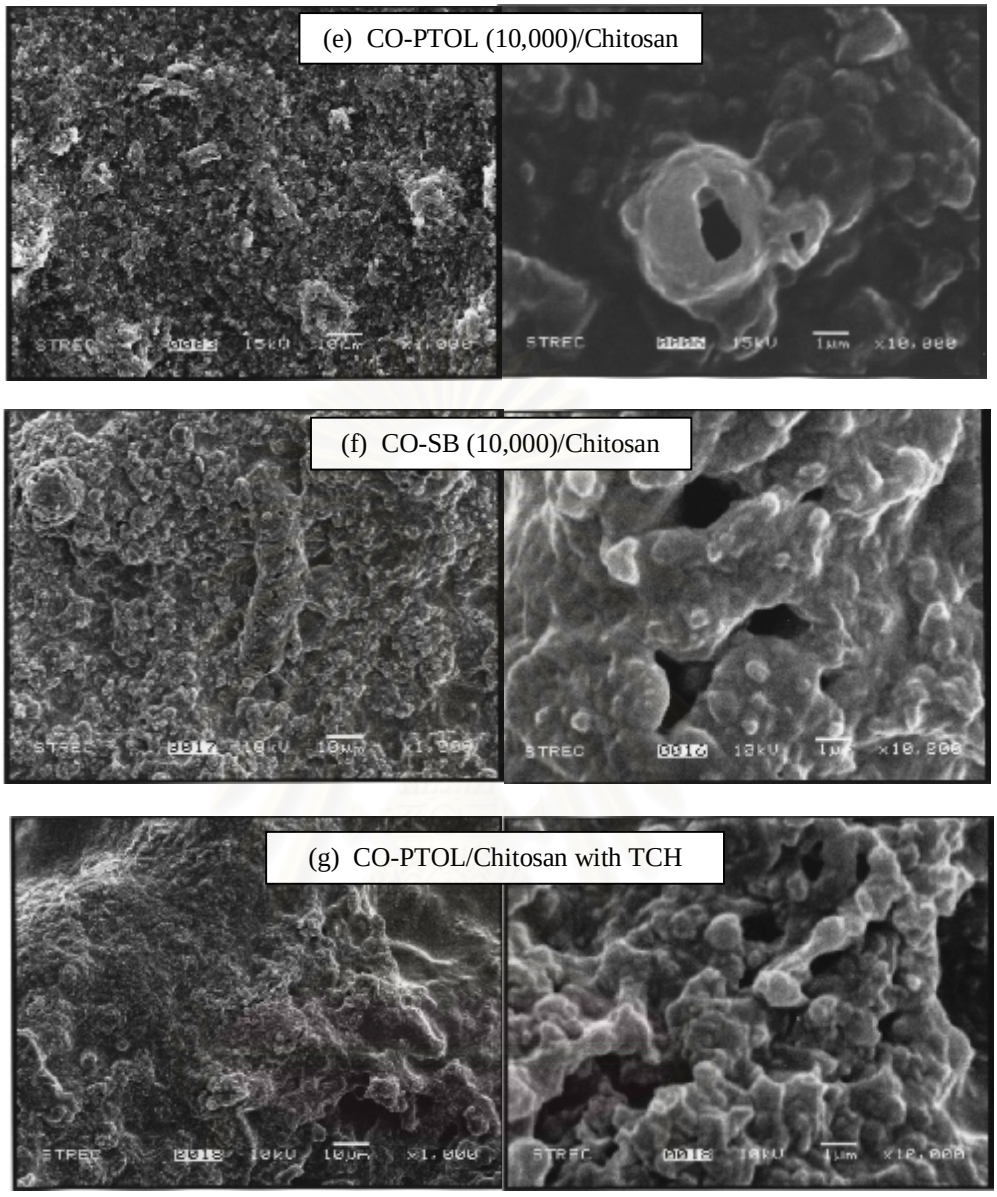

Figure 4.7 **(**Continued) Scanning electron micrographs of the blend films surface (x1000 and x10,000).

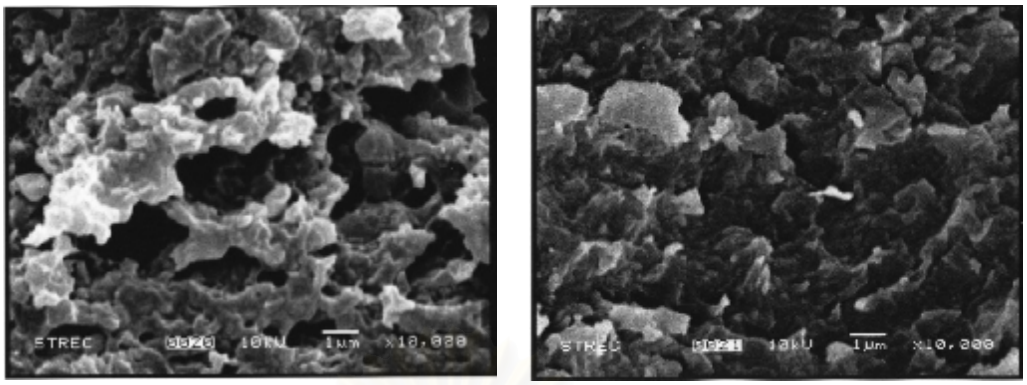

(a) (b)

Figure 4.8 Scanning electron micrographs (cross section) of the blend films with and without TCH ((a) and (b) respectively).

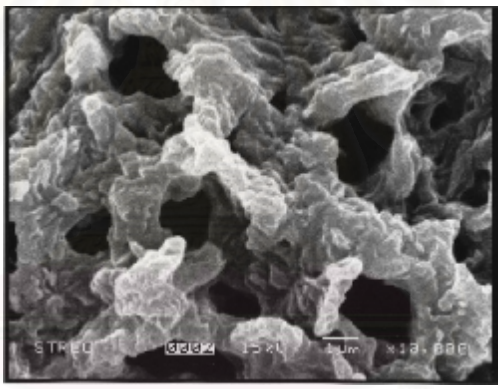

Figure 4.9 Scanning electron micrographs of the blend films surface (x10000) after preparation for about 1 month.

4.3.2 Swelling property

The degree of swelling of film in PBS is demonstrated in Figure 4.10 and Table B1 (Appendix B). It was found that chitosan film exhibited the highest degree of swelling and 30/70 copolymer/chitosan blend film exhibited next below its. The swelling behaviors of the 70/30 copolymer/chitosan blend films in this dissolution system were not significantly different. This is due to the copolymer showed less swelling behavior in this medium. The degrees of swelling capacity are ranging from 200-300%. In blend films, the swelling capability of chitosan decreases due to the hydrophobic effect of the copolymer matrices. This is because the water cannot penetrate well into the hydrophobic copolymer.

Swelling behavior was mainly dependent on film structure and composition (Perugini *et al.*, 2003). Films casted without the presence of copolymer showed higher degree of swelling capacity. Since the chitosan chains were flexible creating more space for water within the matrix. This indicates that chitosan structure is becoming mechanically very fragile and easily fractured.

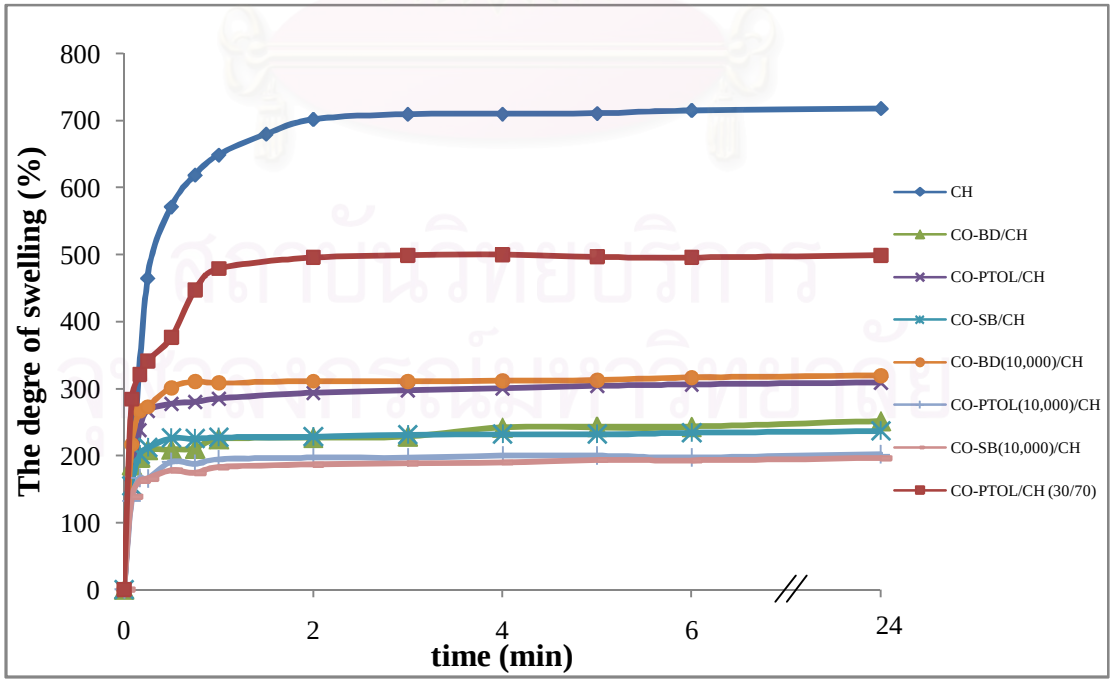

Figure 4.10 Swelling behavior of various ratios of copolymer/chitosan films in PBS.

4.4 *In vitro* tissue adhesion

Adhesive property depended on lactide component and chain entanglement (Cohn *et al.*, 2004). Therefore, it is expected that structure of copolymer might have some effect on adhesive strength. Copolymers that have different arm length and number of arm were synthesized.

Adhesive failure strength (AFS) of blend films is shown in Table 4.5. It is shown that, Film B has maximum AFS while Film D has minimum AFS.

Films A to C are copolymers which similar arm length but different in number of arm blended with chitosan. Adhesive strength increased when number of arm increased. Blend film with the presence of CO-PTOL and CO-SB (Film B and C respectively) represented similar AFS values. This was probably due to the effect of the lower initiating OH (~4 OH) as observed in CO-SB. However, AFS of Film B and C were higher than those of Film A with the presence of CO-BD (linear copolymer). Films D to F are blend films with similar molecular weight. It was found that Film D (CO-BD (10,000)/CH) has the lowest AFS because of high T_g (Table 4.3). CO-BD (10,000) could not change the viscosity with the body temperature. When comparing Film B with Film E, it was indicated that blend film with the presence of the longer arm length copolymer contained the higher AFS value.

Table 4.5 Adhesive failure strength (AFS) of blend films.

Film	*copolymer*	*Adhesive failure strength (AFS)*[a] *(N/cm width)*
A	CO-BD	0.325±0.006
B	CO-PTOL	2.417±0.025
C	CO-SB	2.249±0.035
D	CO-BD (10,000)	0.049±0.008
E	CO-PTOL (10,000)	1.764±0.025
F	CO-SB (10,000)	1.582±0.017

[a]Each value is mean±SD of three determinations.

All above mentioned, Film B (CO-PTOL/CH) give the highest AFS, therefore it is the most suitable copolymer/chitosan blend film for using in the further *in vitro* tetracycline drug release.

4.5 *In vitro* tetracycline hydrochloride release study

In this research, tetracycline hydrochloride was used as model drug release. The percentage of drug content of tetracycline hydrochloride (TCH) was presented in Table 4.6.

Table 4.6 The percentage of drug content.

Formulation	*Blend film*	*Theoretical drug loading (%w/w)*
A	CH	5
B	CO-PTOL/CH	2.5
C	CO-PTOL/CH	5
D	CO-PTOL/CH	10
E	CO-PTOL (10,000)/CH	5

Tetracycline hydrochloride was loaded in the control chitosan and blend films to investigate the drug release profile. Drug release systems containing TCH was designed to modulate the rate desorption resulting in smaller dosages and less frequent administration (Pataro *et al.*, 2003). The dissolution profiles of TCH were present in as graphs to explain and understand the drug released behavior from the films. The dissolution and release rate data of each formulation are given in Tables D1-D5 (Appendix D).

The release studies of TCH from Formulations A to E (Table 4.6) were evaluated in PBS pH 7.4 at 37°C. These dissolution profiles and release rate profiles are shown in Figures 4.11 to 4.13.

4.5.1 Effect of TCH content on the dissolution profiles

The TCH content in copolymer/chitosan film was important for the releasing profiles. Thus, the various TCH contents were studied. The TCH were varied from 2.5, 5 and 10% (w/w), Formulations B to D are presented in Table 4.6. The dissolution profiles and release profiles of TCH in various drug contents are present in Figures 4.11-4.12, Table 4.7 respectively.

The release profiles of Formulation B, C and D are similar. The drug is rapidly released at the first time interval. In initial period, the percentage of drug release of the Formulation B, C and D were 63.41, 38.62 and 29.47% respectively. The increase in drug content increases the amount of drug close to the surface as well as the drug in the matrix (Budhian *et al.*, 2007). The drug released during initial period is predominantly the drug located close to the surface. In our system, the decrease in initial drug release in increasing the drug content probably happens due to uneven drug distribution inside the films. On increasing the drug content, the marginal increase in this surface-associated drug is less as compared to the marginal increase in the total drug. Hence, the initial burst given as a %drug release decreases on increasing the drug content.

At the 7^{th} day, the dissolution percentage of the Formulation B, C and D were 86.84, 84.08 and 89.09%, respectively. The release pattern of B, C and D is not so different because the higher percentage of TCH content probably affected the lower swelling ratio of the film. Therefore, lower swelling films produced less drug release percentage. The increase in drug content in the blend film influenced the absolute release profiles such that both, the cumulative amount of drug released at any time and the induction period increases (Budhian *et al.*, 2007) (Figure 4.12). It was indicated that the amount of drug release from the blend films increased with the increase in drug loading.

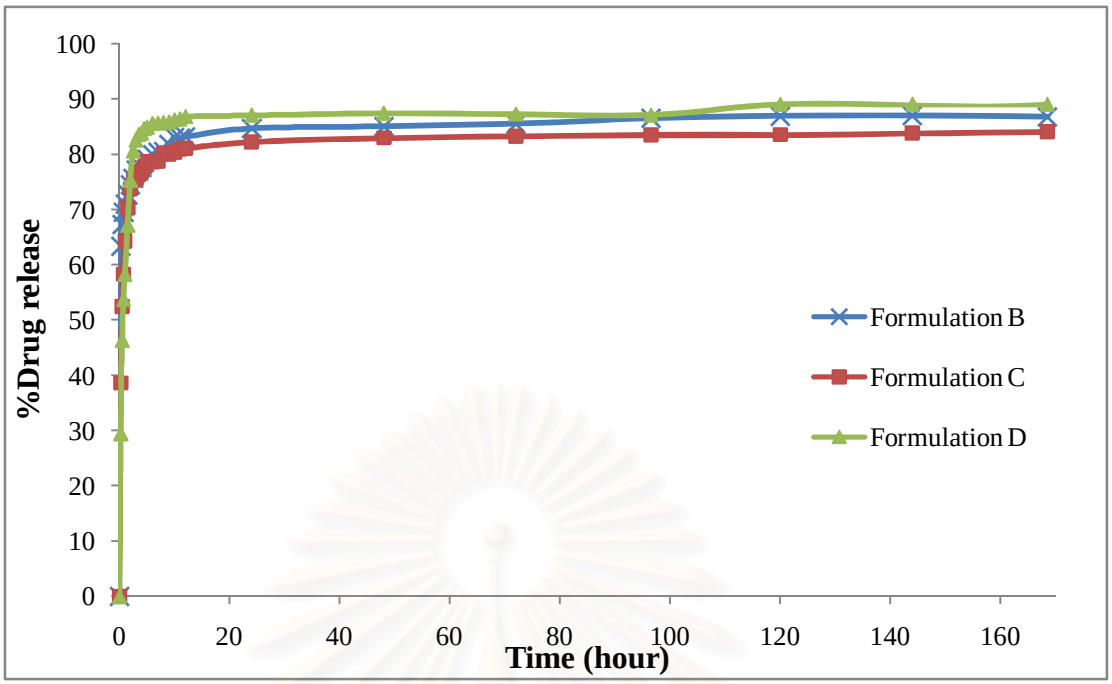

Figure 4.11 The dissolution profiles of TCH from the blend films with various drug loading contents in 7 days interval in PBS pH 7.4 at 37°C.

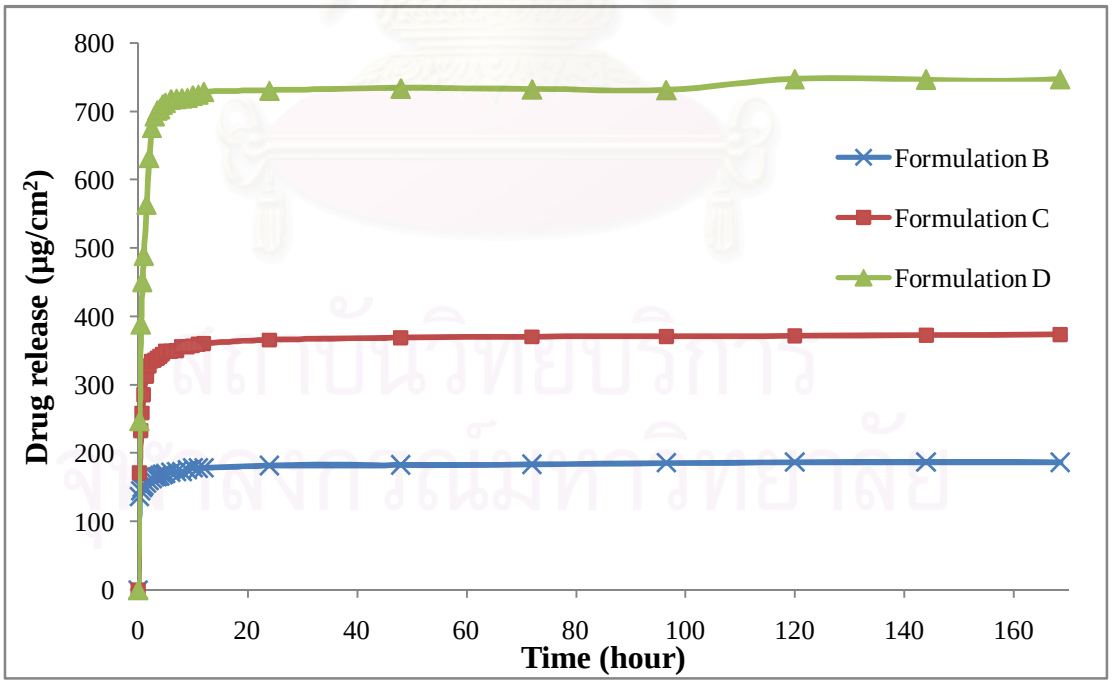

Figure 4.12 The amount of drug released profiles of TCH from the blend films with various drug loading contents in PBS pH 7.4 at 37°C.

In Table 4.7, Formulation D exhibited the highest rate of release value (989.63 μg/cm^2·h) and that Formulation B showed the least value of drug release (544.44 μg/cm^2·h) at first 15 minutes.TCH was released slowly until equilibrium in all formulations.

Table 4.7 The release rate of TCH from the blend films with various drug loading contents in PBS pH 7.4 at 37°C.

Time interval	*Release rate (μg/cm^2·h)*		
	FORM B (2.5% TCH)	*FORM C (5% TCH)*	*FORM D (10% TCH)*
0 – 15 min.	544.44	687.65	989.63
15 min. – 3 h.	10.73	59.77	162.21
3 h. to equilibrium	1.99	4.42	8.23

4.5.2 Effect of the molecular weight of copolymer in matrixes on the dissolution profiles

The next parameter to be considered is the copolymer with different molecular weight. In this study, the %TCH was maintained at 5% (w/w).

The dissolution profiles and the release rate of the various copolymers in chitosan are illustrated in Figure 4.13 and Table 4.8 respectively.

Formulation A, chitosan film (5% TCH), gave the highest percentage of release of TCH (98.28%) over 7 days whereas Formulation C and E released the lower amount of drug at 84.08 and 74.13%. This result is consistent with the swelling property. The degree of swelling capacity of the chitosan film was 718.28 which was higher than 309.35 and 202.17 of the CO-PTOL/CH and CO-PTOL/CH (10,000)

blend film respectively, at over 24 hours. Consequently, the drug could diffuse out from the film more easily.

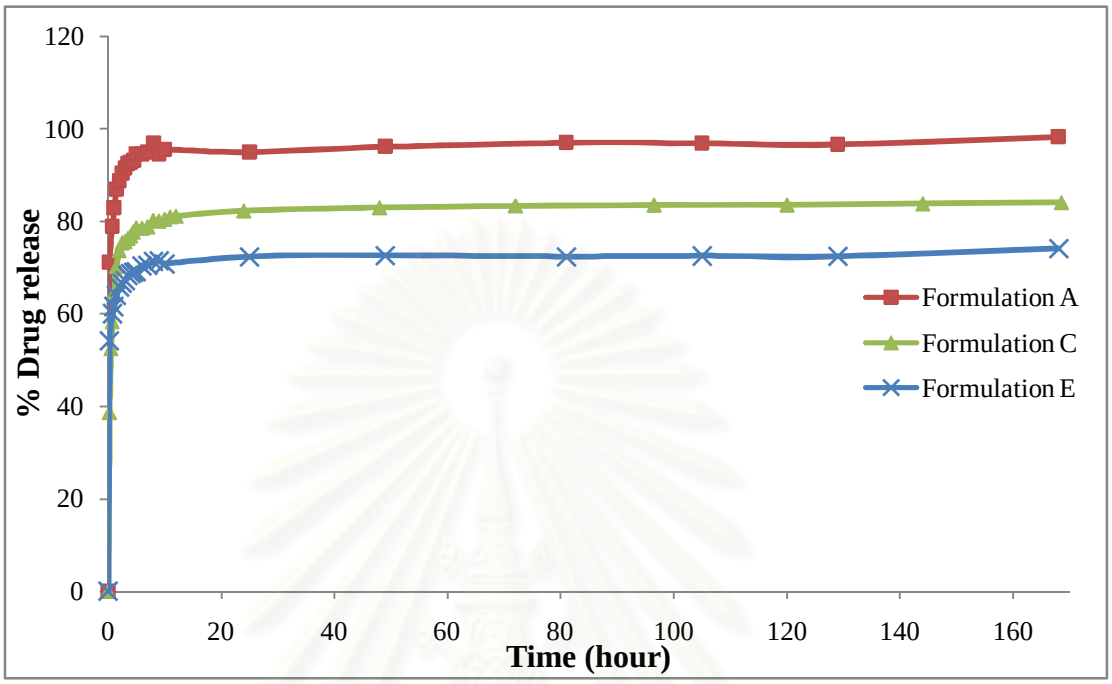

Figure 4.13 The dissolution profiles of TCH from the 5% drug-loaded films with various copolymers in 7 days interval in PBS pH 7.4 at 37°C.

Analysis of the data in Figure 4.13 and Table 4.8 indicated that among the formulations with the various copolymers in chitosan, Formulation C and E with the presence of CO-PTOL and CO-PTOL (10,000) respectively exhibited a significant decrease in release rate when compared with Formulation A.

It was seen that copolymer could help slowing the release rate. Formulation D showed the lowest rate of release value (687.65 μg/cm^2·h) at first 15 minutes.TCH was released slowly until equilibrium in all formulations. This may be attributed to arm length of CO-PTOL is longer than CO-PTOL (10,000). Therefore CO-PTOL could collect more TCH in copolymer hole.

The drug release profiles of the films demonstrated that all the films had rapid initial release rate, probably due to the drug release from the surface region of the films similar to the previous experiments.

Table 4.8 The release rate of TCH from the 5% drug-loaded films with various copolymers in PBS pH 7.4 at 37°C.

Time interval	*Release rate ($\mu g/cm^2 \cdot h$)*		
	FORM A (CH)	*FORM C (CO-PTOL/CH)*	*FORM E (CO-PTOL (10,000)/CH)*
0 – 15 min.	1100.99	687.65	1002.22
15 min. – 3 h.	28.75	59.77	21.78
3 h. to equilibrium	3.98	4.42	4.87

Formulation C could sustain release the TCH within 7 days with high %drug release (84.08%).

Release profile from blend film was compared to a commercially available drug delivery system. Actisite® (Alza Corporation, Palo Alto, CA), poly(ethylene-*co*-vinyl acetate) containing 25% TCH, is the commercial TCH controlled release device. In general, the initial rate of release of Formulation C and Actisite® are high during the first time due to release of drug sequestered on the sample surfaces. It is interesting that the %TCH released after 5 days from Formulation C was about 83.55% that was higher than that released from Actisite (~ 30%) (Kenawy *et al.*, 2002).

Table 4.9 Comparison of Formulation C with other drug delivery device.

Drug release device	*Description of Device*	*Device Degradation Time*
Formulation C	5% (w/w) TCH in CO-PTOL/Chitosan blend film.	Blend film can degrade after removed.
Actisite®	25% (w/w) TCH in ethylene vinyl acetate co-polymer (45% (w/w) vinyl acetate) periodontal monofilament fiber.	The fibers do not degrade, but must be removed after 10 days.

CHAPTER V

CONCLUSIONS AND SUGGESTION

5.1 Conclusions

L-lactide was obtained from synthesis of low molecular weight PLLA followed by ring formation of low molecular weight PLLA. L-lactide, that was recrytallized ethyl acetate, was copolymerized with ε-caprolactone using alcohols with different numbers of hydroxyl groups as co-initiator in the presence of $Sn(Oct)_2$. Two series of low molecular weight copolymers with similar arm length and molecular weight were synthesized and characterized.

From ^{1}H NMR results, all copolymers contain LA/CL mole fraction close to expected mole ratio. However initiating OH of six-arm copolymers, with SB as co-initiator, was lower than theoretical OH. The $\overline{M_w}$, $\overline{M_n}$ and PDI of copolymers were determined. It was found that PDI of the linear and four-arm, star-shaped copolymers was narrow while relatively broad for the six-arm, star-shaped copolymer. The molecular weight was close to targeted value. Moreover, DSC results showed that CO-BD, CO-PTOL, CO-SB and CO-PTOL (10,000) provided preferable T_g at 21.4, 22.8, 25.9 and 20.6 °C respectively. From above analyses, it can be concluded that SB is not suitable to be used as co-initiator in copolymerization of copolymer as tissue adhesive and drug release system.

During film preparation, copolymer was incorporated into chitosan by the modified spontaneous emulsification-solvent diffusion method. The suitable ratio of blend film was 70/30 copolymer to chitosan (w/w). Copolymer particles were dispersed in chitosan matrix which was observed from SEM micrographs. In addition, unexpected pores were observed in blend films. The pores and pore size were increased with the increasing time. Adhesive strength of blend films was investigated by T-peel test. CO-PTOL/CH film (Film B) has the highest adhesive strength while the lowest adhesive strength was found in CO-BD (10,000)/CH (Film D) due to high

T_g. Due to high adhesive strength, Film B is the most suitable copolymer/chitosan blend film for using as tissue adhesive.

The tetracycline hydrochloride (TCH) release from the blend film was investigated in PBS at 37°C. Drug release system containing TCH was designed to modulate the desorption rate resulting in smaller dosages and less frequent application. In general, the mechanism of drug release from copolymer/chitosan film can be explained by diffusion when film is swelling. At various drug loading (Formulations B to D), the similar dissolution profiles were observed. However, the Formulation C can sustain the release of TCH within 7 days compared with chitosan film which was consistent with swelling behavior. Furthermore, Formulation C could release drug with high %drug release (84.08%). Therefore, it is the most suitable TCH drug release system.

5.2 Suggestion for future work

For further study, polymer matrix should be prepared using different methods including multilayer film, bead or film forming solution to improve adhesive property and drug controlled release. Moreover, the study on wound healing with the utilization of the combination of various drugs in the same drug release system should be employed.

REFERENCES

Agrawal, S. K.; DeLong, N. S.; Coburn, J. M.; Tew, G. N.; and Bhatia, S. R. Novel drug release profiles from micellar solutions of PLA-PEO-PLA triblock copolymers. *Journal of Controlled Release* **112** (2006): 64-71.

American Society for Testing and Materials, Annual book of ASTM standards/American Society for Testing and Materials ASTM D 1876-01, Standard test method for peel resistance of adhesives (T-peel test), Volume 15.06, 2006, pp. 121-123.

Aoyagi, S.; Onishi, H. and Machida, Y. Novel chitosan wound dressing loaded with minocycline for the treatment of severe burn wounds. *International Journal of Pharmaceutics* **330** (2007): 138–145.

Baimark, Y.; Niamsa, N.; Morakot, N.; Threeprom, J. and Srisuwan, Y. Preparation and Morphology Study of Biodegradable Chitosan/Methoxy Poly(ethylene glycol)-*b*-Poly(ε-caprolactone) Nanocomposite Films. *International Journal of Polymer Analysis and Characterization* **12** (2007): 457–467.

Budhian, A.; Siegel, S. J. and Winey, K. I. Controlling the In Vitro Release Profiles for a System of Haloperidol-Loaded PLGA. *International Journal of Pharmaceutics* **16** (2007): 1-37.

Choi, J.; Kim, I.-K. and Kwak, S.-Y. Synthesis and characterization of a series of star-branched poly(ε-caprolactone)s with the variation in arm numbers and lengths. *Polymer* **46** (2005): 9725-9735.

Cohn, D. and Lando, G. Tailoring lactide/caprolactone co-oligomers as tissue adhesives. *Biomaterials* **25** (2004): 5875–5884.

Dash, A. K. and Cudworth, G. C. Therapeutic Applications of Implantable Drug Delivery Systems. *Journal of Pharmacological and Toxicological Methods* **40** (1998): 1-12.

Dutkiewicz, S.; Lapienis, D. G. and Tomaszewski, W. Synthesis of Poly(L(+) Lactic Acid) by Polycondensation Method in Solution. *FIBRES & TEXTILES in Eastern Europe* **11** (2003): 66-70.

English, J. P.; McNeely G. W. and Dunn, R. L. Method for making a biodegradable adhesive for soft living tissue. United States Patent 4,804,691 (February 1989).

Ferruti, P.; Penco, M.; D'Addato, P.; Ranucci, E. and Deorganghenghi, R. Synthesis and properties of novel block copolymers containing poly(lactic-glucolic acid) and poly(ethyleneglycol) segments. *Biomaterials* **16** (1995): 1423– 1428.

Foster, D. T.; Rowedder, L. J.; and Reese, S. K. Management of sports-induced skin wounds. *Journal of Athletic Training* **30** (1995): 135-144.

Gallardo, A. .; Eguiburu, J. L.; Berridi, M. J. Fand Roman, J. S. Preparation and in vitro release studies of ibuprofen-loaded films and microspheres made from graft copolymers of poly(L-lactic acid) on acrylic backbones. *Journal of Controlled Release* **55** (1998): 171-179.

Kenawy, E. -R.; Bowlin, G. L.; Mansfield, K.; Layman, J.; Simpsonc, D. G.; Sandersb, E. H. and Wneka, G. E. Release of tetracycline hydrochloride from electrospun poly(ethylene-co-vinylacetate), poly(lactic acid), and a blend. *Journal of Controlled Release* **81** (2002): 57–64.

Kim, C. Controlled release dosage form design. Pennylvia: Technology Publishing Company Book, 2000

Kitayama, T.; Nishiura, T. and Hatada, K. PMMA-block-poly-(butylene)-b-PMMA prepared with α-ω-dilithiated polybiodegradable- isobutylene and its characterization. *Polymer Bulletin* **26** (1991): 513–520.

Kricheldorf, H. R. and Lee, S. R. Polylactones: 32. High-molecular-weight polylactides by ring-opening polymerization with dibutylmagnesium or butylmagnesium chloride. *Polymer* **36** (1995): 2995-3003.

Kricheldorf, H. R. and Serra, A. Polylactones 6. Influence of Various Metal Salts on the Optical Purity of Poly(L-Lactide). *Polymer Bulletin* **4** (1985): 497-502.

Kricheldorf, H. R. and Thiessen, H. H. Telechelic polylactones functionalized with trimethoxysilyl groups. *Polymer* **46** (2005): 12103-12108.

Korhonen, H.; Helminen, A. and Seppala, J. V. Synthesis of polylactides in the presence of co-initiations with different numbers of hydroxyl groups. *Polymer* **42** (2001): 7541-7549.

Kumar, N.; Ravikumar, M. N. V. and Domba, A. J. Biodegradable block copolymers. *Advanced Drug Delivery Reviews* **53** (2001): 23–44.

Lee, J. H.; Go, A. K.; Oh, S. H.; Lee, K. E. and Yuk, S. H. Tissue anti-adhesion potential of ibuprofen-loaded PLLA–PEG diblock copolymer films. *Biomaterials* **26** (2005): 671–678.

Mai-ngam, K.; Prahsarn, C.; Seetapan, N. and Chumningan, P. Thermo-responsive chitosan-*g*-poly-*N*-isopropylacrylamide for tissue adhesives, *Proceeding of the 8th Polymers for Advanced Technologies International Symposium* Budapest, Hungary, 13-16 September 2005.

Mecerreyes D.; Jérôme R. and Dubois Ph. Novel macromolecular architectures based in aliphatic polysters: Relevance of the

"coordination-insertion" ring-opening polymerization. *Advances in Polymer Science* **147** (1999): 1-59.

Montanaro, L.; Arciola, C. R.; Cenni, E.; Ciapetti, G.; Savioli, F.; Filippini, F. and Barasanti, L. A. Cytotoxicity, blood compatibility and antimicrobial activity of two cyanoacrylate glues for surgical use. *Biomaterials* **22** (2001): 59–66.

Pataro, A.L.; Franco, C.F.; Santos, V.R.; Cortes, M.E. and Sinisterrab, R.D. Surface effects and desorption of tetracycline supramolecular complex on bovine dentine. *Biomaterials* **24** (2003): 1075–1080.

Paul, W. and Sharma, C. P. Chitosan, a drug carrier for the 21th century: review. *S.T.P. Pharmasciences* **10** (2000): 5-22.

Penco, M.; Marcioni, S.; Ferruti, P.; D'Antone, S. and Delacticghenghi, R. Degradation behaviour of block copolymers containing poly(lactic-glucolic acid) and poly(ethyleneglycol) segments. *Biomaterials* **17** (1996): 1583–1590.

Peppas, L. B. Polymers in controlled drug delivery. *Medical Plastics and Biomaterials Magazine* (1997): 34.

Perugini, P.; Genta, I.; Conti, B.; Modena, T. and Pavanetto, F. Periodontal delivery of ipriflavone: new chitosan/PLGA film delivery system for a lipophilic drug. *International Journal of Pharmaceutics* **252** (2003): 1–9.

Reece, T. B.; Maxey, T. S. andKron, I. L. A prospectus on tissue adhesives. *The American Journal of Surgery* **182** (2001): 40S–44S.

Sezer, A. D.; Hatipoğlu, F.; Cevher, E.; Oğurtan, Z.; Baş, A. L. and Akbuğa, J. Chitosan Film Containing Fucoidan as a Wound Dressing for Dermal

BurnHealing: Preparation and *In Vitro/In Vivo* Evaluation. *AAPS PharmSciTech* **8** (2007): E1-E8.

Sinha, V. R.; Singla, A. K.; Wadhawan, S. Kumaria, R.; Bonsal, K. and Dhawan. S. Chitosan microsphere as a potential carrier for drugs. *International Journal of pharmaceutics* **274** (2004): 1-33.

Stridsberg, K. M.; Ryner, M. and Albertsson, A. C. Controlled ring-opening polymerization: polymers with designed macromolecular architecture. *Advances in Polymer Science* **157** (2002): 41-65.

Wang, F.; Lee, T. and Wang, C.-H. PEG modulated release of etanidazole from implantable PLGA/PDLA discs. *Biomaterials* **23** (2002): 3555-3566.

Yokoyama, M. Block copolymers as drug carriers. *Critical Reviews in Therapeutic Drug Carrier Systems* **9** (1992): 213–248.

Younes, H.M.; Grimaldo, E. B. and Amsden B. G. Synthesis, characterization and in vitro degradation of a biodegradable elastomer. *Biomaterials* **25** (2004): 5261–5269.

Zhong, Z.; Ankoné, M. J. K.; Dijkstra, P. J. and Birg, C. Calcium methoxide initiated ring-opening polymerization of ε-caprolactone and L-lactide. *Polymer Bulletin* **46** (2001): 51-57.

APPENDICES

APPENDIX A

^{1}H NMR SPECTRUM, GPC AND DSC CHROMATOGRAM

^{1}H NMR spectrum

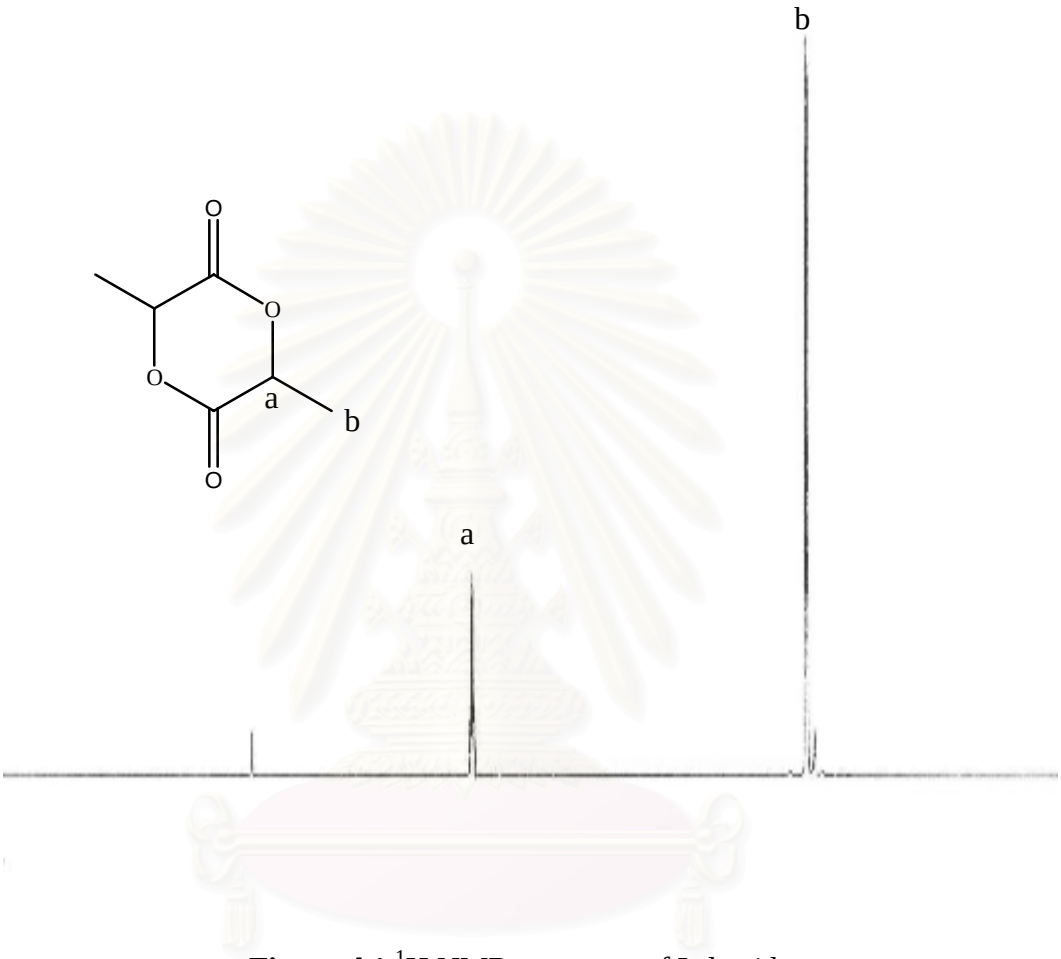

Figure A1 ^{1}H NMR spectrum of L-lactide.

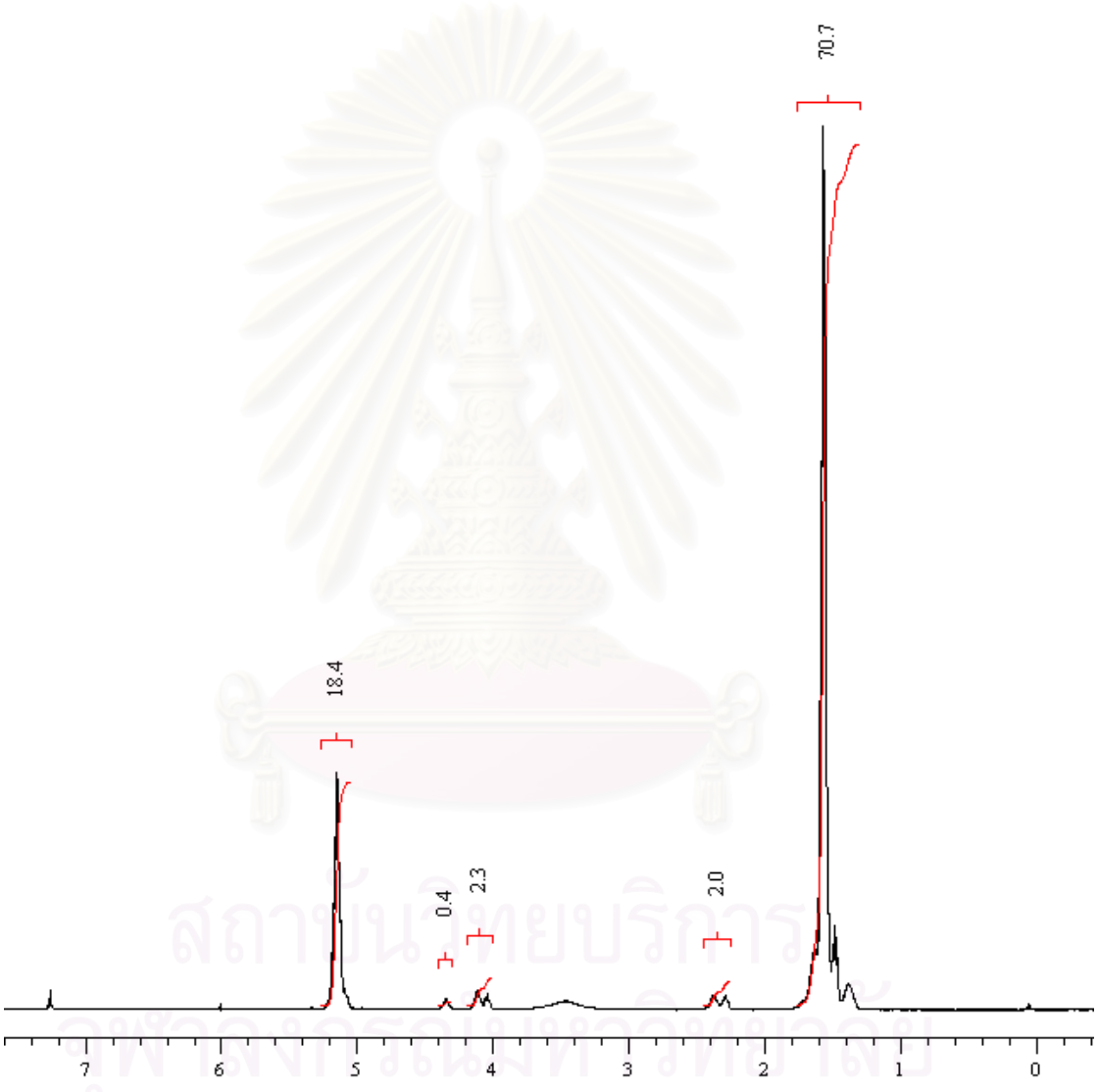

Figure A2 ^{1}H NMR spectrum of P(LA-*co*-CL) prepared by using 1,4-butanediol as co-initiator with similar arm length.

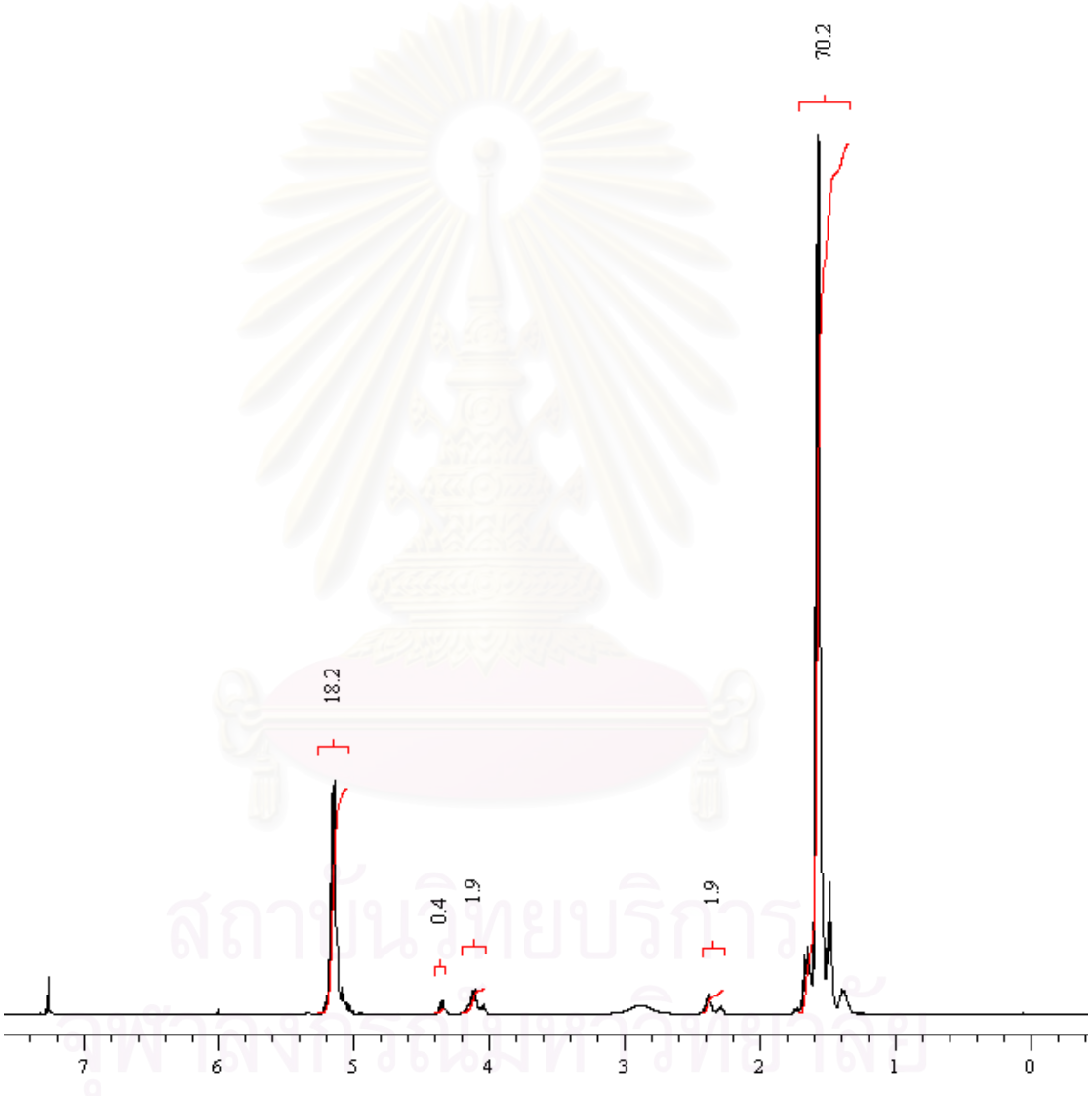

Figure A3 ^{1}H NMR spectrum of P(LA-*co*-CL) prepared by using pentaerythritol as co-initiator with similar arm length.

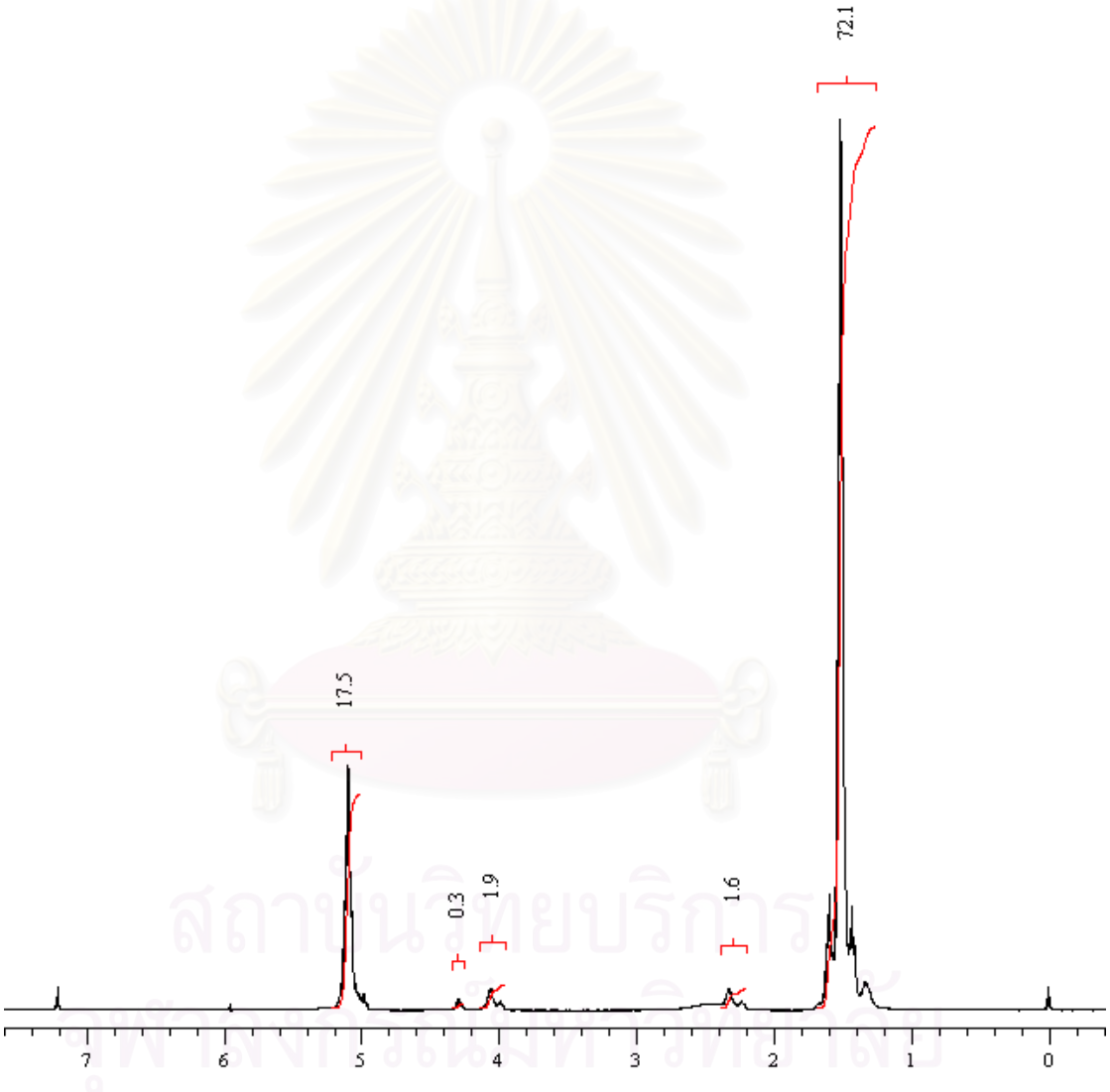

Figure A4 ^{1}H NMR spectrum of P(LA-*co*-CL) prepared by using D-sorbitol as co-initiator with similar arm length.

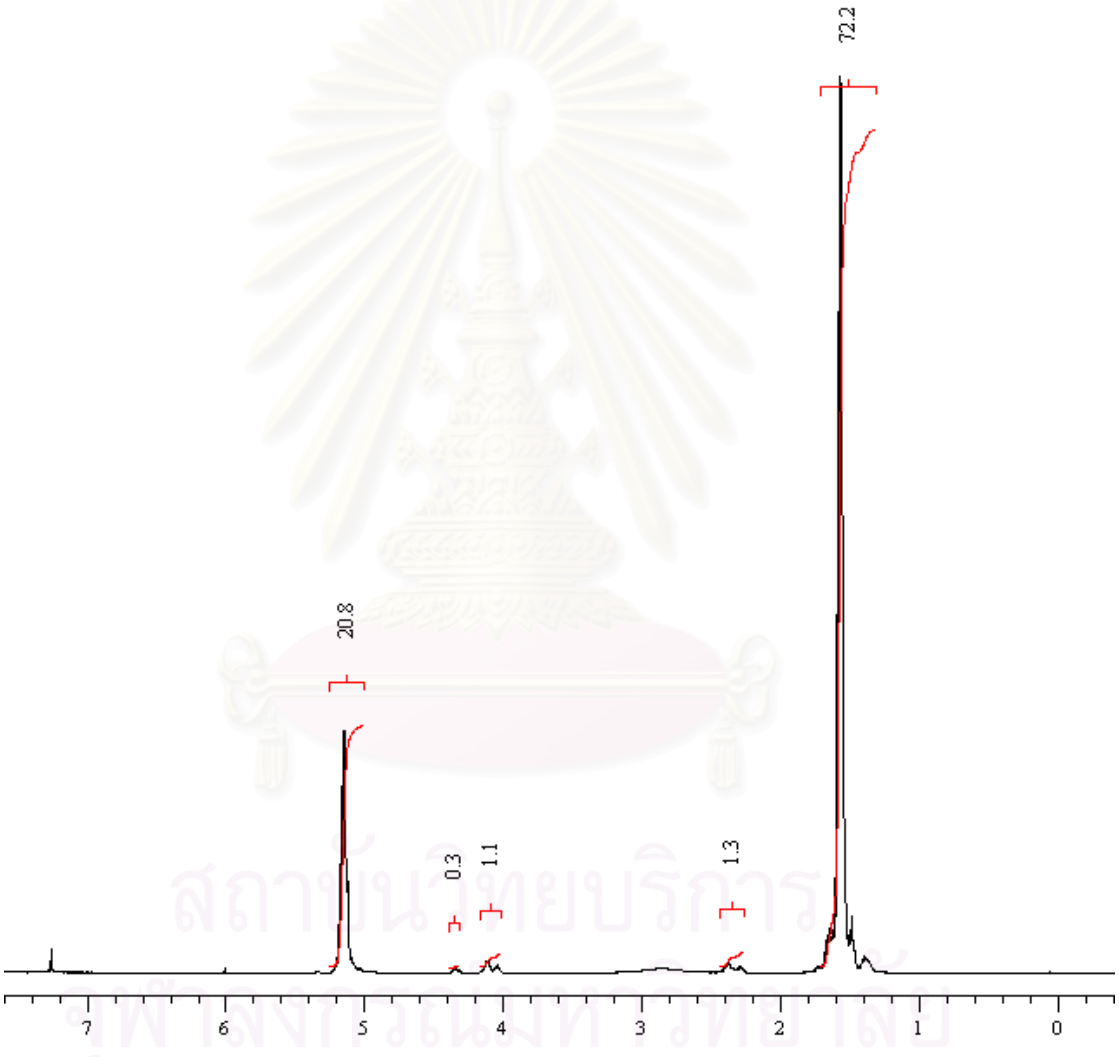

Figure A5 ^{1}H NMR spectrum of P(LA-*co*-CL) prepared by using 1,4-butanediol as co-initiator with similar molecular weight.

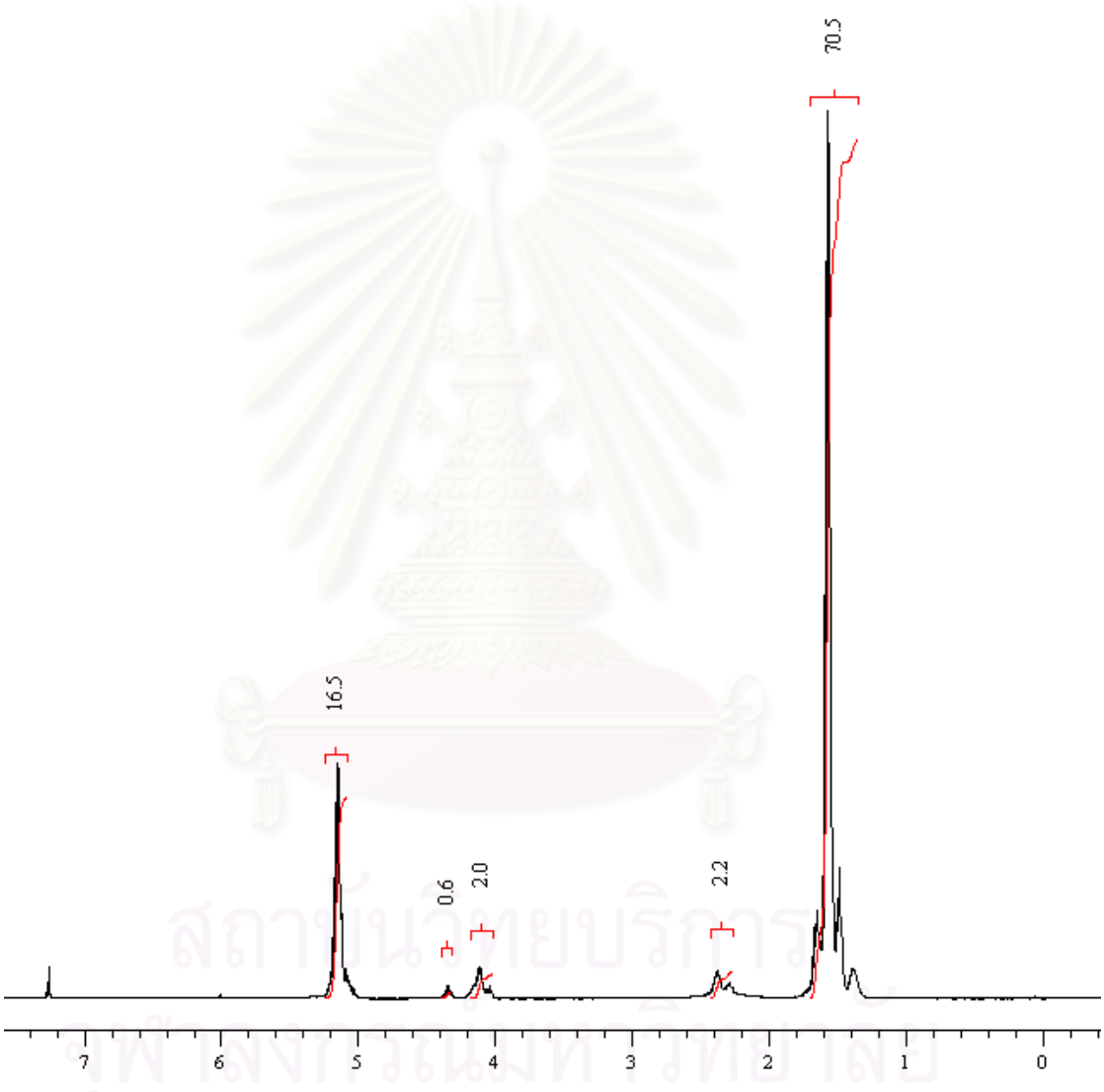

Figure A6 ^{1}H NMR spectrum of P(LA-*co*-CL) prepared by using pentaerythritol as co-initiator with similar molecular weight.

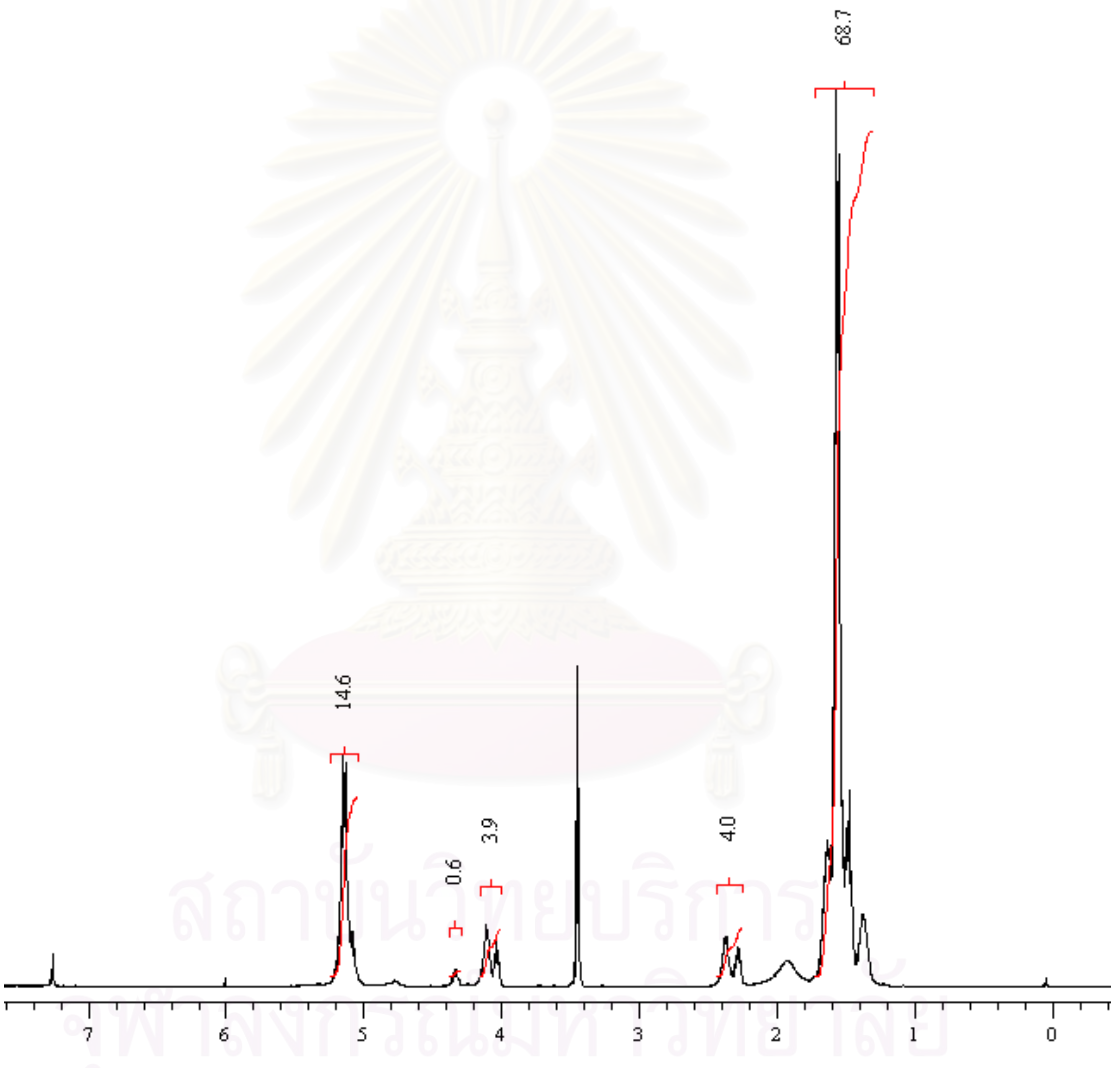

Figure A7 ^{1}H NMR spectrum of P(LA-*co*-CL) prepared by using D-sorbitol as co-initiator with similar molecular weight.

GPC chromatogram

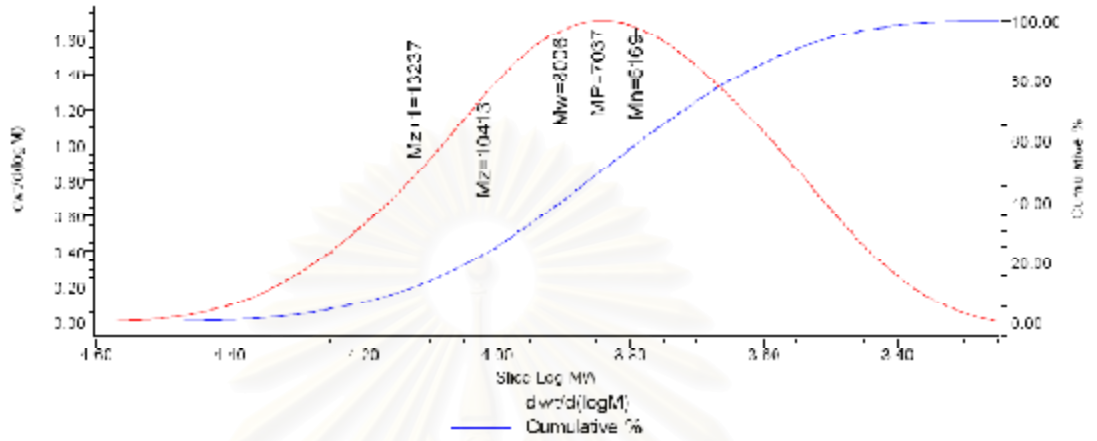

Figure A8 The chromatogram of P(LA-*co*-CL) prepared by using 1,4-butanediol as co-initiator with similar arm length.

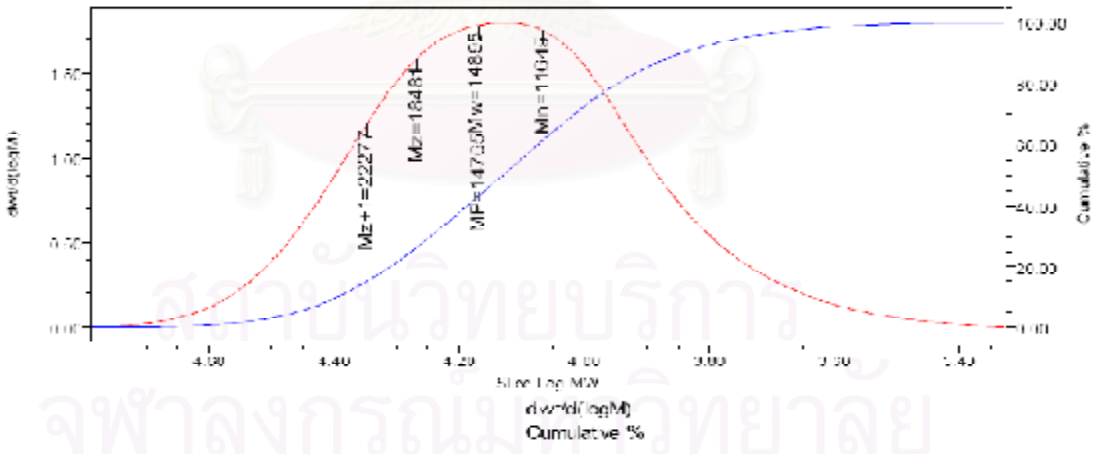

Figure A9 The chromatogram of P(LA-*co*-CL) prepared by using pentaerytritol as co-initiator with similar arm length.

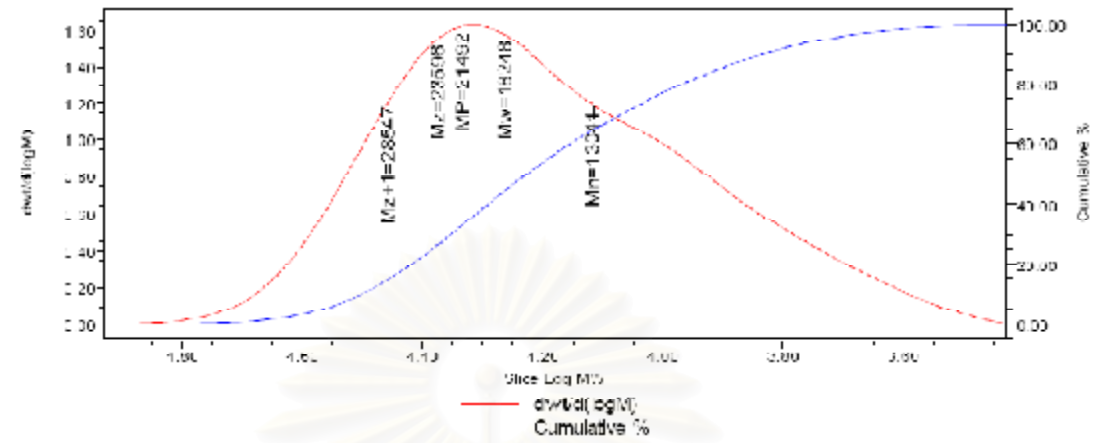

Figure A10 The chromatogram of P(LA-*co*-CL) prepared by using D-sorbitol as co-initiator with similar arm length.

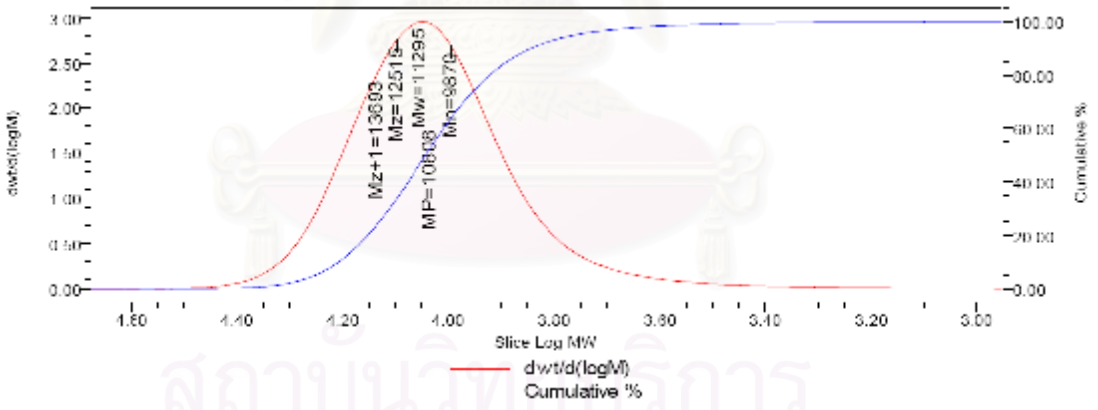

Figure A11 The chromatogram of P(LA-*co*-CL) prepared by using 1,4-butanediol as co-initiator with similar molecular weight.

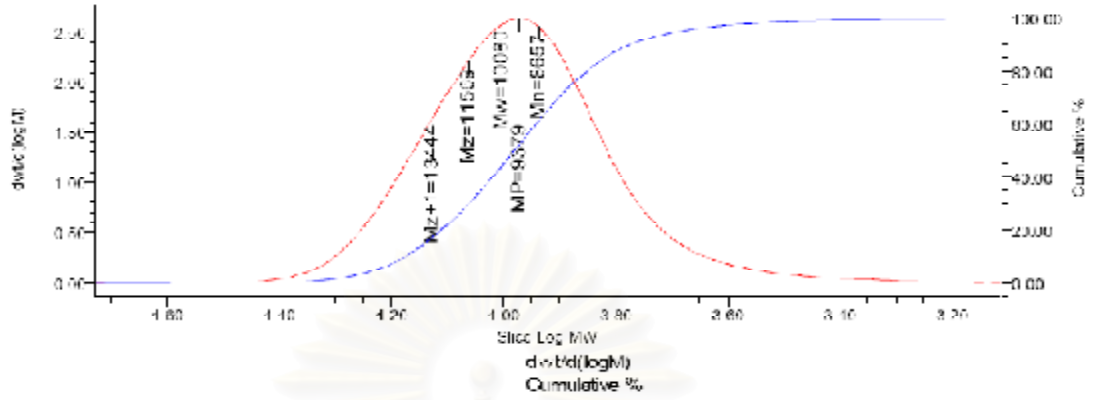

Figure A12 The chromatogram of P(LA-*co*-CL) prepared by using pentaerythritol as co-initiator with similar molecular weight.

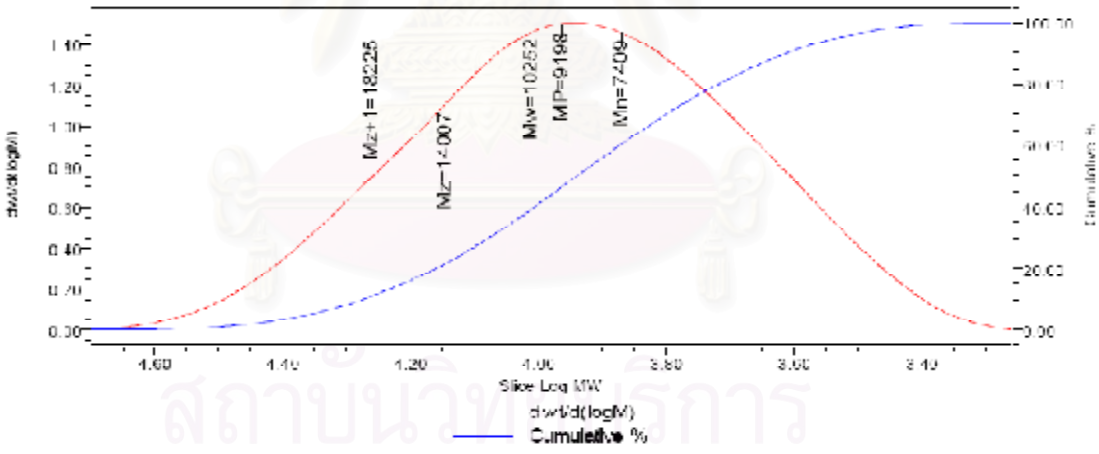

Figure A13 The chromatogram of P(LA-*co*-CL) prepared by using D-sorbitol as co-initiator with similar molecular weight.

DSC chromatogram

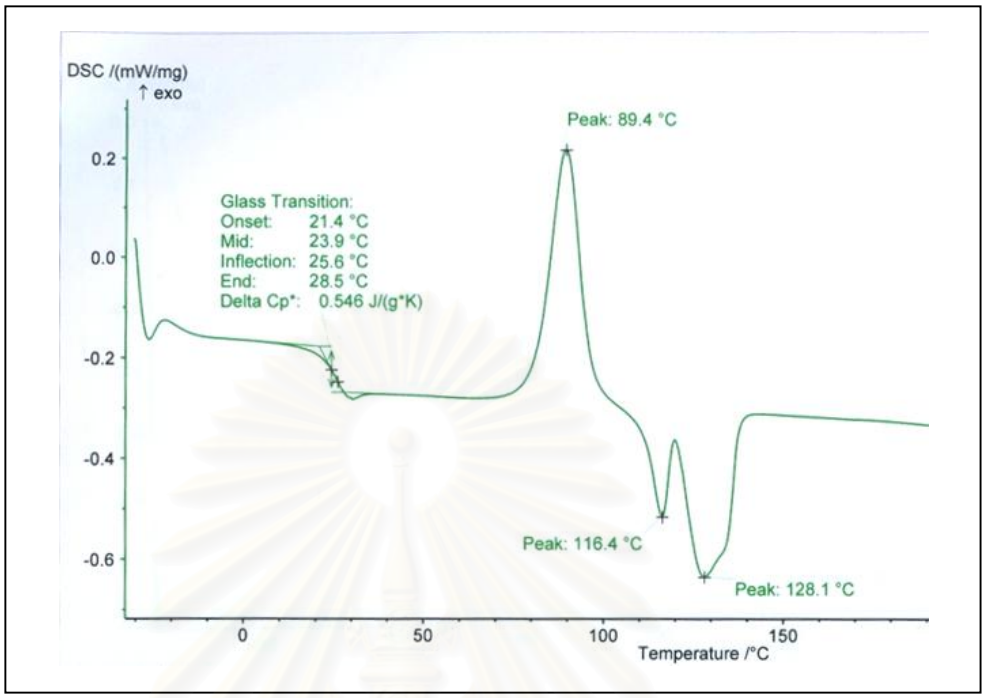

Figure A14 DSC chromatogram of P(LA-*co*-CL) prepared by using 1,4-butanediol as co-initiator with similar arm length.

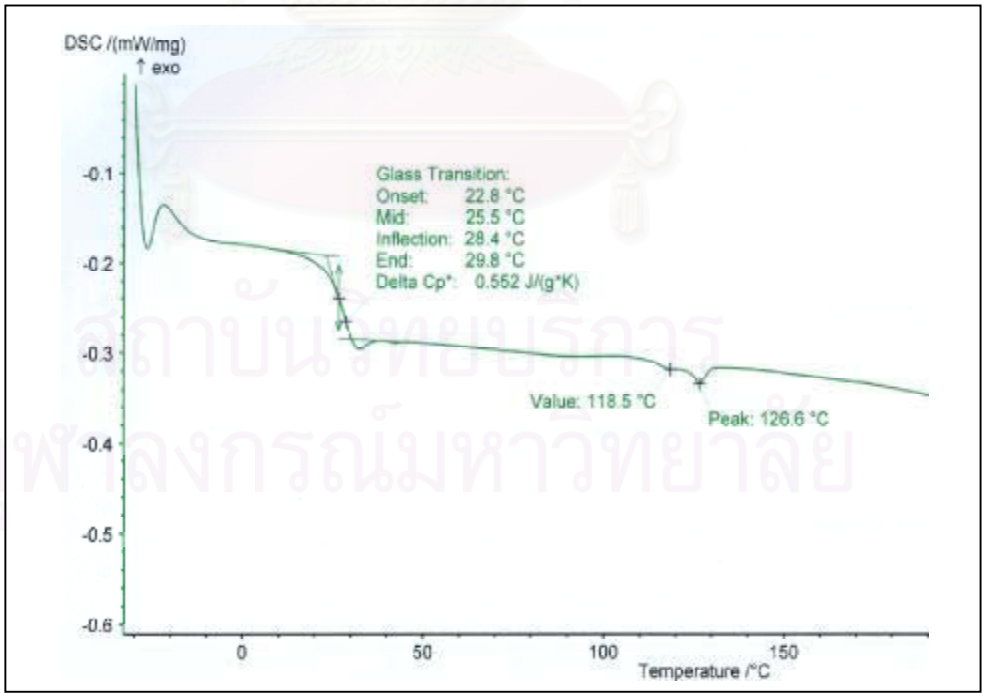

Figure A15 DSC chromatogram of P(LA-*co*-CL) prepared by using pentaerytritol as co-initiator with similar arm length.

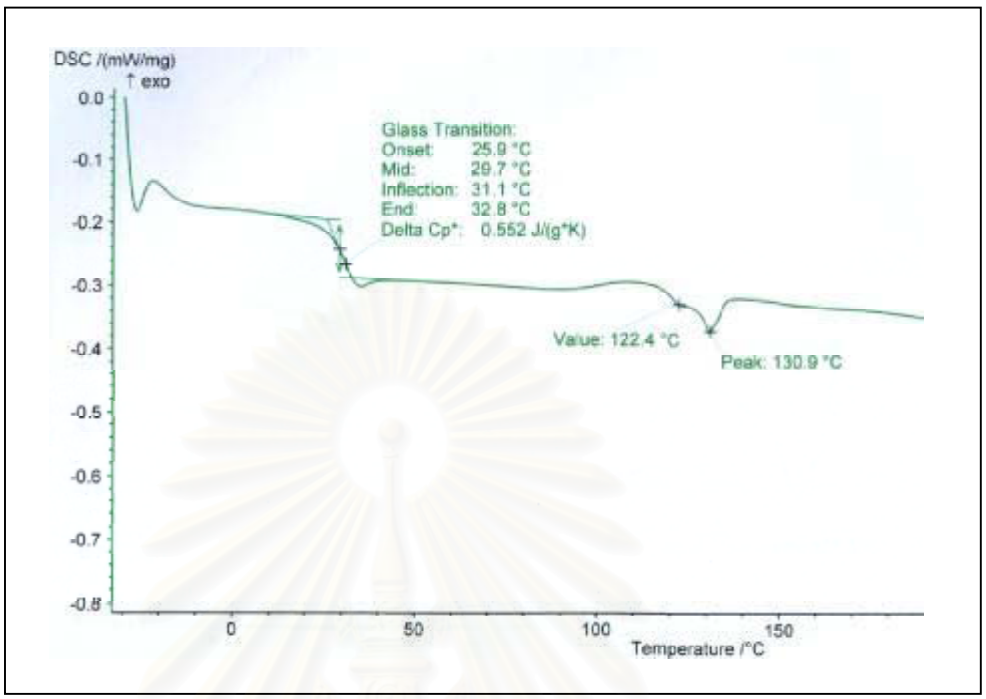

Figure A16 DSC chromatogram of P(LA-*co*-CL) prepared by using D-sorbitol as co-initiator with similar arm length.

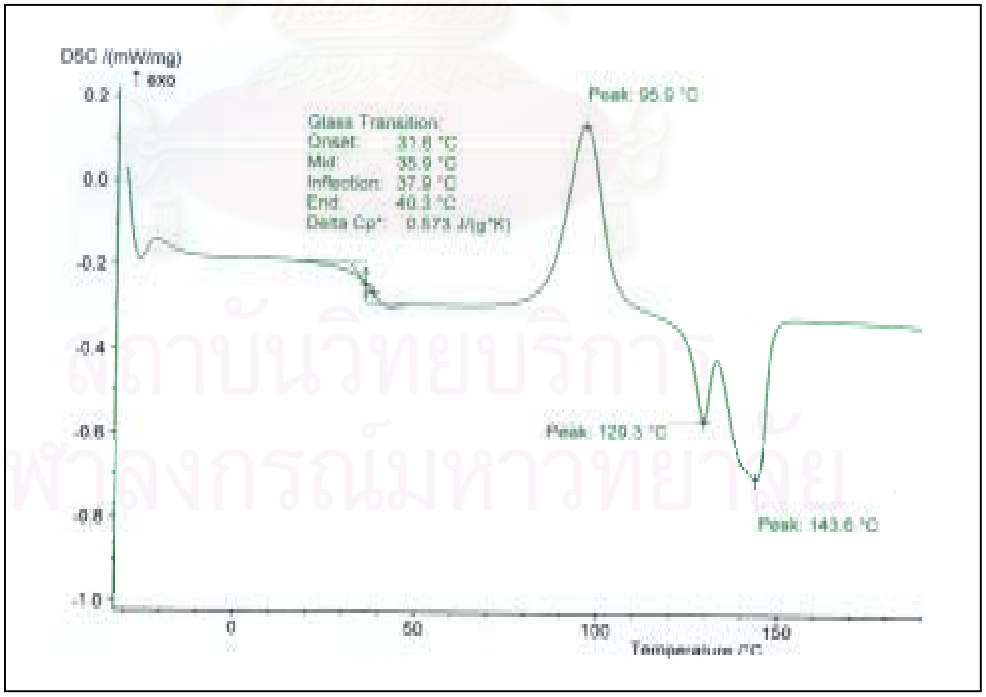

Figure A17 DSC chromatogram of P(LA-*co*-CL) prepared by using 1,4-butanediol as co-initiator with similar molecular weight.

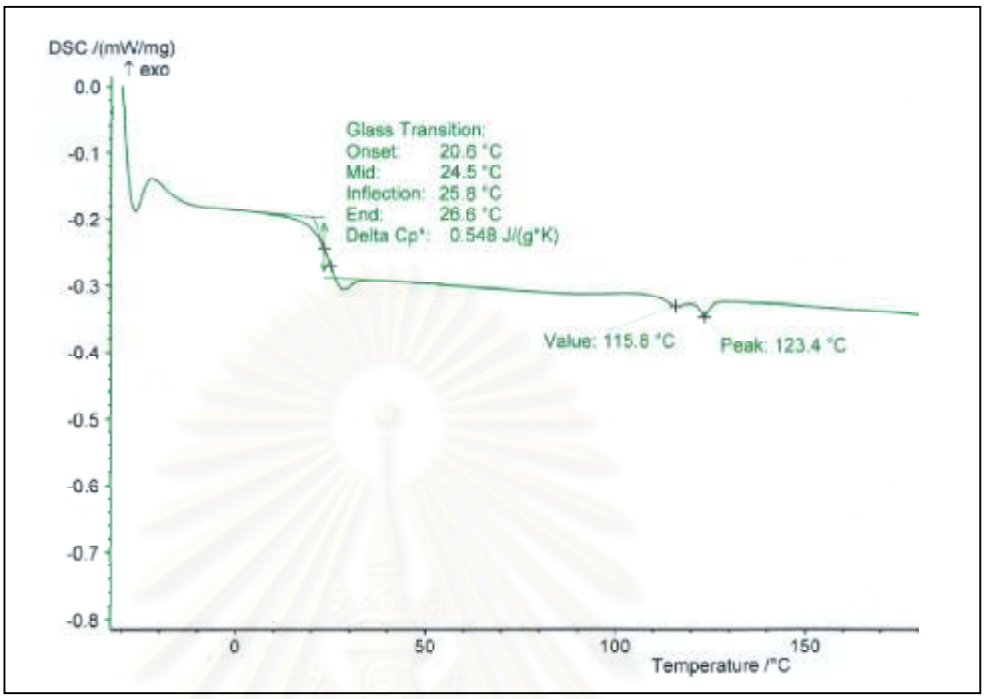

Figure A18 DSC chromatogram of P(LA-*co*-CL) prepared by using pentaerythritol as co-initiator with similar molecular weight.

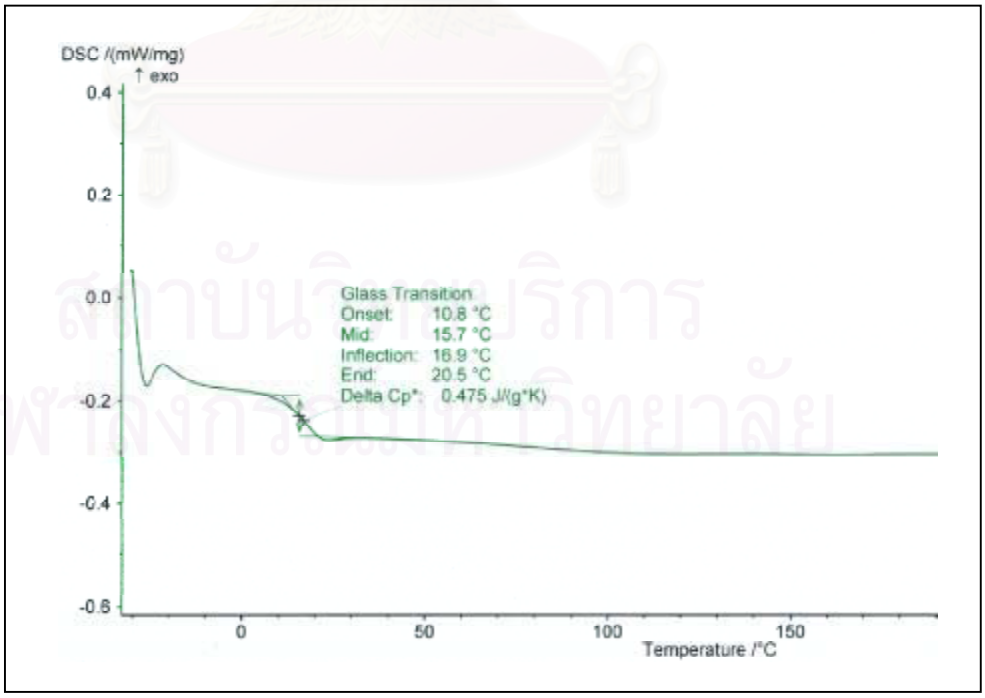

Figure A19 DSC chromatogram of P(LA-*co*-CL) prepared by using D-sorbitol as co-initiator with similar molecular weight.

APPENDIX B

THE DEGREE OF SWELLING

Table B1 The swelling percent of blend films in phosphate buffer saline (pH 7.4).

Time (hour)	CH	CO-BD/CH	CO-PTOL/CH	CO-SB/CH
	degree of swelling ± SD	degree of swelling± SD	degree of swelling± SD	degree of swelling± SD
0	0.00±0.00	0.00±0.00	0.00±0.00	0.00±0.00
0.08	-	185.69±5.64	153.93±9.96	155.40±6.05
0.17	-	197.65±1.12	238.05±12.19	201.78±16.57
0.25	464.83±9.21	208.60±3.60	267.48±9.87	212.08±15.30
0.50	571.67±11.56	209.22±9.65	277.83±5.43	226.44±25.53
0.75	618.83±6.58	210.84±11.91	280.43±5.74	225.63±19.26
1	649.29±7.23	224.64±17.84	285.50±9.47	227.90±18.75
1.5	680.00±9.16	-	-	-
2	702.06±1.39	226.88±23.02	294.17±14.76	228.76±24.23
3	709.86±10.05	228.62±24.65	297.73±12.71	231.76±24.60
4	710.49±6.03	241.94±13.28	301.00±13.31	232.50±25.98
5	711.18±14.23	243.44±10.52	304.30±13.75	232.11±25.58
6	715.38±11.15	243.34±12.11	306.55±14.26	234.78±23.34
24	718.28±11.04	251.68±13.54	309.35±14.02	237.22±22.83

Table B1 (continued) The swelling percent of blend films in phosphate buffer saline (pH 7.4).

Time (hour)	CO-BD (10,000)/CH	CO-PTOL (10,000)/CH	CO-SB (10,000)/CH	CO-PTOL/CH (30/70)
	degree of swelling ± SD	degree of swelling± SD	degree of swelling± SD	degree of swelling± SD
0	0.00±0.00	0.00±0.00	0.00±0.00	0.00±0.00
0.08	216.80±9.30	133.08±5.49	139.36±8.42	284.32±27.29
0.17	266.95±6.68	167.00±7.99	162.89±10.82	320.96±19.67
0.25	273.37±6.73	165.47±3.53	166.25±4.30	341.39±7.20
0.50	301.95±17.63	190.79±6.96	178.52±5.81	376.47±10.59
0.75	310.91±23.28	187.76±7.22	174.61±2.98	447.26±9.05
1	308.93±23.95	194.64±3.61	183.19±4.62	479.29±11.34
2	311.63±28.97	197.00±0.24	187.33±6.95	495.89±11.00
3	311.16±26.26	197.01±3.53	188.87±9.09	499.04±7.18
4	312.31±26.76	200.25±9.40	190.35±8.31	499.99±3.02
5	312.97±27.82	200.03±8.41	194.10±7.27	496.73±3.93
6	316.78±29.93	197.24±7.08	193.40±6.95	495.87±1.82
24	319.87±31.11	202.17±7.20	196.83±6.60	499.26±3.22

APPENDIX C

CALIBRATION CURVE OF TETRACYCLINE HYDROCHLORIDE

Calibration curve of tetracycline hydrochloride

The concentration versus absorbance of tetracycline hydrochloride in phosphate buffer saline pH 7.4 at 276.7 nm is presented in Table C1. The standard curve of tetracycline hydrochloride in these solution media is illustrated in Figure C1.

Table C1 Absorbance of tetracycline hydrochloride in PBS at 276.7 nm.

Concentration (ppm)	Absorbance
5	0.168
10	0.338
20	0.661
30	0.973
40	1.270
50	1.535

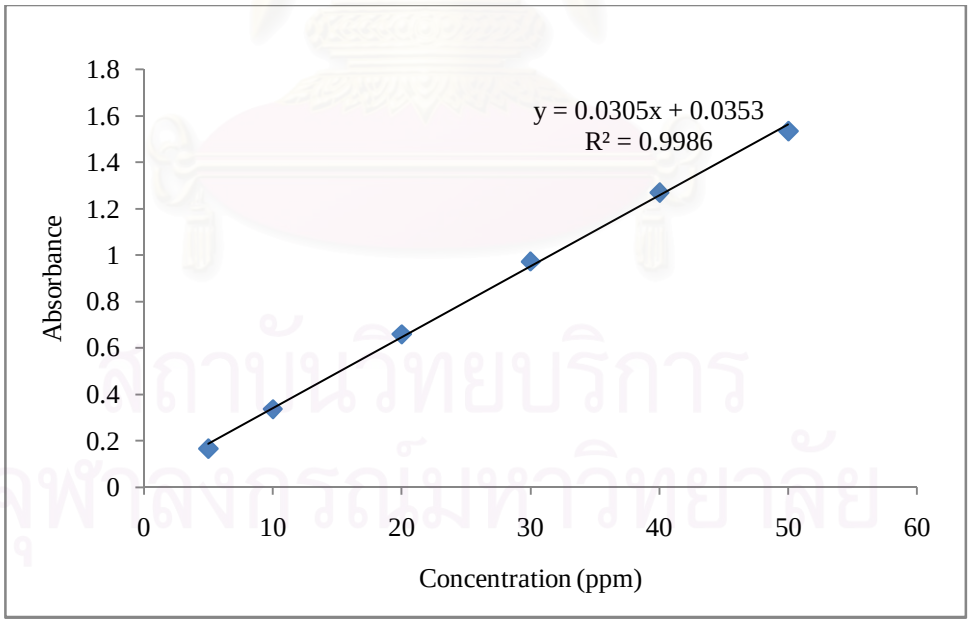

Figure C1 Calibration curve of tetracycline hydrochloride in PBS at 276.7nm.

APPENDIX D

PERCENTAGE OF DRUG RELEASE

Table D1 Percentage of TCH from blend film (Formulation B) in PBS at 37°C.

Time (hour)	%drug release	µg/cm^2
0	0.00±0.00	0.00±0.00
0.25	63.41±1.35	136.11±0.49
0.5	67.35±1.22	144.59±0.48
0.75	69.51±0.64	149.25±3.93
1	71.01±1.04	152.47±3.89
1.5	72.72±1.09	156.15±4.12
2	74.52±0.34	160.02±3.55
2.5	75.68±0.24	162.50±3.35
3	77.13±0.68	165.62±4.14
3.5	77.09±1.04	165.55±5.01
4	77.67±1.01	166.80±4.98
4.5	78.55±0.95	168.67±4.69
5	79.17±2.56	170.05±8.15
6	79.90±1.29	171.59±5.74
7	80.46±1.23	172.78±5.04
8	80.50±0.94	172.85±4.35
9	81.83±1.05	175.72±5.22
10	83.06±0.70	178.35±4.18
11	82.94±1.22	178.09±4.76
12	83.16±1.57	178.59±5.90
24	84.68±0.76	181.83±3.61
48	85.08±0.23	182.68±3.57
72	85.53±0.38	183.65±3.43
96.5	86.52±0.59	185.76±2.03
120	86.95±1.70	186.66±2.58
144	87.02±2.02	186.79±1.65
168.5	86.841.35	186.42±1.73

Table D2 Percentage of TCH from blend film (Formulation C) in PBS at 37°C.

Time (hour)	%drug release	μg/cm^2
0	0.00±0.00	0.00±0.00
0.25	38.62±1.69	171.91±10.10
0.5	52.45±1.51	233.46±10.88
0.75	58.31±2.57	259.26±3.58
1	64.31±0.85	286.17±8.31
1.5	70.25±1.22	312.68±12.94
2	73.70±2.52	327.96±13.92
2.5	75.31±1.45	335.151±1.92
3	75.57±1.43	336.271±0.43
3.5	76.34±1.98	339.58±6.34
4	76.89±1.42	342.05±5.16
4.5	77.65±0.72	345.52±7.41
5	78.59±1.56	349.60±4.26
6	78.58±1.85	349.54±4.40
7	78.75±1.31	350.36±5.52
8	80.19±3.14	356.62±4.92
9	80.04±1.93	356.02±3.44
10	80.39±1.75	357.61±3.11
11	80.95±1.62	360.13±5.93
12	81.11±1.56	360.84±6.17
24	82.25±1.89	366.01±12.31
48	82.97±1.93	369.26±14.67
72	83.31±1.76	370.74±13.61
96.5	83.49±1.13	371.54±11.87
120	83.55±1.50	371.81±11.92
144	83.80±1.58	372.92±11.84
168.5	84.08±1.69	374.13±11.26

Table D3 Percentage of TCH from blend film (Formulation D) in PBS at 37°C.

Time (hour)	%drug release	μg/cm^2
0	0.00±0.00	0.00±0.00
0.25	29.47±0.56	247.41±2.80
0.5	46.31±0.62	388.73±2.57
0.75	53.74±0.88	451.17±4.14
1	58.27±0.70	489.15±3.76
1.5	67.21±0.88	564.21±4.19
2	75.33±0.66	632.43±7.15
2.5	80.59±0.64	676.55±4.44
3	82.61±1.53	693.49±7.47
3.5	83.66±0.64	702.32±5.14
4	83.89±0.75	704.27±7.26
4.5	84.65±1.40	710.68±11.35
5	84.95±1.39	713.20±11.43
6	85.55±2.04	718.17±14.63
7	85.67±2.33	719.16±16.14
8	85.71±2.33	719.50±16.27
9	85.88±2.37	720.92±16.41
10	86.24±2.83	723.93±19.72
11	86.43±2.71	725.54±8.71
12	86.83±2.30	728.89±14.66
24	87.08±2.48	730.99±16.10
48	87.46±2.30	734.23±14.17
72	87.29±1.41	732.80±8.17
96.5	87.15±1.78	731.65±12.31
120	89.07±2.03	747.72±11.35
144	89.04±2.21	747.47±12.70
168.5	89.09±1.76	747.86±9.29

Table D4 Percentage of TCH from chitosan film (Formulation A) in PBS at 37°C.

Time (hour)	%drug release	μg/cm^2
0	0.00±0.00	0.00±0.00
0.25	71.10±1.50	250.56±31.89
0.75	78.91±1.02	276.95±23.78
1	82.88±0.89	284.08±25.82
1.5	86.96±0.85	295.33±29.08
2	88.77±0.80	303.50±28.60
2.5	90.42±0.57	307.50±29.32
3	91.50±0.57	310.44±32.09
3.5	92.46±0.27	315.37±32.93
4	92.69±0.41	317.20±33.19
4.5	93.09±0.37	318.57±34.76
5	94.48±0.86	319.17±35.52
6	94.56±1.00	325.04±34.93
7	95.00±0.73	325.43±34.73
8	96.92±4.28	329.35±34.87
9	94.58±0.47	330.26±36.29
10	95.52±0.82	327.87±44.68
25	95.00±0.70	334.42±39.63
49	96.14±1.33	335.50±35.98
81	97.01±1.61	334.30±36.75
105	96.90±2.19	334.90±35.36
129	96.65±1.52	334.60±38.87
168	98.28±0.95	341.72±28.14

Table D5 Percentage of TCH from blend film (Formulation E) in PBS at 37°C.

Time (hour)	%drug release	μg/cm^2
0	0.00±0.00	0.00±0.00
0.25	54.21±2.51	275.25±3.73
0.75	60.06±1.15	305.53±4.56
1	61.59±0.87	320.89±3.85
1.5	63.99±0.46	336.70±4.35
2	65.79±1.23	343.71±4.81
2.5	66.65±0.64	350.11±6.59
3	67.25±0.13	354.31±8.23
3.5	68.31±0.13	358.05±8.51
4	68.71±0.36	358.93±7.74
4.5	68.98±0.27	360.48±7.54
5	69.10±0.44	365.93±11.59
6	70.39±0.43	366.24±12.02
7	70.48±0.36	367.91±11.16
8	71.33±0.50	375.15±12.25
9	71.51±0.40	366.29±10.17
10	70.87±2.23	369.88±7.07
25	72.37±0.93	367.85±5.63
49	72.66±0.16	372.30±9.24
81	72.39±1.09	375.57±3.07
105	72.54±0.90	375.13±2.84
129	72.43±1.55	374.17±3.18
168	74.13±1.62	380.54±6.12

VITA

Ms. Sumana Sriputtirat was born on Friday 5th March, 1982, in Sakonnakhon, Thailand. In 2005, she graduated with a Bachelor's degree of Science in Chemistry, from Chulalongkorn University. After that, she has studied for a Master's degree of Science in Petrochemistry and polymer science, Faculty of Science, Chulalongkorn University, and completed the program in 2007.

Address: 791/4 Raungsawat Road, Tambol Dhatcherngchoom, Amphur Maung, Sakonnakhon Province 47000.